TECHNICAL REPORT ARBRL-TR-02188

THE PARTICLE DYNAMICS OF TARGET PENETRATION

James Dehn

September 1979

US ARMY ARMAMENT RESEARCH AND DEVELOPMENT COMMAND
BALLISTIC RESEARCH LABORATORY
ABERDEEN PROVING GROUND, MARYLAND

Destroy this report when it is no longer needed.
Do not return it to the originator.

SECURITY CLASSIFICATION OF THIS PAGE *(When Data Entered)*

REPORT DOCUMENTATION PAGE		READ INSTRUCTIONS BEFORE COMPLETING FORM
1. REPORT NUMBER Technical Report No. ARBRL-TR-02188	2. GOVT ACCESSION NO.	3. RECIPIENT'S CATALOG NUMBER
4. TITLE *(and Subtitle)* THE PARTICLE DYNAMICS OF TARGET PENETRATION		5. TYPE OF REPORT & PERIOD COVERED Final
		6. PERFORMING ORG. REPORT NUMBER
7. AUTHOR(s) James Dehn		8. CONTRACT OR GRANT NUMBER(s)
9. PERFORMING ORGANIZATION NAME AND ADDRESS US Army Ballistic Research Laboratory ATTN: DRDAR-BLT Aberdeen Proving Ground, MD 21005		10. PROGRAM ELEMENT, PROJECT, TASK AREA & WORK UNIT NUMBERS 1L161102AH43
11. CONTROLLING OFFICE NAME AND ADDRESS US Army Armament Research and Development Command US Army Ballistic Research Laboratory		12. REPORT DATE SEPTEMBER 1979
ATTN: DRDAR-BL Aberdeen Proving Ground, MD 21005		13. NUMBER OF PAGES 109
14. MONITORING AGENCY NAME & ADDRESS(*If different from Controlling Office*)		15. SECURITY CLASS. *(of this report)* UNCLASSIFIED
		15a. DECLASSIFICATION/DOWNGRADING SCHEDULE

16. DISTRIBUTION STATEMENT *(of this Report)*

Approved for public release; distribution unlimited.

17. DISTRIBUTION STATEMENT *(of the abstract entered in Block 20, if different from Report)*

18. SUPPLEMENTARY NOTES

19. KEY WORDS *(Continue on reverse side if necessary and identify by block number)*

Penetration
KE penetrator
Modeling

20. ABSTRACT *(Continue on reverse side if necessary and identify by block number)* (mba)
New approaches are proposed for describing some of the principle features of target penetration by a projectile in the ordnance velocity range. These features include the following observed facts: (1) curved trajectories including the possibilities of perforation, embedment or ricochet, (2) loss of mass by erosion, and (3) breakup of the projectile into sizable pieces. Each of the approaches proposed is illustrated by examples. In addition, a considerable amount of literature on the subject is reviewed in order to place these new approaches in context. NOTE: This report has been written from an historical

(Continued)

(Item 20 Continued)

perspective. If the reader is more interested in new models than in the history which preceded them, it would be helpful to skip the first two sections and begin with Section III on page 29. Sections IV and V develop and illustrate the basic ideas of this report concerning a constant mass penetrator. Section VI is also historical and could well be omitted at a first reading. Section VII extends the theory to the case of a variable mass penetrator, while Section VIII considers a model of projectile breakup. By a judicious selection of topics of interest the reader's task should be simplified.

TABLE OF CONTENTS

3

LIST OF ILLUSTRATIONS

5

LIST OF TABLES

I. INTRODUCTION

A. General Introduction

In order to put this report in context a survey of some penetration models will be given first. For this purpose it is convenient to divide these models into elementary, intermediate and advanced types. We will not attempt a complete survey of all such models. Instead, we will refer to or quote other surveys where possible and content ourselves with an analysis of some of the more popular models currently in use. A recent general survey of penetration models has been given by Backman and Goldsmith[1].

B. Elementary Models

A principle feature of elementary models is that they are very easy to use and require little calculation. They are usually constructed by choosing certain experimental variables which are felt to be important. These are incorporated together with some adjustable constants into an arbitrary functional form which serves the ad hoc purpose of producing at least qualitatively correct behavior. The constants are then adjusted to give a reasonable or even "best" fit to the data which is available in certain ranges of the allowed values of the experimental variables. The final result is an interpolation formula which is useful within these measured ranges.

One reason for choosing a particular functional form rather than standard multivariate interpolation formulas such as those of Newton or Lagrange might be ease of calculation, although this reason has less force in our day of convenient electronic calculators. A better reason might be given if the functional form chosen is reminiscent of physical laws so that it can be helpful in mentally organizing a mass of data. We must bear in mind, however, that such functional forms are not based on physical laws and are purely empirical. A danger can arise if the user begins to place too much confidence in such formulas and uses them for extrapolation beyond the measured ranges of the experimental variables. At best the predictions of such an extrapolation are highly tentative and are explicitly described as such. At worst such predictions can be absurd without the user even realizing this fact.

Numerous examples of elementary or empirical models exist and many of them have been surveyed by Zook[2]. We will select one for further analysis since it is both ambitious and popular. This model consists

---

[1]M. E. Backman and W. Goldsmith, "The Mechanics of Penetration of Projectiles Into Targets," Int. J. Eng. Sci. 16, 1-99 (1978).

[2]J. Zook, "An Analytical Model of Kinetic Energy Projectile/Fragment Penetration," BRL MR 2797, 1977.

of the two Thor equations[3]. Five experimental variables were chosen: striking mass (m_0), projectile presented area (A), striking velocity, that is, speed (V_0) and obliquity (θ_0), and plate target thickness (T). Five adjustable constants for each target-projectile material combination were incorporated together with these variables into each of two arbitrary functional forms, one for the residual speed (V_1)

$$V_1 = V_0 - 10^{a_1} (TA)^{a_2} (m_0)^{a_3} (\sec \theta_0)^{a_4} (V_0)^{a_5} \tag{1}$$

and another for the residual mass (m_1)

$$m_1 = m_0 - 10^{b_1} (TA)^{b_2} (m_0)^{b_3} (\sec \theta_0)^{b_4} (V_0)^{b_5} \tag{2}$$

remaining after perforation. Here we use numerical subscripts instead of letters to anticipate multiplate target applications. For example, V_1 is the speed remaining after perforation of target plate number one, which of course becomes the striking speed for target plate number two with V_2 remaining and so forth. Similarly we have m_1 and θ_1. These equations were fitted to a particular data set for steel cylinders impacting ten different target plate materials and the constants were adjusted to give a least squares type of best fit.

In the Thor equations dimensions are preserved by suitable choices for the power of ten factors which govern the values of a_1 and b_1. In Equation (1) the fitting procedure gave positive values for a_2 and a_4 in all ten cases while a_3 was always negative and a_5 was positive but less than unity for eight target materials and negative for two, magnesium and aluminum. Since a_2 and a_4 are positive these parts of Equation (1) are reminiscent of physical behavior. The factor (TA) is, roughly speaking, the volume of the plug which is often punched out of thin target plates by blunt projectiles and $a_2 > 0$ implies that the larger this plug is the smaller the residual speed will be. This is reasonable since more energy must be spent punching out and accelerating a larger plug. One might think that an association of T with $\sec \theta_0$ should also have been made. A factor $L = T \sec \theta_0$ is the line-of-sight thickness of the plate and $(T \sec \theta_0)^{a_4}$ with $a_4 > 0$ would imply that a larger L due either to larger T or larger θ_0 means a smaller V_1, which is also reasonable. Unfortunately, there is no easy way to split the factor $(T)^{a_2}$ as given to remind us of both plugs and line-of-sight thickness.

The authors of the Thor report cited above went on to assume that for compact projectiles the area (A) is proportional to the two-thirds power of the striking mass and absorbed $(A)^{a_2}$ into the mass factor,

---

[3]*Project Thor Technical Report No. 47, 1961.*

changing a_3 to a_3^* and of course a_1 to a_1^*. When this is done, T is left free to be associated with sec θ_0 and equality of a_2 and a_4 would remind us of line-of-sight thickness. Usually a_2 and a_4 differ by about 25 percent so such an interpretation is not impossible. The new value given for a_3^* is not $a_3 + 0.67$ as we might expect. Usually it is more like $a_3/3$.

If we set V_1 in Equation (1) equal to zero and interpret V_0 as the perforation limit speed $V_{0\ell}$ we have for the compact projectile

$$(m_0)^{-a_3^*} (V_{0\ell})^{1-a_5} = (10)^{a_1^*} (T)^{a_2} (\sec \theta_0)^{a_4} . \qquad (3)$$

If a_3^* were (- .5) and a_5 were zero, then squaring Equation (3) and multiplying by one-half would give

$$\frac{1}{2} m_0 V_{0\ell}^2 = \frac{1}{2} (10)^{2a_1^*} (T)^{2a_2} (\sec \theta_0)^{2a_4} . \qquad (4)$$

This result reminds us of a threshold energy for perforation proportional to the square of something which resembles a line-of-sight thickness. For magnesium, aluminum, titanium and homogeneous steel target plates, a fit to the data set gave a_3^* closer to (- .4) than (- .5). In addition a_5 was usually close to zero, especially for steel. However, for copper and lead a_3^* was closer to (- .2) while a_5 was about (.8). This gives $(m_0 V_{0\ell})^{0.2}$ on the left side of Equation (3) so that by taking the fifth power, we have

$$(m_0 V_{0\ell}) = (10)^{5a_1^*} (T)^{5a_2} (\sec \theta_0)^{5a_4} \qquad (5)$$

which is suggestive of a threshold momentum. When a_5 is negative as for magnesium and aluminum we obtain a threshold value for a variable $m_0 V_{0\ell}^x$ where x > 2 and physical reminders are difficult to find.

If we use $V_{0\ell}$ from Equation (4) in Equation (1) for a compact projectile with $a_3^* = - .5$ and $a_5 = 0$ we obtain

$$V_1 = V_0 - 10^{a_1^*} (m_0)^{-.5} (T)^{a_2} (\sec \theta_0)^{a_4} = V_0 - V_{0\ell} . \qquad (6)$$

Thus the Thor prediction for the most common target plates is a roughly linear relation between V_1 and V_0. This is in contrast to the hyperbolic relation $V_1 \approx (V_0^2 - V_{0\ell}^2)^{1/2}$ so often proposed using simple physical

11

considerations and presumably confirmed by numerous experiments. If we put Equation (5) in Equation (1) for a compact projectile with $a_3{}^* = .2$ and $a_5 = .8$

$$V_1 = V_o - 10^{a_1{}^*} (m_o)^{-.2} (T)^{a_2} (\sec \theta_o)^{a_4} (V_o)^{.8} = V_o{}^{.8} (V_o{}^{.2} - V_{o\ell}{}^{.2})$$

(7)

which also contrasts with the hyperbolic relation. The latter of course is derived for zero obliquity and constant striking mass. The Thor attempt to include non-zero obliquity and mass erosion in a simplistic formula can of course lead to such contrasts.

These relations are noted here to show that Equation (1) is not only easy to use but can be reminiscent of some sort of physical behavior and so aid in mentally organizing a mass of data, provided we take note of such relations. If we do not, the formula can be as confusing as the data itself.

In Equation (2) b_2 and b_5 were always found to be positive. Positive b_2 implies that a thicker target plate or larger plug will cause greater mass loss which is reasonable. Positive b_5 implies that higher velocity projectiles will suffer more erosion which is not in accord with experience for unbroken projectiles as we will see below. However, if one looks only at the largest piece of a broken projectile, then positive b_5 can describe experiment. In most cases $b_3{}^*$ is positive and not much less than unity which suggests the not unreasonable form

$$m_1 = m_o [1 - f (V_o, \theta_o, T)].$$

(8)

In the single case of titanium $b_3{}^* = - .024$. This is inconsistent with with the other target materials used and could lead one to suspect the data and/or the fitting procedure. The thought that titanium is somehow different and that the Thor results are revealing a new phenomenon should be resisted since we are dealing with an empirical formula not based on any physical law.

For eight target materials b_4 was found to be positive which is reasonable since greater mass loss is expected for a greater line-of-sight thickness. For two target materials b_4 was found to be negative with $b_4 = -.172$ for magnesium and $b_4 = - .361$ for aluminum. This leads to the surprising prediction that a greater line-of-sight thickness due to an increase in obliquity means less mass loss. In addition, it is inconsistent with the other target materials used, although interestingly enough, the value found for a_5 for these same two materials was also inconsistent with the other materials. Again we might suspect the data and/or the fit. Indeed, at least for aluminum two obvious blunders can

12

be found which might help to account for the negative value of b_4. In experiments 256 and 257 the residual mass was reported to be three or four times the striking mass. If a simple typographical blunder is not responsible then possibly a failure to pick out the remains of the steel projectile could be the cause. For example, if a large piece from the aluminum target were chosen instead of the projectile or if a piece of the target adhering to the projectile were included in the weighing procedure, perhaps an explanation could be found. This type of mistake is commonly called a blunder to distinguish it from an experimental error which can be reduced but not removed entirely. Again we should resist the temptation of thinking that new properties of magnesium and aluminum might be revealed and await discovery, reminding ourselves that we are dealing with a purely empirical formula. An argument might be made that target pieces adhering to the projectile should be recorded as the residual mass since this combination can inflict more damage behind the target. If we accept this argument, then to be consistent we should always record the masses of target pieces. This is desirable, but was never done in the Thor collection.

If we try to verify an increase in residual mass with increasing obliquity (negative b_4) in the Thor data sets for magnesium and aluminum we quickly find that the data is too sparse and inaccurate to make a judgment. If we hold three factors constant for magnesium, namely, $T = .75$ inches, $m_0 = 240$ grains and $V_0 = 5,400$ ft/sec, we find m_1 equal to 195.7, 165.4 and 230.7 grains respectively for θ_0 equal to $0°$, $60°$ and $70°$. It is difficult to believe that a $10°$ increase in obliquity could lead to a forty percent increase in residual mass, and similar behavior is not found elsewhere. Such data is usually labeled anomalous and calls for a repetition of the experiment before inclusion into a formula fit. If we keep $T = 1$ inch, $m_0 = 120$ grains and $V_0 = 5,000$ ft/sec, we find $m_1 = 104.5$ and 119.0 (average 111.75) grains at $\theta_0 = 0°$, $m_1 = 103.7$ grains at $45°$ and 105.2 and 106.5 (average 105.85) grains at $60°$. Here we have more than one experiment in two cases at least and the trend is not inconsistent with decreasing or even constant m_1 as a function of θ_0 in view of the experimental errors involved. Other data with T, m_0 and V_0 constant was not obtained. If we allow V_0 to vary a bit we find for $T = 1$ inch and $m_0 = 240$ grains that for $\theta_0 = 0°$ and $V_0 = 4,649$ ft/sec, $m_1 = 214.7$ grains; for $\theta_0 = 45°$ and $V_0 = 4,763$ ft/sec, $m_1 = 202.2$ grains; and for $\theta_0 = 60°$ and $V_0 = 5,000$ ft/sec, $m_1 = 185.0$ grains. In addition we find for $T = 2$ inches and $m_0 = 240$ grains that for $\theta_0 = 0°$ and $V_0 = 5,000$ ft/sec, $m_1 = 213.3$ and 219.0 (average 216.15) grains while for $\theta_0 = 45°$ and $V_0 = 5,500$ ft/sec, $m_1 = 174.7$ and 190.7 (average 182.7) grains. Admittedly this information is complicated by the fact that increasing V_0 should also decrease m_1, but there is no evidence to support an increase of m_1 with increasing θ_0.

The residual mass data for aluminum is even more sparse than for magnesium and, as we have noted, contains some blunders. About the only example close to what we want is for $T = 0.5$ inches and $m_0 = 240$ grains where we find that $m_1 = 229.8$ grains for $\theta_0 = 45°$ and $V_0 = 2,662$ ft/sec

13

while m_1 = 222.1 grains for θ_o = 60° and V_o = 2,638 ft/sec. Here the slight decrease in V_o should tend to increase m_1, yet in spite of this m_1 decreases slightly as θ_o increases. Of course with experimental errors in the order of 10 to 20 percent for m_1 and at least 10 percent for V_o it is difficult to say anything about m_1 as a function of θ_o from this information.

What are we to make of a negative value for b_4 or a_5 in the cases of magnesium and aluminum? The fitting error was no worse for these materials than for the other eight. An explanation can be found for this anomaly in the arbitrary functional form of the model in which a simple product of variables is strung together and given adjustable exponents fitted to a data set which is unevenly weighted over the measured ranges and which contains large experimental errors and occasional blunders. If a different mathematical form had been chosen to fit the same data set, the result could well be a decrease in residual mass with increasing obliquity. The same result might be obtained if the same mathematical form were fitted to a different (more accurate, more evenly weighted) data set. These observations serve to illustrate the recognized but sometimes ignored fact that purely empirical models add nothing to our fundamental understanding and can give erroneous predictions if they are used for extrapolation.

For example, a fit of Equation (1) to another data set might give a negative value for a_4, implying that V_1 would increase with increasing obliquity, contrary to experience. Or, it might give a value of a_5 greater than unity, implying a decrease in V_1 as V_o increases with the absurd prediction of embedment or ricochet rather than perforation at sufficiently high V_o. This kind of possibility is not idle speculation as is clear from a recently published extension of the Thor procedure to tungsten fragments penetrating steel and aluminum targets[4]. There it was found that a fit of Equation (2) to the data for steel targets gave a value of b_3 greater than unity, implying a decrease in residual mass with increasing striking mass with complete disappearance of m_1 for sufficiently large m_o. Fortunately, the authors point out this particular danger. Hopefully users of their formula will bear this in mind and explicitly mention this behavior if they are bold enough to use this formula for extrapolation. It is interesting to note in this report that b_4 is positive for aluminum as well as for steel in contrast to the negative value found in the Thor case. This tends to confirm the observations made above on the nature of purely empirical formula fits to particular data sets.

Thor Report No. 47 does not make it clear exactly how the residual speed was measured. It merely states that most of the data was provided by BRL but that other sources were also included (no reference given).

---

[4]G. L. Holloway, M. B. Danish and J. A. Matts, "Penetration Relations for Tungsten Alloy Fragments versus Selected Target Materials," ARBRL-TR-02087, 1978. (AD #C015203)

14

Other Thor Reports before and after No. 47 are also of little help. It is very likely that velocity screens were used, although depth of penetration into a catcher material is also a possibility. In making such measurements for oblique impacts it is common practice to cock the target plate at the desired angle but to leave the velocity screens or witness plates normal to the axis of the gun which is used to launch the projectiles. This is done not only because of space limitations or convenience, but also because the deviation of the projectile from its original flight path is not known ahead of time and would require additional experiments and equipment to determine if it could not be calculated. This practice can lead to errors in the reported magnitude of the residual velocity since only one component of this velocity is being measured. In cases where the obliquity is not large or the impact speed is not greatly different from the exit speed, the neglect of an exit velocity component perpendicular to the line of fire is not serious since the deviation is small. However, for large obliquities and marginal perforations this neglect can lead to serious errors. This practice is illustrated in Figure 3 (p 40) of Thor Report No. 47 where the assumption of normal impact on a second target is explicitly mentioned (last line of p. 38).

C. Intermediate Models

Intermediate models are harder to use and require more calculation, but not enough to preclude a description of the main features of practical problems using a reasonable expenditure of time and money. They are based on some type of physical law which is assumed to govern the motion of the projectile through the target and usually they treat the projectile as a point mass and contain other simplifying assumptions as well as adjustable constants. They come under the general heading of particle physics and as such can be called semi-empirical or semi-theoretical. Although they require more effort to use than elementary models, they can be used with some confidence in tentative extrapolations beyond the measured ranges of the variables. The degree of confidence we assign to such extrapolations will depend on the kind of physical laws that are assumed to apply and the extent of the agreement between model predictions and known facts. Ideally such models will predict at least qualitatively correct behavior even for the extreme values permitted for the variables.

A simple example of this type of model is contained in a 1963 paper by Recht and Ipson[5]. Using a result of Jameson and Williams[6] that projectile and target plug residual speeds are practically the same, these authors wrote an energy balance as follows:

---

[5] R. F. Recht and T. W. Ipson, "Ballistic Perforation Dynamics," Transactions of the ASME, p. 384, 1963.

[6] R. L. Jameson and J. S. Williams, "Velocity Losses of Cylindrical Steel Projectiles Perforating Mild Steel Plates," BRL R 1019, 1957. (AD #142447)

$$\frac{1}{2} m_o V_o^2 = \frac{1}{2} (m_o + m_p) V_1^2 + W + E \tag{9}$$

where m_p is the plug mass, W is the work done in shearing out this plug and E is the energy lost in other ways. The authors assume that E can be equated to the energy transfer which might occur in a free collision between m_o and m_p as if the rest of the target were not present. Since momentum conservation in such a free collision is

$$m_o V_o = (m_o + m_p) V_{1f} \tag{10}$$

with the subscript f standing for free collision, we have

$$E = E_f = \frac{1}{2} m_o (V_o^2 - V_{1f}^2) = \frac{1}{2} m_o V_o^2 - \frac{1}{2} m_o \left(\frac{m_o V_o}{m_o + m_p}\right)^2 \tag{11a}$$

or

$$E = \frac{1}{2} m_o V_o^2 \left(\frac{m_p}{m_o + m_p}\right)\left(\frac{2 m_o + m_p}{m_o + m_p}\right) \quad . \tag{11b}$$

We have put Equation (11a) into the equivalent form (11b) in order to point out that the authors implicitly assumed in their paper that the factor $(2 m_o + m_p)/(m_o + m_p)$ can be set equal to unity when they wrote their Equation (2). Of course this requires m_o to be zero to be strictly correct or at least $m_o \ll m_p$ to be approximately true. In case $m_o = m_p$ (a not unreal situation in some cases), this factor is equal to 1.5 (not too far from unity) and it approaches 2 if $m_o \gg m_p$. We will not make this approximation here and will note the consequences.

At the perforation limit, $V_1 = 0$ and $V_o = V_{o\ell}$. In this case a combination of Equation (11a) and Equation (9) gives us

$$W = \frac{1}{2} m_o V_{o\ell}^2 \left(\frac{m_o}{m_o + m_p}\right)^2 \tag{12}$$

which is the authors' Equation (4) except for the second power of the mass ratio instead of the first power given by the authors. This of course does not affect their argument based on high-speed machining studies that W can be taken to be independent of $V_o > V_{o\ell}$ to a good approximation, since the dynamic shear stress is also approximately constant.

16

Now if we put Equations (11a) and (12) in Equation (9) and solve for V_1, we obtain

$$V_1 = \left(\frac{m_o}{m_o + m_p}\right)^{3/2} \left(V_o^2 - V_{o\ell}^2\right)^{1/2} \tag{13}$$

which is the authors' Equation (5) except for the 3/2 power of the mass ratio instead of their first power. This is interesting because Equation (13) above is exactly the authors' Equation (14) which they obtained by postulating an extra factor of

$$\left(\frac{m_o}{m_o + m_p}\right)^{1/2}$$

to account for perforation of thick plates. If $m_p \ll m_o$ in Equation (13), then we have the simple hyperbolic relation mentioned in the previous subsection.

Another tradition exists in this category of models which analyze the particle dynamics of penetration. It consists of assuming a force field in which the projectile moves while it is in the target, solving Newton's second law, and comparing with experiment. Newton himself apparently followed this procedure in his theory of gravitation. A learning exercise used in some physics texts asks the student to assume various forms for a gravitational force field, a simple one being

$C (m_1)^{a_1} (m_2)^{a_2}/(r)^{a_3}$, where the notation is obvious. Then the student is required to fit the adjustable constants C, a_1, a_2 and a_3 to Kepler's data and to give values for these constants as well as their average error, for example, $a_3 = 2 \pm .002$. Explanations for this error in addition to experimental uncertainties are then elicited, for example, perturbations by the other planets, and so forth. This method is so powerful that Newton's contemporaries, Robins and Euler, soon applied it to projectile penetration of dense media[7]. They assumed a constant force field opposing the motion and for constant projectile mass and zero obliquity their equation

$$m_o \, dv/dt = -a \tag{14}$$

is easily solved. A generalization of Equation (14) to include a speed-dependent force field is

---

[7] W. Johnson, *Impact Strength of Materials*, N.Y.: Crane, Russak, 1972, cc. 9-10.

17

$$m_o \, dv/dt = - (a + b\,v + c\,v^2) \tag{15}$$

where a, b and c are constants. This equation with b = 0 is usually attributed to Poncelet (c.1830), while the same equation with a = 0 is generally associated with Resal (c. 1895). Of course Equation (15) is also easily solved[8].

Robertson's 1943 report[9] is an example of a paper which solves Equation (15) with b = 0. This author factors the constant a into Aa' where A is the "area of impression" of the projectile and a' is called a "shatter coefficient". He also allows A to be a function of the depth of penetration, but he proposes no explicit form for A except in the case of a cylinder when A is taken to be a constant πR^2 for a non-deforming cylinder of radius R. He also lets C = A(1/2 γ ρ_t) where ρ_t is the density of the target material and γ is a dimensionless constant which he calls the "inertial coefficient". He then uses the relation dv/dt = v dv/d$_z$ where z is the depth of penetration to integrate Equation (15) once using limits V_o and V_1 for v and 0 and T for z, obtaining

$$V_1 = e^{-cT/m_o} (V_o{}^2 - V_{o\ell}{}^2)^{1/2} \tag{16}$$

where $V_{o\ell}{}^2 = (a/c)(e^{2\,cT/m_o} - 1)$. Here 2 cT = γ ρ_t A T = γ m_p where m_p is the plug mass and 1/2 ρ_t (a/c) = (a'/γ). The ratio (a/c) has the dimensions of a velocity squared while (a'/γ) has the dimensions of a stress. Here the same type of hyperbolic form as above has been obtained directly from Newton's law with an analytical rather than an empirical form for the limit speed. Of course this form contains the adjustable constants a' and γ.

Lambert and coworkers[10] suggest a generalization of Equations (13) and (16) to include obliquity and rod length, namely,

[8]W. Gröbner and N. Hofreiter, "Integraltafel. Erster Teil. Unbestimmte Integrale".

[9]H. P. Robertson, "The Mechanics of Armor Perforation," NDRC, Armor and Ordnance Report No. A-227 (OSRD No. 2043), 1943.

[10]J. P. Lambert and G. H. Jonas, "Towards Standardization in Terminal Ballistics Testing: Velocity Representation," BRL Report 1852, 1976; J. P. Lambert and B. E. Ringers, "Standardization of Terminal Ballistics Testing, Data Storage and Retrieval," ARBRL-TR-02066, 1978; and J. P. Lambert, "The Terminal Ballistics of Certain 65 Gram Long Rod Penetrators Impacting Steel Armor Plates," ARBRL-TR-02072, 1978.

$$V_1 = \left(\frac{m_o}{m_o + (m')/3}\right)\left(V_o{}^p - V_{o\ell}{}^p\right)^{1/p}. \tag{17}$$

The constant p is 2 plus an empirical factor which depends on rod diameter, obliquity and target thickness. $V_{o\ell}$ is an empirical factor related to these quantities as well as to the rod mass and length. The mass m' bears a strong resemblance to the plug mass, m_p. If the exponential factor in Equation (16) is expanded in powers of (m_p/m_o), neglecting powers higher than the first, it becomes $1 - (\gamma/2)(m_p/m_o)$. If the mass ratio in Equation (17) is similarly expanded we have $1 - 1/3 \ (m'/m_o)$ where $m' = \rho_t \ (\pi R^2) \ T \ (\sec \theta_o)^{3/4}$ with R the rod radius. If $\sec \theta_o$ had been chosen to the first power we would have a line-of-sight thickness and m' roughly equal to m_p. A choice of $\gamma = 2/3$ would complete the first order equivalence of m' and m_p. A similar expansion of the mass ratio in Equation (13) gives $1 - 3/2 \ (m_p/m_o)$.

Zook[2] has continued this tradition by applying the solution of Equation (15) to that portion of the Thor data which was obtained for zero obliquity. This was a wise restriction because, as we shall see below in the body of the present paper, Equation (15) is only applicable to the case of zero obliquity. Like Robertson, Zook factors the constant a in Equation (15) and writes $a = C_1 \ A \ H_t$ where A is the cross-sectional area of the projectile and H_t is the Brinell hardness of the target material. Similarly, he writes $c = C_3 \ A \ \rho_t$ so that his C_3 is half of Robertson's "inertial coefficient", γ. Unlike Robertson he retains the constant b and proposes the form $b = C_2 \ A \ \sqrt{H_t \ \rho_t}$. However, he made no attempt to justify this geometric mean type of form, nor to justify the use of a hardness coefficient of any type much less the Brinell hardness which is, of course, only one of the many such parameters which appear in the literature. Consequently, a, b and c remain adjustable or empirical constants in an analytical theory.

Backman and Finnegan[11] modified Equation (15) to be

$$m_o \ dv/dt = - A \ (a_1 + c_1 \cos^2 \psi \ v^2) \tag{18}$$

where ψ is the angle between the projectile's current line-of-flight (tangent to the trajectory) and the current normal to the spherical surface which is in contact with the deforming target. In order to

---

[11]M. E. Backman and Finnegan, "Dynamics of the Oblique Impact and Ricochet of Non Deforming Spheres Against Thin Plates," NWC TP 5844, 1976.

19

determine the projectile motion for oblique impacts they also postulate the following rule. The force opposing the motion is directed through the center of the sphere and lies antiparallel to the current contact surface normal mentioned above. Given this postulate, one can then resolve this force into a resistive component antiparallel to the current line of flight and a lift component perpendicular to this line. Torques tending to rotate the sphere are neglected and the change in speed, Δv, is calculated for time step, Δt, from the resistive force component, while the change in direction is calculated from the lift component. Next, the change of position during the following time interval is calculated using the values of the speed and curvature. Finally, a critical penetration depth, P^*, for plate failure is assumed, beyond which depth part of the resistive force component is assumed to vanish over a portion of the contact surface specified by an assumed angle α^*. Thus, the model contains four adjustable constants, a_1, c_1, P^* and α^* which are determined from data obtained at zero obliquity. The constants a_1 and c_1 were found by a best fit to Equation (13) above using the Recht-Ipson power of unity. The constants P^* and α^* were chosen to match observation of crater formation at zero obliquity. Additional postulates about a kind of virtual origin for the sphere at the beginning of its motion also enabled the authors to calculate crater shapes for ricochet and embedment from the projection of one side of the tube which is swept out by the sphere along its trajectory. Since A is a point at the moment of impact with zero force pointing along the normal to the target face, an initial depth of penetration must be assumed in order to begin the calculation. In addition, the outcome will depend somewhat on the size of the time steps which are chosen and very definitely on the spherical cap which is taken to be the contact surface at any instant.

An advantage of this model is its ability to predict exit angles as well as exit speeds for oblique impacts. In addition to perforation phenomena, ricochet and embedment phenomena are also treated, something which is rarely if ever done by other models in this category. An unsatisfactory feature of this model is the somewhat arbitrary nature of the rules which have been selected for calculating force components and crater shapes. Still, it appears to be the most advanced example of its kind in the particle mechanics tradition of penetrator models. In using a numerical time and space step method for calculating the projectile trajectory, this model resembles some of the computer code techniques usually reserved for solving the field equations which are referred to in the next subsection.

D. Advanced Models

Even Newton's law of gravitation has been superceded by tensor field equations which predict the existence of gravitational waves and are currently being used in "black hole" theories designed to explain certain astrophysical observations[12]. Similarly, a large number of investigators

[12] L. L. Smarr and W. H. Press, "Our Elastic Spacetime: Black Holes and Gravitational Waves," American Scientist 66(1) Jan-Feb 1978, p. 72.

have abandoned particle physics descriptions and turned to solutions of the field equations of continuum mechanics in an effort to model the penetration process. A summary of such efforts can be found in a paper by Jonas and Zukas[13] who also review a number of particle models. We will content ourselves here with a few quotations from their paper:

"Computer codes are invaluable for obtaining a qualitative picture of penetrator and target deformation. They provide details not normally obtainable from ballistic experiments. Yet, it is not unfair to state that, on the whole, they have not improved our understanding of penetration phenomenology, except possibly in the hypervelocity regime."

With few exceptions

"....the present state-of-the-art in computations is best summarized by a paraphrase of Richard's Law, to wit: 'One good guess is worth a thousand computer runs'."

"Aside from the above considerations, codes in their present form cannot be relied upon for quantitative data (except by accident) in the ordnance velocity regime."

"It is necessary to add here that despite these limitations, code results for deformation fields often bear reasonable resemblance to those found experimentally."

"Refinements in theory will be to little avail however until characterization of materials at the strain rates appropriate to ballistic impact conditions (up to 10^5 s^{-1}) is achieved, for errors in input will outweigh any gains in modeling."

"The last and most difficult hurdle to overcome will be determination of reliable and computationally suitable models for the onset of fracture and the characterization of failed material."

"The use of such codes is neither straightforward nor inexpensive. A typical code will output about 10^7 words of information and cost upwards of $1000 per run. Of necessity much of the output is presented in plot form. Considerable experience is required to run the codes and frequently manual intervention is called for. In no way can present codes be treated as 'black boxes'."

---

[13]G. H. Jonas and J. A. Zukas, "Armor Penetration: Theory and Experiment," USA BRL, invited paper at the 14th Annual Meeting of the Society of Engineering Science, Lehigh University, PA, 1977. Also published as "Mechanics of Penetration: Analysis and Experiment," Int. J. Eng. Sci. 16, 879, 1978.

Although Newton's gravitational law has been superceded for some purposes it is still extremely useful for most terrestial and solar system phenomena. Similarly, while continuum models may be useful for some purposes and may eventually become routine, our present requirements for further fundamental understanding as well as our needs for relatively simple, inexpensive methods of making quantitative predictions for at least the main features of practical problems prompt us to investigate further the possibility of constructing a better particle model. The purpose of the present paper is to construct such a model so we can describe the penetration process in a simple yet rational manner. This should have the double effect of increasing our understanding and providing a useful tool for making predictions.

II. LIMITATIONS OF A SPEED-DEPENDENT FORCE FIELD

Even the most general force field usually considered (Equation (15) above) is severely limited. We can note this by writing it in vector form as follows:

$$\vec{F} = - (a + b v + c v^2) \hat{v} = - (\frac{a}{v} + b + c v) \vec{v} \tag{19}$$

where $\hat{v} = \vec{v}/v$ is a unit vector in the current direction of the velocity $\vec{v}$ which has magnitude v. If $\vec{r}$ is a position vector from the coordinate origin to the center of mass of the projectile, then in Cartesian coordinates $\vec{r} = x \hat{i} + y \hat{j} + z \hat{k}$ where $\hat{i}$, $\hat{j}$ and $\hat{k}$ are constant unit vectors and of course $\vec{v} = \dot{\vec{r}} = \dot{x} \hat{i} + \dot{y} \hat{j} + \dot{z} \hat{k}$ with $v = (\dot{x}^2 + \dot{y}^2 + \dot{z}^2)^{1/2}$. Here the Newtonian dot convention for time derivative is being used. In most discussions of this force field in the past, the fact that $\vec{F}$ is being taken antiparallel to $\vec{v}$ is mentioned at least implicitly by the statement that only zero (or normal) obliquity is being considered. Attempts are then sometimes made to "patch up" the result in order to make application to impacts at non-zero obliquity. These attempts are, of course, in vain since a direct consequence of $\vec{F}$ being anti parallel to $\vec{v}$ at the beginning of the motion is that the motion is necessarily rectilinear. This is immediately obvious because, if there is no force component perpendicular to $\vec{v} = \vec{v}_0$ at time zero, there never will be such a force component and the projectile must continue to move along its original straight-line path. In short, curvilinear motion is impossible in such a force field. Since curvilinear motion, including extreme cases such as ricochet, is observed experimentally, then a different force field must be used if we hope to describe the projectile motion.

This observation about rectilinear motion can also be demonstrated by solving Newton's second law for a constant mass particle with Equation (19) as the force. We may write

$$[m_o \frac{d}{dt} + (\frac{a}{v} + b + c v)] \vec{v} = 0 \tag{20}$$

where for convenience we have factored the equation into an operator (in brackets) and an operand, $\vec{v}$. If we take the scalar or dot product of this equation with $\hat{v}$, using $\vec{v} \cdot \hat{v} = v$, we obtain the usual separable scalar equation

$$m_o \frac{dv}{dt} + (a + b v + c v^2) = 0 . \tag{21}$$

As noted above in the introduction, the solution can be looked up in standard integral tables. If our interest is in obtaining $v = v(s)$ where s is the displacement or distance traveled along the trajectory, we can use the relation $dv/dt = v \, dv/ds$, since $v = ds/dt$. As we have seen, Robertson has done this for the special case $b = 0$, while Zook has done it for the general case. Our interest here is in obtaining $v = v(t)$ instead. If we define the discriminant

$$q = 4 ac - b^2 \tag{22}$$

then for $q < 0$,

$$v = \frac{1}{2c} (h^+ - A h^- e^{-Bt})/(1 - A e^{-Bt}) \tag{23}$$

where $h^{\pm} = -b \pm \sqrt{-q}$, $A = (2 c v_0 - h^+)/(2 c v_0 - h^-)$ and $B = \sqrt{-q}/m_0$, using the initial conditions $v = v_0$, $s = 0$ at $t = 0$, with

$$s = (\frac{m_0}{c}) \ln (\frac{1 - A e^{-Bt}}{1 - A}) + (\frac{h^+}{2c}) t . \tag{24}$$

Alternative solutions for this case which involve hyperbolic tangents will not be considered here because of the physical requirement that v decrease with increasing time.

For $q = 0$, $a + b v + cv^2 = c (V + v)^2$ where $V = \sqrt{\frac{a}{c}} = \frac{b}{2c}$, so

$$v = [(V + v_0)^{-1} + (\frac{c}{m_0}) t]^{-1} - V \tag{25}$$

and

$$s = (\frac{m_0}{c}) \ln [1 + (\frac{c}{m_0})(V + v_0) t] - Vt. \tag{26}$$

For $q > 0$,

$$v = [\sqrt{q} \tan (C - Dt) - b]/(2c) \tag{27}$$

$$s = [2 m_0 \ln \{\cos (C - Dt)/\cos (C)\} - b t]/(2c) \tag{28}$$

where $C = \arctan [(2c v_0 + b)/\sqrt{q}]$ and $D = \sqrt{q}/(2 m_0)$. Our main interest here is to note from Equations (23), (25) and (27) that $v = v(t)$ can be

24

found explicitly.

If we write Equation (20) in Cartesian component form we have, for example,

$$[m_o \frac{d}{dt} + (\frac{a}{v} + b + c\,v)]\,\dot{x} = 0 \tag{29}$$

with similar equations for the other two components, that is, with the same operator multiplying $\dot{y}$ or $\dot{z}$. Each of these equations is separable and we obtain, using Equation (15) or (21),

$$\frac{d\dot{x}}{\dot{x}} = \frac{d\dot{y}}{\dot{y}} = \frac{d\dot{z}}{\dot{z}} = -\frac{1}{m_o}(\frac{a}{v} + b + c\,v)\,dt = \frac{dv}{v} \quad . \tag{30}$$

By integrating once, we have

$$\frac{\dot{x}}{v_{ox}} = \frac{\dot{y}}{v_{oy}} = \frac{\dot{z}}{v_{oz}} = \exp[\frac{1}{m_o} f(t)] = \frac{v}{v_o} \tag{31}$$

where $f(t) = -\int_0^t (\frac{a}{v} + b + c\,v)\,dt$. This completes our demonstration, since Equation (31) says that the velocity components $\dot{x}$, $\dot{y}$ and $\dot{z}$ at any time t are always in the ratio that they were initially when the components were v_{ox}, v_{oy} and v_{oz}. In other words, the motion is rectilinear and the projectile will continue along the line of $\vec{v}_o$. This implies that $s = r$, the position vector, so that only one Cartesian axis is needed to describe the motion. A simple coordinate rotation will make any one component serve as well as another.

Since v is known explicitly as a function of time we can also find $f(t)$ explicitly as a function of time. This can be done with integral tables or more simply by using Equations (23), (25) or (27) in Equation (31). If we integrate Equation (31), using initial conditions $z = y = z = s = r = 0$ at $t = 0$, we have

$$\frac{x}{v_{ox}} = \frac{y}{v_{oy}} = \frac{z}{v_{oz}} = \frac{s}{v_o} = \frac{r}{v_o} \tag{32}$$

where s is given by Equations (24), (26) or (28).

25

While it is certainly possible to obtain explicit solutions for $v(t)$ and $s(t)$ when we use the force field of Equation (15), we have no real interest in doing so because we know that this field cannot describe the curved trajectories of real projectiles, except in the limiting cases of very thin target plates or very high velocity projectiles when the motion is in fact approximately rectilinear.

Before proceeding it is interesting to note that Equations (27) and (28) reduce to Robertson's case described in the previous section for $b = 0$, $q = 4\,ac > 0$ ($a > 0$, $c > 0$). In particular they become

$$v = \sqrt{\frac{a}{c}}\ \tan\left\{\tan^{-1}\left(v_0\sqrt{\frac{c}{a}}\right) - \sqrt{ac}\ t/m_0\right\} \tag{33}$$

and

$$s = (m_0/c)\ \ell n\left[\cos\left\{\tan^{-1}\left(v_0\sqrt{\frac{c}{a}}\right) - \sqrt{ac}\ t/m_0\right\}\Big/\cos\left\{\tan^{-1}\left(v_0\sqrt{\frac{c}{a}}\right)\right\}\right]. \tag{34}$$

At the perforation limit $v_0 = v_{o\ell}$, we require $v = 0$ when $s = T$, the target thickness. From Equation (33) we find that this occurs at $t_\ell = (m_0/\sqrt{ac})\ \tan^{-1}(v_{o\ell}\sqrt{c/a})$. If we use this value of t in Equation (34) and let $s = T$, we find

$$v_{o\ell} = \sqrt{a/c}\ \tan\left\{\cos^{-1}\left(e^{-cT/m_0}\right)\right\} \tag{35}$$

which vanishes as $T \to 0$ or $m_0 \to \infty$ and increases without limit as $T \to \infty$ or $m_0 \to 0$. Since

$$\tan^2\left\{\cos^{-1}\left(e^{-cT/m_0}\right)\right\} = \frac{1}{\cos^2\left\{\cos^{-1}\left(e^{-cT/m_0}\right)\right\}} - 1 = e^{2cT/m_0} - 1, \tag{36}$$

then Equation (35) is obviously the same as Robertson's $v_{o\ell}$, given above after Equation (16). When perforation occurs for $v_0 > v_{o\ell}$, then $t = t_1$, $v = v_1$ and $s = T$. From Equation (34) we can find t_1 or the argument of the cosine involving t_1 and use this in Equation (33) to obtain

26

$$v_1{}^2 = \frac{a}{c}\tan^2\left\{\cos^{-1}\left[e^{cT/m_0}\cos\left\{\tan^{-1}\left(v_0\sqrt{\frac{c}{a}}\right)\right\}\right]\right\}$$

$$= \frac{a}{c}\left[e^{-2cT/m_0}\sec^2\left\{\tan^{-1}\left(v_0\sqrt{\frac{c}{a}}\right)\right\} - 1\right]$$

$$= \frac{a}{c}\left[e^{-2cT/m_0}\left(1 + v_0{}^2\frac{c}{a}\right) - 1\right]$$

$$= e^{-2cT/mo}\left[v_0{}^2 - \frac{a}{c}\left(e^{-2cT/m_0} - 1\right)\right]$$

$$= e^{-2cT/m_0}\left[v_0{}^2 - v_{0\ell}{}^2\right] \tag{37}$$

which is Robertson's result in Equation (16) above. In Equation (37) we have used Equation (36) and the identity $\sec^2 x = 1 + \tan^2 x$.

Even for rectilinear motion during zero obliquity impacts the force $F = [-(a + b\,v + c\,v^2)]$ might not describe all the observed phenomena in a natural way. If $a > 0$, then there is still a force $F = -a$ acting to reverse the motion when v vanishes in a thick enough target. Thus ricochet can be described since the rebound conditions, $\dot{v} < 0$, $v = 0$, $0 < s < T$ for $t < \infty$, and the ricochet conditions, $v < 0$, $s = 0$, $t < \infty$ can be met. However, embedment cannot be described since embedment requires $F \to 0$ as $v \to 0$, $0 < s < T$ as $t \to \infty$ and by assumption $F \to -a$ as $v \to 0$. If $a = 0$ because $a = a(v_0)$ vanishes, then embedment can be described. However, embedment will occur only for a particular v_0 or v_0's (depending on the functional form of $a(v_0)$) instead of over a continuous range of v_0 as observed. We could define $a(v_0)$ to be zero over a continuous range of v_0, but this seems somewhat artificial. If $a = -a' < 0$, then $F = a' - b\,v - c\,v^2$ and again embedment cannot be described. Neither can ricochet be described since F turns positive in finite time as $v \to 0$ and the mass accelerates before reaching a turning point ($v = 0$) an unphysical behavior which is not observed. A perforation/embedment limit requires $F \to 0$, $v \to 0$, $s \to T$ as $t \to \infty$ and can be described only if $a = 0$, so that $s_{max} = \frac{m_0}{c}\ln\left(1 + \frac{c}{b}v_{0\ell}\right)$ or $v_{0\ell} = \frac{b}{c}(e^{cT/m_0} - 1)$. Robertson's

27

case (b = 0) then implies $v_{o\ell}$ = 0 which agrees with Equation (35) for a = 0. Since finite values for $v_{o\ell}$ are observed, then Robertson's case should not be used. A ricochet/embedment limit requires F → 0, v → 0, s → 0 as t → ∞ and cannot be described since the requirement a > 0 prevents F → 0. If we define $a(v_o)$ to be zero for all $v_o \leqslant v_{o\ell}$, then we eliminate all possibility of ricochet and have only two regions, embedment for $0 \leqslant v_o \leqslant v_{o\ell}$ and perforation for $v_o > v_{o\ell}$. Ricochet or rebound after penetration for low speed, zero obliquity impact has not been well explored experimentally, but seems possible.

In summary the force F = $[-(a + b v + c v^2)]$ can describe only rectilinear motion and so is limited to zero obliquity impacts. Although perforation can always be described for thin enough targets, and ricochet can be described if a > 0, embedment over a continuous range of v_o can only be described by defining $a(v_o)$ to be zero over this range.

III.   FORCES DEPENDENT ON DEPTH OF PENETRATION AS WELL AS SPEED

As we have seen, the constant a in Equation (15) has been modified
to be proportional to some type of projectile area multiplied by a
"shatter" or "hardness" coefficient. The area dependence is reasonable.
In addition there is a more physical interpretation for the constant
coefficient of proportionality. Johnson[7] points out the usefulness of
dividing impact regimes according to the ratio $(\rho \, v^2/\bar{\sigma})$ which is approx-
imately equal to twice the crater volume for simple cases. Here $\bar{\sigma}$ is
the mean flow stress and ρ the density. This suggests adopting the
form

$$a = a_2 \, \bar{\sigma} \, \bar{A} \tag{38}$$

so that Recht and Ipson's $W = \int_0^T a_2 \, \bar{\sigma} \, \bar{A} \, ds = a_2 \, \bar{\sigma} \, \bar{A} \, T$, which is constant

if $\bar{\sigma}$ and $\bar{A}$ are constant. They argue from machining studies that $\bar{\sigma}$ is a

constant, while $\bar{A}$ is a constant at least for a non-deforming blunt
cylinder hitting end-on at zero obliquity. For most metals, except soft
ones like tin and lead, their plastic shear strength is not very depen-
dent on shearing speed[14], so $\bar{\sigma}$ constant is a good approximation.

However, for many projectiles A depends somewhat on depth of pene-
tration, although a constant average presented area like that in Equa-
tion (38) may be quite adequate to represent the shearing force. For a
sphere with radius R, the cross-sectional area at the original target

plate impact plane is $\pi[R^2 - (R - s)^2] = \pi[2 \, R \, s - s^2]$ where s is the

depth of penetration. This becomes a constant $\pi \, R^2$ for $s \geqslant R$ which
applies for the rest of its motion through a thick target. For a thin
target it may be more appropriate to use an average value proportional

to $\pi \, R^2$ for $\bar{A}$ in Equation (38). For a cylinder with a conical nose the

cross-sectional area at the impact plane is $\pi \, \tan^2 \phi \, s^2$ where ϕ is the
constant half-angle of the cone vertex. This becomes the constant $\pi \, R^2$
when the cylindrical portion of the projectile (of radius R) enters the
target.

In addition to shearing forces there are also frictional forces
which depend on the contact area between projectile and target and which
may be given the simple form

$$F_f = \mu_f \, P \, A_c \tag{39}$$

---

[14]P. W. Bridgman, _Studies in Large Plastic Flow and Fracture_, N.Y.,
McGraw Hill, 1952, p. 284.

where μ_f is a constant coefficient of sliding friction and P is the pressure. In order to write this simple form we must assume that the stress is isotropic as for a fluid, an approximation which should improve with higher speeds. If we retain all components of the general stress tensor we will obtain a much more complicated form which is probably not necessary for our purpose. Here we will take P to have a constant average value during the motion. However, we will take into account the variation of A_c with depth of penetration s. For a sphere the area of the contact surface is $2 \pi R s$, which becomes $2 \pi R^2$ for $s \geqslant R$. For a conical nose at zero obliquity the contact area is $\pi R (R^2 + s^2)^{1/2}$ where R is the radius of the cone base as well as the radius of the cylindrical body. When the body of this projectile enters the target the nose contact area becomes the constant $\pi R (R^2 + h^2)^{1/2}$ where h is the cone height and an additional cylindrical area $2 \pi R s$ of the body comes into contact with the target. In general A might be reasonably represented by the form $A_o = \overline{A}_1 + C_1 s + C_2 s^2$ with $\overline{A}_1$, C_1 and C_2 constant and usually with $C_2 < C_1$.

For oblique impact and for irregular projectile shapes like those coming from naturally fragmenting warheads or armor spall and debris, the areas important for shear and friction forces will be more complicated, although a quadratic form in s is probably still adequate for an average contact area. Projectile deformation will increase the contact area as s increases. Tumbling and yawed impact present additional problems while projectile erosion further complicates matters. Erosion will be considered in a later section of this report.

For constant mass projectiles we will adopt a force field which depends on depth of penetration in a simple way namely $- (a_o + d_1 s + d_2 s^2)$, where a_o, d_1 and d_2 are constants. This form is suggested by the shear stress, friction and deformation considerations given above. It seems to be a reasonable way to represent the "plug shear", "penetration" and "deformation" processes described by Recht and Ipson in their 1974 paper[15]. The "bulging or dishing" response of a thin target plate also depends on how far the projectile tip has progressed beyond the original impact plane. An initial elastic response dependent on the first power of s is expected, followed rapidly by an inelastic response dependent on higher powers of s, much as in the form we have chosen. However, the "breeching or petaling" mode of plate failure described by these authors is not expected to depend on depth of penetration. Instead it seems to be dependent on speed and will be included in the speed-dependent part of our force field. It is of more importance for thin plates and high

[15]R. F. Recht and T. W. Ipson, "Ballistic Penetration Resistance and Its Measurement," Proceedings of the First International Symposium on Ballistics, Orlando, Florida, 1974.

obliquities since the plugging mode of failure is more common near zero obliquity. For example, thin aluminum plates fail by petaling when $\theta_o > 30°$ while thin steel plate failure has been described as "hinging"[11].

When a body moves through a fluid its motion is opposed by a viscous or internal friction force which is proportional to the first power of the speed. This is in addition to the sliding friction force mentioned above which depends only on the contact area and pressure. For a sphere of radius R Stokes' force is $6\pi R\mu v$, where μ is the coefficient of viscosity. Thus the constant b in Equation (15) can be given a simple physical interpretation. The viscosity of solids is a well-known physical concept[16] and for common metals it has been measured at high speeds[17].

For a body moving through a fluid another force proportional to the square of the speed called the drag force is also considered. Since we expect metal-metal projectile-target penetration to be a non-linear process we should also consider a force dependent on v^2 as well as v. This could include such non-linear processes as conversion of kinetic energy into heat energy (or even radiant electromagnetic and mechanical energy). For example, Johnson[7] estimates the temperature rise in a penetration to be $v^2/(2 C_p J)$ where J is Joule's mechanical equivalent of heat. Using $C_p = 0.1$ cal/(gm-deg) for the specific heat of steel or aluminum, we calculate a temperature rise of about 100°C when v is 0.3 km/sec. In addition, a v^2 term could represent the energy transferred to pieces which are separated from the target such as the plug sheared out at low obliquity, the petaling or hinging mentioned above and the energy used in accelerating ejecta from the impact side of a target plate as well as assorted bits of spall and other debris emerging from the rear. This is the usual inertial reaction interpretation.

Our complete force field is then of the form

$$F = - [a_o + b_1 v + b_2 v^2 + d_1 s + d_2 s^2]. \tag{40}$$

Admittedly this is an oversimplification which contains for example no cross product terms in s and v and no explicit functions of pressure, temperature, time or other factors which might be included. However, we have given simple physical interpretations for the coefficients

[16]E. A. Evans, "Viscosity of Solids," in *American Institute of Physics Handbook*, N.Y., McGraw-Hill, 1957, c. 2h.

[17]S. K. Godunov, A. A. Deribas and V. I. Mali, "Influence of Material Viscosity on the Jet Formation Process During Collisions of Metal Plates," *Fiz. Goreniya i Vzryva* <u>11</u> (1) 3, 1975, and V. I. Mali, V. V. Pai and A. I. Skovpin, "Investigation of the Breakdown of Flat Jets," *Ibid.*, 10 (15), 775, 1974.

a_0, b_1, b_2, d_1 and d_2 which should eventually enable us to estimate their values from experimental data obtained in studies other than penetration studies. If we can use such values and successfully predict the outcome of penetration experiments, then we have gained some fundamental insight into the penetration process, since these coefficients will no longer be purely empirical constants. If we cannot do this, we will have to be content with calling them empirical constants. Still, if we can adjust them to known data and successfully predict the unknown, we will in any case have a relatively simple method for solving practical problems without a large expenditure of time and money.

A more general form than Equation (40) which includes higher powers of s and v as well as cross product terms was attributed to Thompson[18] by Murff and Coyle[19], although in practice they used Equation (40) with $b_2 = d_2 = 0$ and found it adequate to describe embedment in semi-infinite soil targets. Their suggestion of an infinite series of terms ($s^n v^m$) did not include suggestions for physically interpreting these terms and so would reduce the coefficients of these terms to empirical constants.

---

[18]L. G. Thompson, et al., "The Effect of Soil Parameters on Earth Penetration of Projectiles," Technical Report to Sandia Laboratories, Texas A&M Research Foundation, July 1969.

[19]J. D. Murff and H. M. Coyle, "Prediction Method for Projectile Penetration," J. Soil Mech. Foundations Division, Proc. ASCE 99, 1033, 1973.

IV. SPECIAL AND GENERAL SOLUTIONS DESCRIBING THE MOTION

As we have seen in Section II, Equation (15) as it stands permits only rectilinear motion. However, we can write it in a component form which will permit curvilinear motion, provided we require the coefficients in our force field to be anisotropic. This is a reasonable thing to do in any case even for a semi-infinite target since the forces parallel and perpendicular to the impact surface at the point of impact must be different. Thus, even for small obliquities the trajectory will be curved. This is because the impact surface is an interface between materials of different properties, commonly metal and air in cases of Army interest. If the impact surface is planar and effectively of infinite extent but the target thickness T is finite, this will have a strong anisotropic influence too. The message that a projectile has struck the front face of a target plate is rapidly transmitted by shock wave to the rear surface where transmission and reflection occur. Because of this the resistance offered by the plate perpendicular to the surface plane is different from that parallel to this plane. In the special case where $d_1 = d_2 = 0$ in Equation (40), Newton's law becomes

$$m_o \ddot{x} + a_{ox} + b_{1x} \dot{x} + b_{2x} (\dot{x})^2 = 0 \qquad (41)$$

and

$$m_o \ddot{z} + a_{oz} + b_{1z} \dot{z} + b_{2z} (\dot{z})^2 = 0 \qquad (42)$$

where the y-component is ignorable because of the symmetry of an oblique impact on a plate of thickness z = T. If we allowed $a_{ox} = a_{oz}$, $b_{1x} = b_{1z}$ and $b_{2x} = b_{2z}$ we would be right back to Equation (15) with its rectilinear motion and other limitations. Now, however, we can find explicit solutions for x(t) and z(t) which have the *same* form as Equations (24), (26) and (28) but which are not in the same ratio for all time since $a_{ox} \neq a_{oz}$, $b_{1x} \neq b_{1z}$ and $b_{2x} \neq b_{2z}$. Thus curvilinear motion can be described. However, both ricochet and embedment cannot be described without artificial definitions for a_{oz}. We can describe either perforation and ricochet or perforation and embedment but not perforation, ricochet and embedment, all three as a continuous function of v_o for given obliquity.

Now consider the special case in which $b_2 = d_2 = 0$ in Equation (40), leading to

$$m_o \ddot{x} + a_{ox} + b_{1x} \dot{x} + d_{1x} x = 0 \qquad (43)$$

and

$$m_o \ddot{z} + a_{oz} + b_{1z} \dot{z} + d_{1z} z = 0 \qquad (44)$$

33

for a plate target. Not only is curvilinear motion possible because of the anisotropy of the force field coefficients, but ricochet, embedment and perforation can all be described as a single function of v_o. The solutions for each Equation (43) and (44) are well known since we recognize this differential equation form as that of the damped harmonic oscillator with constant imposed force a_{os}. This force we have already interpreted as that needed to remove enough material from the target to make way for the passage of the projectile. If s now represents either x or z (or y also in the general case), we can write the solution for each component as the superposition

$$s = A_{1s} e^{\gamma_s^+ t} + B_{1s} e^{\gamma_s^- t} + \delta_s \qquad (45)$$

where $\delta_s = -a_{os}/d_{1s}$, $\gamma_s^{\pm} = -\alpha_s \pm \beta_s$, $\alpha_s = b_{1s}/(2 m_o)$ and $\beta_s = (\alpha_s^2 - d_{1s}/m_o)^{1/2}$. If we take the time derivatives of the component displacements and impose the initial conditions $x = z = 0$, $\dot{x} = v_{ox}$ and $\dot{z} = v_{oz}$ at $t = 0$, we have

$$s = \frac{1}{2\beta_s} \left[\left(v_{os} + \delta_s \gamma_s^- \right) e^{\gamma_s^+ t} - \left(v_{os} + \delta_s \gamma_s^+ \right) e^{\gamma_s^- t} \right] + \delta_s \qquad (46)$$

and

$$\dot{s} = \frac{1}{2\beta_s} \left[\left(v_{os} + \delta_s \gamma_s^- \right) \left(\gamma_s^+ \right) e^{\gamma_s^+ t} - \left(v_{os} + \delta_s \gamma_s^+ \right) \left(\gamma_s^- \right) e^{\gamma_s^- t} \right] \qquad (47)$$

for each component. The usual cases for real, zero and imaginary β_s will be studied in the next section. For the moment we will merely point out that ricochet, embedment and perforation can all be described as a single function of v_o.

As we have seen, part of the constant a_{os} consists of the term $a_{2s} \bar{\sigma} \bar{A}_s$ which should depend on the target thickness since a thicker target requires a greater force to shear out more material. However, this increase does not continue indefinitely and for semi-infinite targets the influence of the rear surface interface is never felt so the force is T-independent. Such behavior can be represented by using components of the line-of-sight thickness $L = T/\cos \theta_o$, namely,

34

$L_x = L \sin \theta_o = T \tan \theta_o$ and $L_z = \cos \theta_o = T$ in a form like $a_{2s} \, \bar{\sigma} \, \bar{A}_s =$

$f(L_s) = (a_{1s}/a_{3s}) (1 - e^{-a_{3s} L_s})$, $(s = x, z)$. Thus for thin targets $f(L_s) \approx a_{1s} L_s$ while for semi-infinite targets $(L_s \to \infty)$, $f(L_s) \to (a_{1s}/a_{3s})$. Another part of a_{os} is the friction force which can be taken as a constant (on the average) proportional to the impact speed with the form $\mu_{fs} \, P \, A_{cs} \, v_{os} = c_{1s} \, v_{os}$. Thus we can write $a_{os} = f(L_s) + c_{1s} \, v_{os} \approx a_{1s} L_s + c_{1s} v_{os}$ for thin targets. For any target we can write the z-component of the force as

$$F_z = - [f(L_z) + c_{1z} \, v_{oz} + b_{1z} \, \dot{z} + d_{1z} \, z] \tag{48}$$

which is not zero at $t = 0$. In addition, the influence of target thickness $L_z = T$ has been included in the force governing the motion. This form also enables us to require the force to vanish as $t \to \infty$ for any case of embedment, including the two limiting cases, the ricochet/embedment limit and the perforation/embedment limit. At the ricochet limit (when $v_o = v_{oRL}$) $\dot{z} = z = 0$ as $t \to \infty$ and Equation (48) becomes

$$0 = - [f(T) + c_{1z} \, v_{ozRL}] \tag{49}$$

while at the perforation limit (when $v_o = v_{oPL}$) $\dot{z} = 0$, $z = T$, and

$$0 = - [f(T) + c_{1z} \, v_{ozPL} + d_{1z} \, T] . \tag{50}$$

These equations may be solved simultaneously to obtain $f(T) = d_{1z} T v_{ozRL} / (v_{ozPL} - v_{ozRL})$ and $c_{1z} = - d_{1z} T/(v_{ozPL} - v_{ozRL})$ so that $f(T)$ and c_{1z} both depend on d_{1z}. The constant term in Equation (45) then becomes

$$\delta_z = - a_{oz}/d_{1z} = - [f(T) + c_{1z} \, v_{oz}]/d_{1z}$$
$$= T (v_{oz} - v_{ozRL})/(v_{ozPL} - v_{ozRL}) \tag{51}$$

which is negative for $v_{oz} < v_{ozRL}$. Since the physical requirement of finite s and $\dot{s}$ requires

$$\gamma_s^- < \gamma_s^+ < 0 \tag{52}$$

35

in Equation (45), at least for their real parts, we see that z tends eventually to be negative in the ricochet regime. When z returns to zero, the problem ceases and the exit velocity component $\dot{z}$ will be negative. At the ricochet limit $\delta_z = 0$ and $z \to 0$, $\dot{z} \to 0$ as $t \to \infty$. For $v_{ozRL} < v_{oz} < v_{ozPL}$, $T > \delta_z > 0$ and embedment occurs since $z_{max} < T$. For $v_{oz} > v_{ozPL}$, $\delta_z > T$, and perforation occurs.

If we substitute $[f(T) + c_{1z} v_{oz}] = - d_{1z} \delta_z$ in Equation (48), we have

$$F_z = - [b_{1z} \dot{z} + d_{1z} (z - \delta_z)] \tag{53}$$

where δ_z is seen to play the role of the eventual value of z as t becomes arbitrarily large and $F_z \to 0$, $\dot{z} \to 0$. Because of this δ_z will be called a final position parameter.

Similarly, for the x-component

$$F_x = - [f(L_x) + c_{1x} v_{ox} + b_{1x} \dot{x} + d_{1x} x]. \tag{54}$$

We also require $F_x \to 0$, $\dot{x} \to 0$ at the ricochet limit, so

$$0 = - [f(L_x) + c_{1x} v_{oxRL} + d_{1x} x_{RL}] \tag{55}$$

and

$$0 = - [f(L_x) + c_{1x} v_{oxPL} + d_{1x} x_{PL}] \tag{56}$$

at the perforation limit where $\dot{x}$ also vanishes. The limiting values x_{RL} and x_{PL} are not usually known. From these relations we find $f(L_x) = - d_{1x} (x_{RL} v_{oxPL} - x_{PL} v_{oxRL})/(v_{oxPL} - v_{oxRL})$ and $c_{1x} = - d_{1x} (x_{PL} - x_{RL})/(v_{oxPL} - v_{oxRL})$ which may be substituted into Equation (54) to obtain

$$F_x = - [b_{1x} \dot{x} + d_{1x} (x - \delta_x)] \tag{57}$$

where

$$\delta_x = - [x_{PL} v_{oxRL} - x_{RL} v_{oxPL} - (x_{PL} - x_{RL}) v_{ox}]/(v_{oxPL} - v_{oxRL}) \tag{58}$$

plays a role similar to δ_z. Of course δ_z in Equation (51) can be calculated from experimental data for a given θ_o to within the accuracy possible for these types of limit measurements. However, the limit values in Equation (58) are not usually measured and it is necessary to estimate δ_x from its definition. This can also be done for δ_z.

36

In summary, we have introduced a soluble set of equations (Equations (43) and (44)) and pointed out their ability to describe curvilinear motion, including the extremes of ricochet, embedment and perforation. A discussion of the constant force term a_{oz} (composed of shear and frictional parts) led us to the general position parameter δ_z given in Equation (51) and its x-analog in Equation (58). In this country it is customary to determine the perforation limit speed v_{ozPL} for given target thickness, and from Equation (51) we see that $\delta_z = T$ when $v_{oz} = v_{ozPL}$. From Equation (45) with $s = z$, we also see that $z = \delta_z = T$ (since $t \to \infty$). In Germany[20] it is common to determine that thickness of target plate which will just stop the projectile for given striking speed. This limit thickness, T_ℓ, of course corresponds to the limit speed, v_{ozPL}, so again, from Equations (45) and (51) $z = (\delta_z)_\ell = T = T_\ell$ when $v_{oz} = v_{ozPL}$. For an effectively semi-infinite target neither v_{ozPL} nor T_ℓ is ever reached experimentally. Thus, even for the highest striking velocity $v_{oz} < v_{ozPL}$ and by Equations (45) and (51) we have $z_\infty = (\delta_z)_\infty < T = T_\ell$. In other words, the maximum depth of penetration in a semi-infinite target is less than the limit thickness. Experimentally[20] it is found that the ratio $T_\ell/(\delta_z)_\infty$ decreases as v_o increases and seems to approach 1.5 as v_o approaches the longitudinal sound speed in the target material (at least for steel targets and short steel rods). Because of spalling, dishing, petalling and other finite target effects as well as projectile erosion and breakup, T_ℓ is roughly an exponential function of v_o in the ordnance range.

If we allow b_{2s} and/or d_{2s} to be non-zero in the components of Equation (40), then we have a set of non-linear equations. The general closed-form solution to any one of these equations is not known at present and will be the subject of future work. If need be, we can always write approximate solutions in series form. However, we will first try to answer the question of how well we can describe the available data for ordnance velocity penetrations using Equations (43) and (44). These are the simplest forms we can expect to use to describe curvilinear motion resulting in perforation, embedment or ricochet depending in a continuous manner on v_o and θ_o.

[20]V. Hohler, E. Schneider and A. Stilp, "Endballistik von Splittern I-V, Berichte E 6/73, E4/74, E4/75, E9/75 and E 7/75 (1973-1975) Ernst-Mach-Institut, Freiburg.

V. ILLUSTRATIONS OF MOTIONS IN THE SIMPLEST FORCE FIELD

In this section we wish to illustrate some of the capabilities of the force with components $F_s = - (a_s + b_s \dot{s} + d_s s)$. We will not give an exhaustive analysis. Rather we will show the type of agreement with experiment which might be expected by showing this agreement in a few simple cases. For convenience we reproduce the z-component of the solution for the equation of motion as well as its time derivative, dropping numerical subscripts:

$$z = \frac{1}{(\gamma_z^+ - \gamma_z^-)} \left[(v_{oz} + \delta_z \gamma_z^-) e^{\gamma_z^+ t} - (v_{oz} + \delta_z \gamma_z^+) e^{\gamma_z^- t} \right] + \delta_z \tag{59}$$

$$\dot{z} = \frac{1}{(\gamma_z^+ - \gamma_z^-)} \left[(v_{oz} + \delta_z \gamma_z^-) \gamma_z^+ e^{\gamma_z^+ t} - (v_{oz} + \delta_z \gamma_z^+) \gamma_z^- e^{\gamma_z^- t} \right] \tag{60}$$

where $\gamma_z^{\pm} = - \alpha_z \pm \beta_t$, $\alpha_z = \frac{b_z}{2m_o}$, $\beta_z = \sqrt{\alpha_z^2 - d_z/m_o}$ and

$$\delta_z = - T (v_{ozRL} - v_{oz})/(v_{ozPL} - v_{ozRL}) = - a_{oz}/d_z. \tag{61}$$

As is well known, β_z can be real, zero or imaginary. If β_z is real or zero, then $d_z \leqslant m_o \alpha_z^2$. For $d_z = 0$ we have a solution analogous to that which describes a body falling through a viscous medium in the earth's gravitational field, $a_{oz} = m_o g$. However we have already seen that such a force field dependent only on the velocity is not adequate for describing an embedment region between ricochet and perforation regions in a plot of exit speed versus striking speed. Experimentally, velocity decreases with time which requires

$$\gamma_z^- < \gamma_z^+ < 0 \tag{62}$$

so that z and $\dot{z}$ will always be finite in Equations (59) and (60). The same is true of course for the other components. Equation (62) implies $\alpha_z^2 \geqslant d_z/m_o > 0$, since $d_z < 0$ would make $\beta_z > \alpha_z$ and $\gamma_z^+ > 0$, leading to a non-physical velocity increase with time. The special case

38

$d_z = m_0 \, \alpha_z^2$ or $\beta_z = 0$ requires the degenerate solution

$$z = e^{-\alpha_z t} \left[v_{oz} - \alpha_z \, \delta_z) \, t - \delta_z \right] + \delta_z \tag{63}$$

$$\dot{z} = e^{-\alpha_z t} \left[v_{oz} - (v_{oz} - \alpha_z \, \delta_z) \, \alpha_z \, t \right]. \tag{64}$$

By rearranging Equations (59) and (60) we can find

$$e^{\gamma_z^+ t} = [\dot{z} - \gamma_z^- \, (z - \delta_z)] / (v_{oz} + \delta_z \, \gamma_z^-) \tag{65}$$

$$e^{\gamma_z^- t} = [\dot{z} - \gamma_z^+ \, (z - \delta_z)] / (v_{oz} + \delta_z \, \gamma_z^+). \tag{66}$$

If we divide Equation (65) by Equation (66) and solve for t, we find

$$t = \frac{1}{(\gamma_z^+ - \gamma_z^-)} \, \ell n \left\{ \frac{[\dot{z} - \gamma_z^- \, (z - \delta_z)] \, (v_{oz} + \delta_z \, \gamma_z^+)}{[\dot{z} - \gamma_z^+ \, (z - \delta_z)] \, (v_{oz} + \delta_z \, \gamma_z^-)} \right\}. \tag{67}$$

In case $\beta_z = 0$ we find from Equations (63) and (64)

$$e^{-\alpha_z t} = [\dot{z} + \alpha_z \, (z - \delta_z)] / (v_{oz} - \alpha_z \, \delta_z) \tag{68}$$

and

$$t = [v_{oz} \, (z - \delta_z) + \delta_z \, \dot{z}] / [\{\dot{z} + \alpha_z \, (z - \delta_z)\} \, (v_{oz} - \alpha_z \, \delta_z)] \tag{69}$$

$$= \frac{1}{\alpha_z} \, \ell n \, [(v_{oz} - \alpha_z \, \delta_z) / \{\dot{z} + \alpha_z \, (z - \delta_z)\}]$$

Now let us illustrate the application of this solution (and the analogous x-component solution) by using some of Backman and Finnegan's

data[11]. Figures 1, 2 and 3 reproduce some of their data for a 1 gram hard steel (SAE 52100) sphere penetrating a 6061 aluminum alloy plate of thickness T = 9.53mm. The sphere diameter was 6.35mm. As before, we will take our z axis anti-parallel to the normal to the impact surface and our origin at the point of impact with the motion occuring in the x-z plane. We note that our choice of axes makes $L_y = 0 = v_{oy}$ so $\delta_y = 0$ and $y = \dot{y} = F_y = 0$ for all t. By convention the obliquity θ_o is the angle measured from the impact face normal to the negative of the striking velocity vector. In order to conform to the conventions of Backman and Finnegan we will measure the exit angle $\theta = \arctan(\dot{x}/\dot{z})$ from the negative of the impact face normal, that is, from the z axis, to the exit velocity vector. Thus for perforations we will have $0 \leqslant \theta \leqslant 90°$, for ricochets we will have $\theta > 90°$, while for embedments θ is undefined. An upper limit of 180° for θ is suggested by the available data near the ricochet/embedment limit, but the data is not good enough to be sure. There are also indications that $\theta \rightarrow 180° - \theta_o$ as $v_o \rightarrow 0$ as we might expect since we are approaching the case of elastic rebound (no penetration) for which the angle of reflection is equal to the angle of incidence. Again experimental evidence is lacking near this limit to confirm or deny such behavior.

At the other extreme of very large striking speed ($v_o \rightarrow \infty$) we expect the exit speed $v \rightarrow v_o$ and the exit angle $\theta \rightarrow \theta_o$. This expectation has been verified by experiments with very thin (aluminum foil) targets and ordnance projectiles which move almost as if the target were not there. In both extremes ($v_o \rightarrow 0$ and $v_o \rightarrow \infty$) the time spent penetrating the target is very small. That is, the ricochet time, t_R, which is the time it takes for z to return to zero, and the perforation time, t_p, which is the time it takes for z to reach the value T, both approach zero for these extreme striking speeds. It is clear from Equation (60) and its x-analog that the solution behaves properly at these two extremes, namely, $\dot{x}_p/|\dot{z}_p| \rightarrow v_{ox}/v_{oz}$ so $\theta = \arctan(\dot{x}_p/\dot{z}_p) \rightarrow \theta_o = \arctan(v_{ox}/v_{oz})$ for very large v_o, while $\theta \rightarrow 180° - \theta_o$ for very small v_o (small $\dot{z}_R < 0$ and $\dot{x}_R \geqslant 0$). For intermediate values of v_o which lead to ricochet, $\theta > 180°$ is a possibility ($\dot{z}_R < 0$, $\dot{x}_R < 0$), but there seems to be no published evidence for this case. For zero obliquity impacts, $\theta_o = 0 = \sin \theta_o$, $x = \dot{x} = 0$, $v_{ox} = v_o \sin \theta_o = 0$ and $L_x = L \sin \theta_o = 0$ [or $(1 - e^{-a_{3x}L_x}) = 0$] so $F_x = 0$ in Equation (54). As $\theta_o \rightarrow 90°$, grazing incidence turns into a near mass and no penetration occurs.
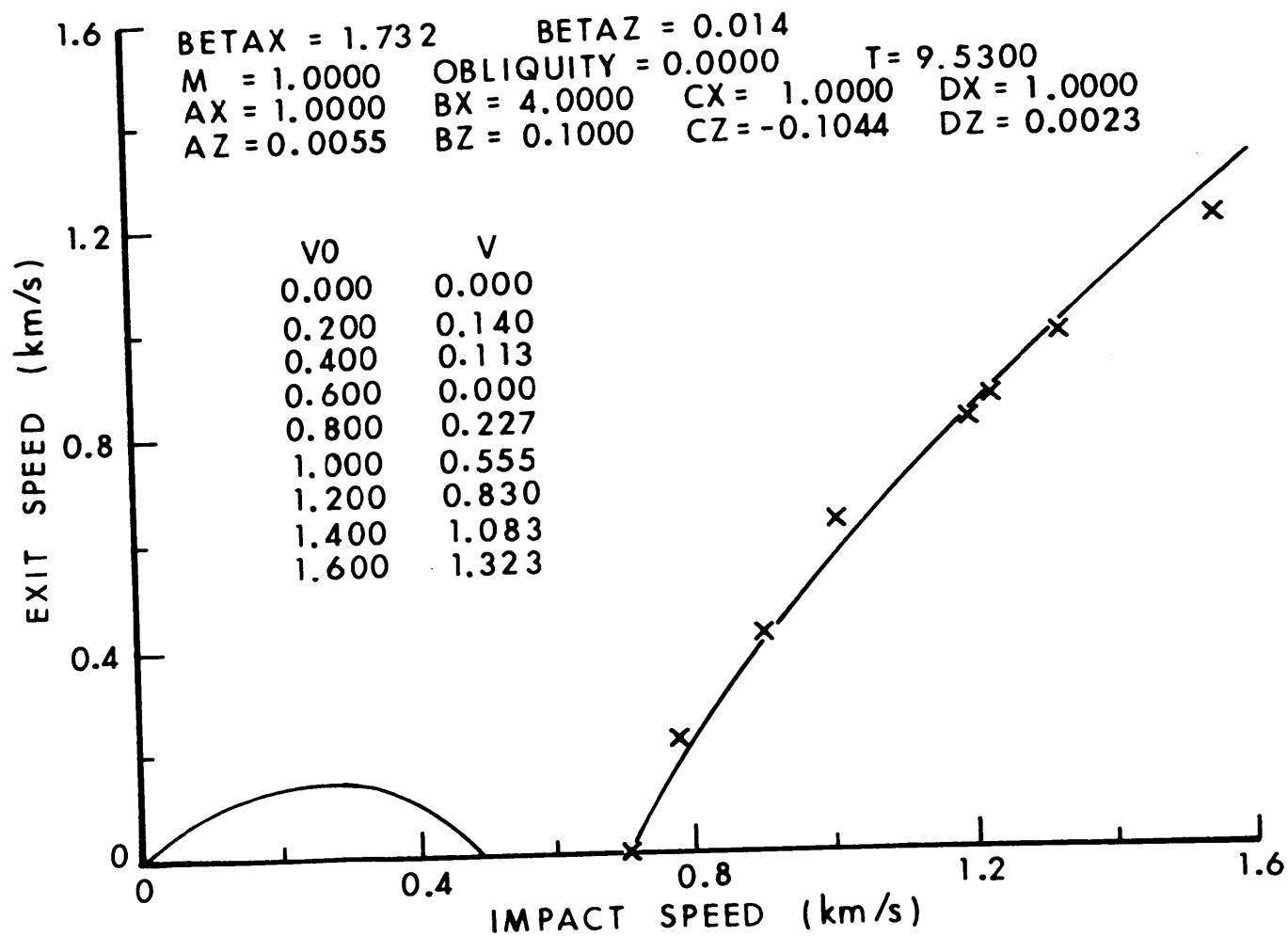
Figure 1. Measured and calculated exit speeds for steel spheres vs aluminum plates at zero obliquity.
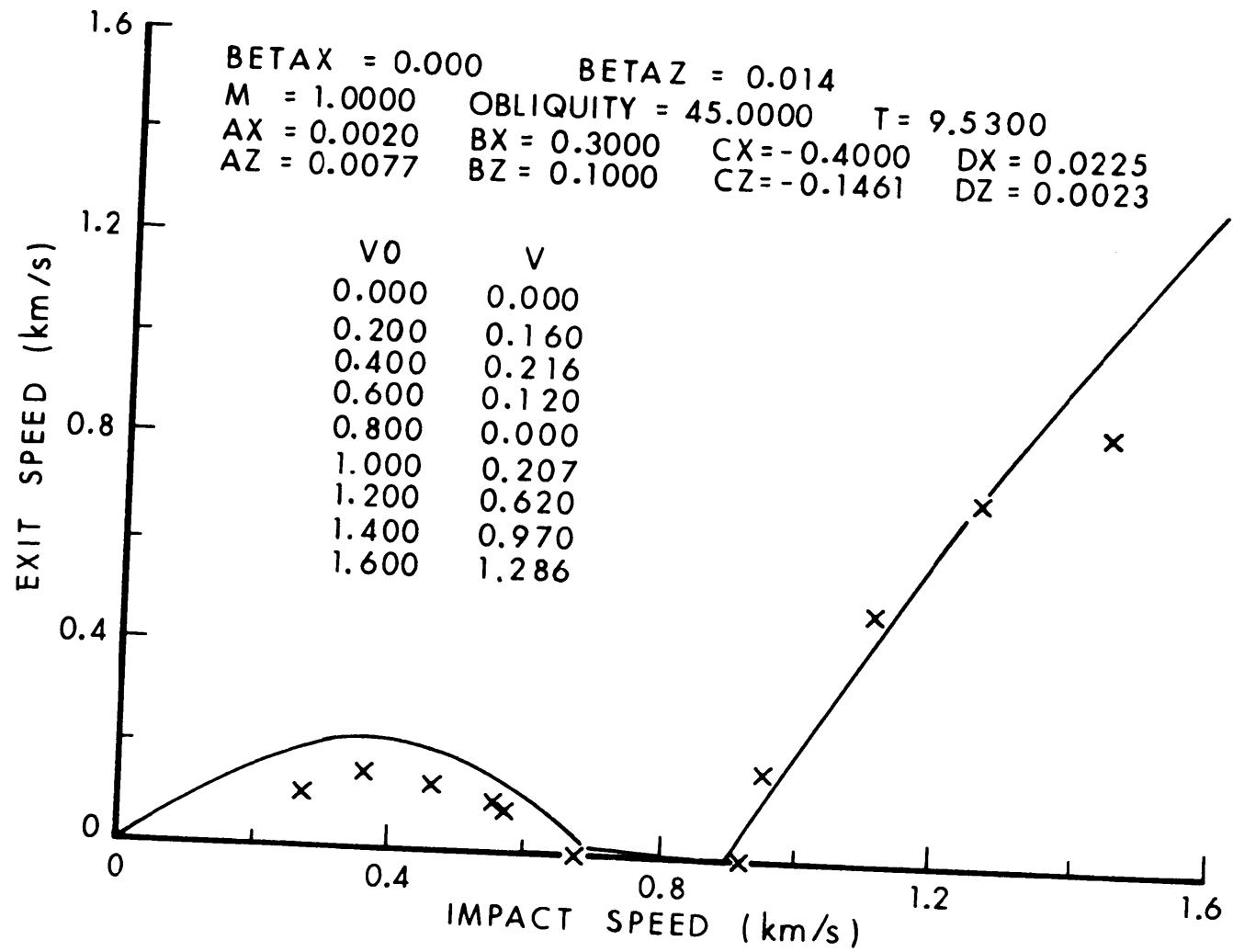
41

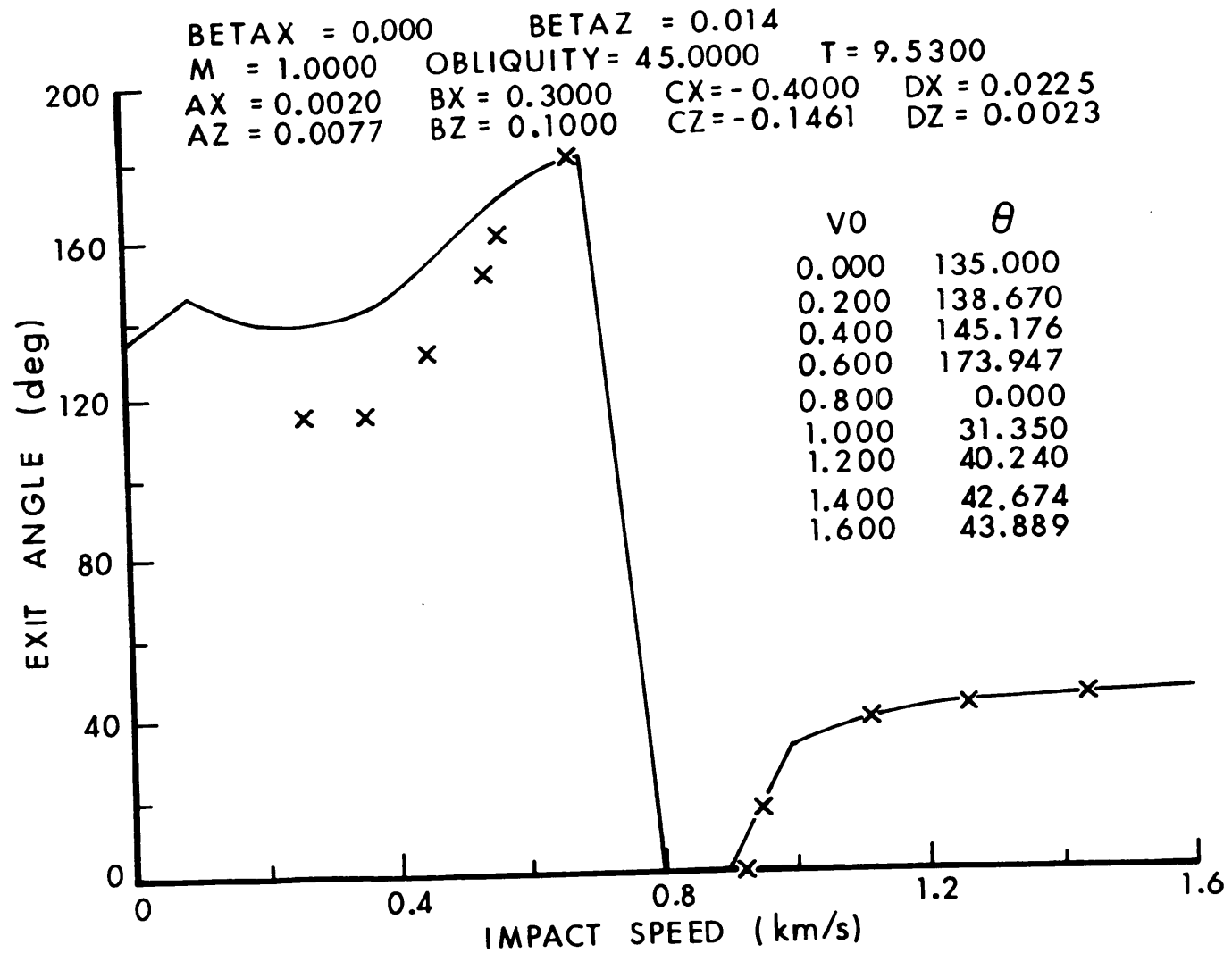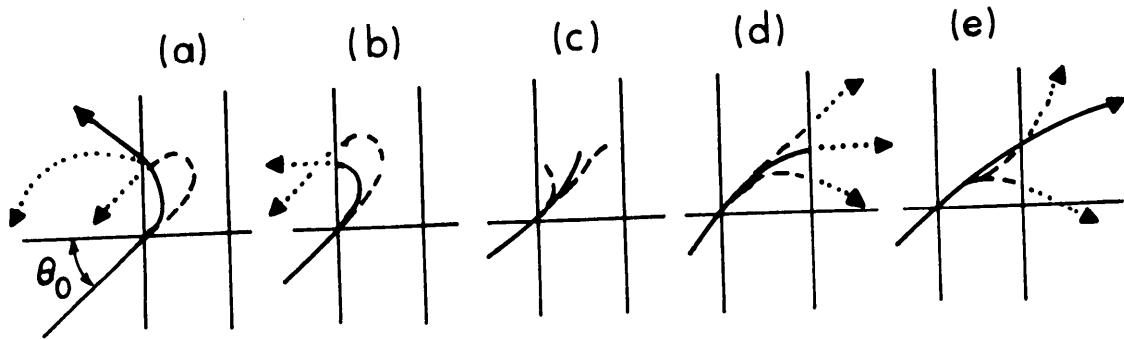Figure 2. Measured and calculated exit speeds for steel spheres vs aluminum plates at 45° obliquity.

Figure 3. Measured and calculated exit angles for steel spheres vs aluminum plates at 45° obliquity.

For real β_z, $\dot{z}$ can vanish only twice. The first time can be found by letting $\dot{z} = 0$ in either Equation (67) or Equation (69) and then $z = z_{max}$ can be found by using this value of t in either Equation (59) or Equation (63). The second zero of $\dot{z}$ occurs as $t \rightarrow \infty$. It is of course possible for $t \rightarrow \infty$ to be the only time that $\dot{z}$ vanishes. This occurs at perforation limits or for embedment in semi-infinite targets.

At the ricochet limit $\dot{z}$ has already vanished once at the turning point $z = z_{max} < T$. For this limit it vanishes again as $z \rightarrow 0$ and $t \rightarrow \infty$. From Equations (67) or (69) we see that this requires $\delta_z = 0$ which is insured by Equations (51) or (61) when $v_{oz} = v_{ozRL}$. At the perforation limit $v_{oz} = v_{ozPL}$ and $\delta_z = T$ in Equation (61) so that $\dot{z}$ vanishing and z approaching T makes $t \rightarrow \infty$ here too. For embedment in a finite target, $\dot{z} \rightarrow 0$ and $z \rightarrow \delta_z < T$ makes $t \rightarrow \infty$. For a semi-infinite target which guarantees embedment even for the largest v_o we can realize, $z_{max} = \delta_z$ as $t \rightarrow \infty$. Since v_{ozPL} increases without limit as T increases without limit in Equation (51), $\delta_z = z_{max}$ depends on v_{oz}.

Figure 4 illustrates schematically some of the trajectories which can occur during target penetration. These trajectories become effectively straight lines when the projectile exits from the target into a low resistance medium like the air. Alternative trajectories are illustrated by solid or dashed lines while dotted lines indicate projections of trajectories if the motion had continued or if a different distribution of target material had been present. For example, if there had been more target material in the upper left of Figure 4(a), then the x coordinate might reach a maximum in finite time and eventually turn negative. The solid line in Figure 4(a) shows a typical ricochet while the dashed line illustrates a possibility which does not seem to have been documented in the literature as mentioned above. In the dashed case illustrated the exit velocity is anti-parallel to the striking velocity and $\theta = 180° + \theta_o$. Smaller or larger values for θ are possible with the latter involving a trajectory which crosses itself. This crossing could occur inside or outside the target. Figure 4(b) illustrates possible trajectories when $v_o = v_{oRL}$, the ricochet limit. Here $v_{ox} = v_{oxRL}$ and $\delta_x = x_{RL}$ in Equation (56) so $x \rightarrow \delta_x$ and $\dot{x} \rightarrow 0$ makes $t \rightarrow \infty$ in the x-component analogs of Equations (67) or (69). If $\dot{x}$ remains positive and approaches zero only as $t \rightarrow \infty$, then x_{RL} is a maximum value which x approaches only as $t \rightarrow \infty$ and the exit angle $\theta_{RL} = 180°$ as illustrated by the solid line in Figure 4(b). If $\dot{x}$ turns negative in finite time and then approaches zero as $t \rightarrow \infty$, then $x_{RL} < x_{max}$ and $\theta_{RL} > 180°$ as shown by the dashed line in Figure 4(b) which is the the limiting case of a dashed line in Figure 4(a). Figure 4(c)

44

(a) RICOCHET ($|\dot{X}| > 0$, $\dot{Z} < 0$, $X = X_R$, $Z = 0$, t_R FINITE)

(b) RICOCHET LIMIT ($\dot{X} = \dot{Z} = Z = 0$, $X = X_{RL}$, $t_{RL} \rightarrow \infty$)

(c) EMBEDMENT ($\dot{X} = \dot{Z} = 0$, $0 < \delta_Z < T$, $0 < \delta_X$, $t \rightarrow \infty$)

(d) PERFORATION LIMIT ($\dot{X} = \dot{Z} = 0$, $Z = T$, $X = X_{PL}$, $t_{PL} \rightarrow \infty$)

(e) PERFORATION ($|\dot{X}| > 0$, $\dot{Z} > 0$, $Z = T$, $X = X_P$, t_P FINITE)

Figure 4. Schematic examples of penetration trajectories.

illustrates by a solid line an embedment trajectory for which $v_{oRL} < v_o < v_{oPL}$ and z approaches a maximum value as $t \to \infty$, $\dot{z} \to 0$. Of course $\dot{z} \to 0$ as $t \to \infty$ even if the final z value $\lessapprox z_{max}$ (solid). The dashed lines in Figure 4(c) illustrate such possibilities. At the perforation limit the available data suggest that the exit angle is close to zero. The solid line in Figure 4(d) illustrates this and, if true, then x_{PL} is a maximum. Since $\dot{x}_{PL} \to 0$ as $t \to \infty$, the other possibility is that $x_{PL} < x_{max}$ if $\dot{x}$ has already vanished once in finite time. This is shown by one dashed curve in Figure 4(d). Of course $\dot{z} \to 0$ and $z \to \delta_z = T$ when $v_o = v_{oPL}$ will make $t \to \infty$ in Equations (67) or (69). Finally, a typical perforation trajectory with the exit angle $\theta < \theta_o$ is shown by the solid line in Figure 4(e). As $v_o \to \infty$, of course, $\theta \to \theta_o$. Another possibility shown by a dashed line is that $\dot{x}$ vanish while $z < T$ so that x_{max} occurs inside the target and the exit angle $\theta < 0$. A third possibility in which a point of inflection ($\ddot{x} = 0$, $\dot{x} > 0$) occurs inside the target in finite time could lead to $\theta > \theta_o$ and is illustrated by another dashed line in Figure 4(e). A similar type of behavior is possible for ricochets also but was not illustrated in Figure 4(a) to avoid crowding and confusion. In short, a variety of trajectories can be described by Equation (59) and its x-analog although not all of them may be realizable for particular projectile and target material combinations. For targets other than plates of homogeneous material or for projectiles with special shapes or motions at impact, it may be necessary to invoke unusual trajectories or to include x-, y- and z-components of motion for an adequate description. We also note that for real $\beta_s \geq 0$ with $s = x$, z (or y if needed) all combinations such as $\beta_x = 0$, $\beta_z > 0$ or $\beta_x = \beta_z = 0$ or $\beta_x > 0$, $\beta_z > 0$, etc. are allowed.

In summary, there are some constraints imposed on the parameters a_{os}, b_s and d_s (for $s = x, z$) from general considerations of plate target penetration with $\beta_s \geq 0$. From Equation (62) and its x analog we have $b_x > 0$, $b_z > 0$, $0 < d_x \leq m_o [b_x / (2 m_o)]^2$ and $0 < d_z \leq m_o [b_z / (2 m_o)]^2$, while from Equations (49) and (50) we have $a_z = d_z V_{ozRL} / (v_{ozPL} - v_{ozRL})$ since $f(T) \approx a_z T$ for thin targets, while $c_z = - d_z T / (v_{ozPL} - v_{ozRL})$ in any case. Similarly we can relate c_x to d_x and a_x to d_x since $f(L_x) \approx a_x T \tan \theta_o$ for thin targets from Equations (55) and (56). We can also find cross constraints between the x and z parameters by equating Equation (67) (or Equation (69)) to its x analog since time

(like mass) is common to all components. For example, at the time of perforation, $\dot{x}_p = v_p \sin \theta_p$, $\dot{z}_p = v_p \cos \theta_p$ and $z_p = T$. Since we know v_p, θ_p and T experimentally and can estimate x_p experimentally, we can obtain cross constraints for as many values of v_o (and θ_o) as are needed. The same can be done for ricochets with $\dot{x} = v_R \sin \theta_R$, $\dot{z} = v_R \cos \theta_R$, $z = 0$ and x_R estimated. In addition (at least for some projectile-target combinations) other conditions must be satisfied in the ricochet region.

For example, from Figure 2 it is clear that $v_R = \sqrt{\dot{x}_R^2 + \dot{z}_R^2}$ goes through a maximum as a function of v_o. Thus at some value of v_o, $dv_R/dv_o = 0$ and $d^2 v_R/dv_o^2 < 0$, which imposes additional cross contraints. Similarly, from Figure 3 (and similar data) it seems likely that θ_R = arc tan $(\dot{x}_R/\dot{z}_R)$ goes through a minimum, so that perhaps $d\theta_R/dv_o = 0$ and $d^2 \theta_R/dv_o^2 > 0$ at some value of v_o.

For the zero obliquity case shown in Figure 1 there is no x-component. There is also no ricochet limit shown although one probably exists. Table I contains estimates made from Figures 11 to 17 of Backman and Finnegan with estimates of error $\pm$ .05mm/µs on the speeds. For this

Table I. Limit Speeds vs θ_o (1 gm Steel Spheres vs 6061 Aℓ plate)

θ_o	0°	20°	45°	60°
$\cos \theta_o$	1	.94	.71	.5
v_{oRL} (mm/µs)	?	.5	.71	1.06
v_{ozRL} (mm/µs)	?	.47	.5	.53
v_{oPL} (mm/µs)	.71	.73	.9	1.2
v_{ozPL} (mm/µs)	.71	.69	.65	.6
$v_{ozPL} - v_{ozRL}$	?	.22	.15	.07

kind of error we can say that v_{ozRL} is approximately .5mm/µs over the whole range, including perhaps $\theta_o = 0°$. However, v_{ozPL} clearly decreases as θ_o increases (T = constant). If we take $a_z = [v_{ozRL}/(v_{ozPL} - v_{ozRL})]d_z$
= [.50/(.71 - .50)] d_z = 2.38 d_z and $c_z = - d_z T/(v_{ozPL} - v_{ozRL})$
= - d_z (9.53)/(.71 - .50) = - 45.38 d_z for $\theta_o = 0°$ with
$0 < d_z \leqslant .25 b_z^2$ for $m_o = 1$ gm, then we only have to estimate b_z in

order to constrain d_z and so a_z and c_z. Gudunov and co-workers[17] have measured the kinematic coefficient of viscosity, ν, for copper, aluminum, lead and steel. They give $\nu = 1.0$ m^2/s for aluminum, 2.5 m^2/s for duraluminum and 5.5 m^2/s for steel. The dynamic coefficient of viscosity is $\mu = \rho\nu$. For example, for aluminum with $\rho = 2.7$ gm/cm^3, $\mu = 2.7 \times 10^4$ gm/(cm-sec). If a Stokes type of law were to hold for a non-deforming sphere penetrating aluminum then $b_z = 6\pi R\mu = 6\pi$ $(\frac{.635 \text{ cm}}{2})$ $(2.7 \times 10^4$ gm/(cm-sec)) $= .16 \times 10^6$ gm/sec $= .16$ gm/μs or 2.5 times this for duraluminum. In this way we can estimate b_z from an experiment of a different type. If we obtain reasonable agreement with penetration experiments, then we will be encouraged to believe that the constant b_z is more than just a fitting parameter. If we take $b_z = .10$ gm/μs and $d_z = .0023$ gm/(μs)^2, we obtain the solid line in Figure 1 calculated for v_0 increments of 0.1 km/s (or 0.1 mm/μs). The X's are the data points of Backman and Finnegan (their Figure 11). The model allows a ricochet region for $0 \leq v_0 \leq .50$ mm/μs with an embedment region for $.50 \leq v_0 \leq .71$ mm/μs. In the perforation region there is rough agreement with experiment but the curvature of the calculated line is less then that of a line fitted through the experimental points. This is probably due to our neglect of the force term $b_{2z} v_z^2$. No attempt was made to optimize the parameters. Since $\theta_0 = 0$, $v_{0x} = 0$ and $L_x = T \tan \theta_0 = 0$ so $\delta_x = x = \dot{x} = 0$ for all time for any x-parameters. The x-parameter values in Figure 1 are dummy values to satisfy the program input requirements of the 9830A Hewlitt-Packard Computer (see Appendix).

In Figures 2 and 3 the data of Backman and Finnegan (their Figures 14 and 15) for the same parameters as in Figure 1 except $\theta_0 = 45°$ is shown by X's. The calculated solid curves were obtained by using $a_x = .002$ gm/(μs)^2, $b_x = .3$ gm/μs, $c_x = - .4$ gm/μs, $d_x = .0225$ gm/(μs)^2 with b_z and d_z the same as for $\theta_0 = 0°$, but with a_z and c_z determined using $v_{ozPL} = .65$ km/s instead of .71 km/s from Table I. No attempt has been made to optimize the agreement which presumably could be improved with some effort. It might be wiser to apply this theory to a greater variety of data first to learn more about the trends shown by the parameters. This will be done in future work before we return to optimizing data fits.

From Table I we noted that $v_{ozRL} = v_{oRL} \cos \theta_0 = .5$ was essentially constant, implying that $v_{oRL} = .5/\cos \theta_0$. We saw however that $v_{ozPL} = v_{oPL} \cos \theta_0$ decreased as θ_0 increased, implying that v_{oPL} is some other function of θ_0. If we postulate that v_{oPL} and v_{oRL} differ by a constant amount, namely, $v_{oPL} = .21 + v_{oRL} = .21 + .5/\cos \theta_0$ so that $v_{ozPL} = .5 + .21 \cos \theta_0$, we can reproduce the values given in Table I. The parameter a_z now becomes $a_z = d_z v_{ozRL}/(v_{ozPL} - v_{ozRL}) = d_z$ $(2.38/\cos \theta_0)$. In our calculation for Figures 2 and 3, we assumed that

d_z had the same value for $\theta_0 = 45°$ as it did for $\theta_0 = 0°$ which made a_z increase as θ_0 increased. If a_z were to be independent of θ_0 we would have to assume d_z proportional to $\cos \theta_0$. Actually, a_z is proportional to the z-components of the projectile presented area and the contact area. Consequently a_z ought to be proportional to $\cos \theta_0$ instead of $(\cos \theta_0)^{-1}$ as assumed. This implies that d_z ought to be proportional to $(\cos \theta_0)^2$. A similar argument applies to c_z which is also proportional to d_z. In future work we will explore the merits of including the dependence of these parameters on obliquity.

If β_s is imaginary, then the motion has a periodic form with decaying amplitude, although for perforations and ricochets less than one full period will be completed before the problem terminates when the projectile exits from the target. For embedments a large number of oscillations would be executed before the motion ceased when t grew arbitrarily large. For imaginary $\beta_z = i \omega_z = i \sqrt{d_z/m_0 - \alpha_z^2}$ with $d_z > m_0 \alpha_z^2 > 0$, for example, we have

$$z = e^{-\alpha_z t} \left[\frac{1}{\omega_z} (v_{oz} - \alpha_z \delta_z) \sin \omega_z t - \delta_c \cos \omega_z t \right] + \delta_z \qquad (70)$$

$$\dot{z} = e^{-\alpha_z t} \left[v_{oz} \cos \omega_z t - \frac{1}{\omega_z} \{\alpha_z v_{oz} - \delta_z (\alpha_z^2 + \omega_z^2)\} \sin \omega_z t \right]$$
$$(71)$$

with analogous relations for the x-component. As before from Equations (70) and (71) we can find

$$e^{-\alpha_z t} \sin \omega_z t = [\delta_z \dot{z} + v_{oz} (z - \delta_z)]/X \qquad (72)$$

$$e^{-\alpha_z t} \cos \omega_z t = \frac{1}{\omega_z} [(v_{oz} - \alpha_z \delta_z) \dot{z}$$
$$(73)$$

$$+ (z - \delta_z) \{\alpha_z v_{oz} - \delta_z (\alpha_z^2 + \omega_z^2)\}]/X$$

49

where

$$X = \frac{1}{\omega_z} [v_{oz}{}^2 + \delta_z{}^2 (\alpha_z{}^2 + \omega_z{}^2)] = \frac{1}{\omega_z} [v_{oz}{}^2 + \delta_z{}^2 (\frac{d_z}{m_o})] \qquad (74)$$

or by dividing Equation (72) by Equation (73)

$$\tan \omega_z t = \omega_z [\delta_z \dot{z} + v_{oz} (z - \delta_z)]/[v_{oz} - \alpha_z \delta_z) \dot{z} \qquad (75)$$

$$+ (z - \delta_z) \{\alpha_z v_{oz} - \delta_z (\alpha_z{}^2 + \omega_z{}^2)\}] \ .$$

The times at which turning points of the motion occur can be found by setting $\dot{z} = 0$ in Equation (75) with the successive values of $\omega_z t$ occurring modulo π. The perforation limit can be represented by the condition that the first maximum of z is equal to the target thickness ($z_{max\ 1} = T$) while the ricochet limit can be represented by $z_{max\ 1} < T$, $z_{min\ 1} = 0$. Since oscillatory embedment is a motion allowed by the general model, provided $d_z > m_o \alpha_z{}^2$, $z_{max\ 1} < T$ and $z_{min\ 1} > 0$, it might be interesting to design an experiment to look for this event since there does not seem to be any information on the subject in the published literature. However, such an experiment would require a motionless target (very massive) since this model takes no account of target motion (a reasonable approximation for many targets during the short times involved for perforations or ricochets). In this paper we will not further explore the possibility that one or more β_s (s = x, y, z) may be imaginary. Of course mixed β_s (one component β real or zero, another imaginary) are allowed in general.

In summary, we have shown how to apply the solutions of Equations (43) and (44) to a particular case of plate target penetration for which experimental exit speeds and angles were available in both ricochet and perforation regimes. The agreement between theory and experiment can certainly be improved, but the overall agreement shows promise. An important improvement in agreement is expected when force terms involving the square of velocity components are included (as they will be in future work). This should take the burden of agreement in the perforation region off the first power terms and allow them to aid the constant and penetration depth terms in improving agreement in the ricochet regime. The reader is urged to use the computer code in the Appendix with somewhat different parameter values in order to get a feel for how this might be possible. We have also noted the considerable variety of trajectories which are allowed by the theory, many of which might be realized in practice with a suitable choice of materials.

50

VI. MASS LOSS, EXPERIMENT AND EXISTING THEORY

A. Comments on the Experimental Data Base

The largest data set which relates to the question of mass loss by a penetrator consists of the Thor collection[3] for steel fragments together with its extension to tungsten fragments[4]. In the Thor collection residual mass was frequently not recorded, but when it was, it was never equal to the striking mass. In the extension to tungsten fragments, the residual mass after perforation was almost always recorded and was always less than the striking mass. In other words, if our aim is to model at least the important features of penetration our model must be amended to include non-constant mass.

"With low striking velocities, the loss in weight of a fragment during perforation is small and is usually ignored. In such cases, the residual velocity, alone, serves as a good measure of the resistance of the target to perforation and the capacity of the residual fragment for perforating another target. As striking velocity increases, the break-up of the fragment becomes more and more pronounced until this aspect of the impact must be taken into account. The residual weight of the fragment must be known as well as the residual velocity before any reasonable estimate can be made of the capacity of the fragment for perforating another target."[3]

There are other data collections concerning rod penetrators and these also record mass loss as a frequent phenomenon of practical interest[21]. In addition many individual reports record mass loss.

There appear to be two basic types of mass "loss". The first can be described as erosion or wearing away of the projectile occuring mostly at the tip or leading edge. This might occur with or without prior distortion of the tip. The second can be described as fracture or breakup of the projectile into pieces of more or less comparable size, differing, say, by no more than an order of magnitude. This phenomenon can be called a mass "loss" only if one chooses to disregard the smaller pieces of the broken projectile and concentrates on the largest surviving piece. This point of view was adopted by those who collected the Thor and extended Thor data sets. An attempt was made to justify this procedure:

"In many experimental cases, the weight of the largest piece of residual fragment approximates the total weight of fragment perforating the barrier target. At any rate, the capacity of a fragment to perforate a primary target beyond an initial barrier can be conservatively estimated by considering only the largest piece of fragment which perforates

---

[21]J. P. Lambert, "The Terminal Ballistics of Certain 65 Gram Long Rod Penetrators Impacting Steel Armor Plate," ARBRL-TR-02072, May 1978. (AD #A057757)

51

the barrier. This approach is justified whenever the hypothetical primary target is one for which damage from the impact of small, slow-moving particles is not anticipated, i.e., damage to such a target will essentially be that caused by the largest, fastest particle that impacts on it."[3]

The authors admit however the desirability of observing more than the largest piece so that one can estimate damage to all types of interior components. However, they seem to ignore the possibility that the projectile might breakup into pieces of comparable size. Suppose, for example, the largest piece were $0.4 \ m_o$, while three other pieces half this size but with comparable residual speed accompanied the largest piece in a debris cone. Then the target damage might be much worse than that estimated by considering only the largest piece. Add to this the target plug, spall and other debris and the practical need for recording more than the largest piece becomes clear. From a theoretical point of view the need for recording the number and sizes of as many such pieces as can be practically measured is also clear. Unfortunately this was not done even in the extension of the Thor data to tungsten fragments which used a similar wallboard collection method and recorded only the largest piece. However, x-rays were used to measure residual speed in some of these later experiments so there may be some unreported fragment mass distribution information still recoverable.

If one is to compare a physical theory with experiment and not merely fit an arbitrary function, at least three things must be known about residual penetrator masses, (1) we must know whether erosion and/or breakup has occurred; (2) if erosion has occurred, we must know its extent and if breakup has occurred we must know the masses of all the pieces; and (3) we must know whether erosion and/or breakup has been caused by the target or by the observation technique. We are interested in events caused by the target. If erosion and/or breakup is caused by use of a recovery medium, this leads to falsification of the data we need. One might imagine firing into the recovery medium alone in order to correct for this falsification. Such a procedure might seem to resemble the calibration procedure which is usually carried out when such a medium is used to determine residual speeds. However, this is not satisfactory for mass determinations. For example, it is entirely possible that incipient cracks produced by the target/projectile encounter will be converted into projectile breakup by the recovery medium, although the projectile emerging from the target was intact. To show that this did not happen would require a pre-conditioning of the projectile comparable to firing it through a target. For observation of residual masses direct methods such as x-rays seem preferable in spite of their difficulties. Some experiments of this type have been performed[22]. However, the Thor data collection and its extension do not contain enough information for

[22]L. Herr and C. Grabarek, "Ballistic Performance and Beyond Armor Data for Rods Impacting Steel Armor Plates," BRL MR 2575, 1976. (AD #B009979L)

comparison with a physical theory in spite of the large number of firings involved. In general, they do not tell us the three pieces of information enumerated above. In addition, they contain very few cases in which only one variable was changed while all others were held constant, something which is essential if fundamental comparisons are to be made.

B. Comments on Previous Models

Some of the advantages and disadvantages of purely empirical models such as the second Thor equation have been pointed out and will be elaborated upon below. Mass erosion and breakup is now being incorporated into some advanced continuum models with of course an increase in the complexities which already exist for such computer-dependent models. In the class of theoretical but simple intermediate models there are at least three which have been proposed to describe mass erosion, although there seem to be none for breakup.

The earliest intermediate erosion model was given by Tate[23]. He adapted a modified hydrodynamic theory first proposed by Hill, Mott and Pack[24], later published by Bishop, Hill and Mott[25] and still later modified by Eichelberger[26]. If we assume that the deceleration is negligible during some part of the penetration then Bernoulli's steady-state equation will hold approximately for the pressure at the stagnation point

$$P = \frac{1}{2} \rho_t u^2 + R = \frac{1}{2} \rho (v - u)^2 + Y \tag{76}$$

where R and Y are strength parameters or stresses above which the target and projectile respectively behave as fluids. Here u is the penetration speed and v is the speed of the rear of the penetrator for zero obliquity impact on a target plate, while ρ_t is the density of the target and ρ is the density of the projectile. Since $u \leqslant v$, we have

$$u = \frac{1}{(1 - \mu^2)} \left[v - \mu \sqrt{v^2 + A} \right] \tag{77}$$

where $\mu = \sqrt{\frac{\rho_t}{\rho}}$ and $A = \frac{2}{\rho_t} (1 - \mu^2) (R - Y)$. Since v and u are the

---

[23]A. Tate, "A Theory for the Deceleration of Long Rods After Impact," J. Mech. Phys. Solids 15, 387, 1967, and "Further Results in The Theory of Long Rod Penetration," Ibid. 17, 141, 1969.

[24]Unpublished Ministry of Supply Report, 1945.

[25]R. F. Bishop, R. Hill and N. F. Mott, Proc Phys Soc 57, 147, 1945.

[26]R. J. Eichelberger, J. Appl. Phys. 27, 68, 1956.

speeds of the back and front end of the rod respectively, then the decrease in length with time is

$$\dot{\ell} = - (v - u) .$$ (78)

The equation of motion of the back end of the rod was taken to be

$$\rho \, \ell \, \dot{v} = - Y,$$ (79)

assuming only a constant deceleration supported by the strength of the rod. Equation (79) is not strictly speaking compatible with Equation (76) which assumes $\dot{v}$ = 0. It is also for the speed of the rear of the rod, not its center of mass. Since dt = - $\rho \, \ell$ dv/Y from Equation (79), we can eliminate dt from Equation (72) and write

$$\frac{d\ell}{\ell} = \frac{\rho}{Y} \, (v - u) \, dv.$$ (80)

If we use Equation (77) in Equation (80) to eliminate u, and integrate from initial values of ℓ = L and v = V we obtain

$$\frac{\ell}{L} = \left[\frac{v + \sqrt{v^2 + A}}{V + \sqrt{V^2 + A}} \right]^{\left(\frac{R-Y}{\mu Y}\right)} \exp \left[\frac{\rho\mu}{2Y(1 - \mu^2)} \left\{ \left[v \sqrt{v^2 + A} - \mu \, v^2 \right] \right. \right.$$ (81)

$$\left. \left. - \left[V \sqrt{V^2 + A} - \mu \, V^2 \right] \right\} \right].$$

Here ℓ cannot vanish for finite V. Tate distinguished several cases. If R > Y, the rod behaves as a fluid until penetration ceases and u = 0

in Equation (77) or $v_c = \mu \sqrt{\frac{A}{1-\mu^2}}$. The length of the rod at this

point, namely ℓ_c, is found by using v_c in Equation (81). Beyond this point the hydrodynamic theory does not apply. Instead the bulk of the rod is taken to be a rigid body, and v in Equations (78) and (79) is taken to be the speed of the center of mass with, of course, u = 0. The center of mass continues to move forward but the tip merely erodes in place. Now dt = - dℓ/v from Equation (78) can be eliminated in Equation (79) to obtain Equation (80) with u = 0. If we integrate from initial values ℓ = ℓ_c and v = v_c to final values ℓ_f and v = 0 we obtain the final length

54

$$\ell_f = \ell_c \exp [- (R-Y)/Y] . \tag{82}$$

If the impact speed $V < v_c$, the tip merely deforms without penetration ($u = 0$) and an integration of Equation (80) from initial values $\ell = L$ and $v = V$ to $\ell = \ell_f$ and $v = 0$ gives

$$\ell_f = L \exp [- (\tfrac{1}{2} \rho V^2)/Y] \tag{83}$$

for the final length of the undeformed portion of the rod which depends exponentially on the ratio of the initial kinetic energy density $\tfrac{1}{2} \rho V^2$ to the rod strength Y. The lack of any penetration is an unreasonable feature and holds only for weak rods versus strong targets. Tate points out that his model only applies to perfectly plastic rod material for which the plastic wave speed $C = 0$. He compares Equation (83) to Taylor's[27] result for the deformation of a rod striking a rigid target, namely,

$$\ell_f = L \exp [- (\tfrac{\rho}{2Y}) V (V + 2C)] \tag{84}$$

which reduces to Equation (83) when $C = 0$.

If $R < Y$, then the rod behaves as a fluid until $u = v_c = \sqrt{-A/(1-\mu^2)}$

$= \sqrt{2(Y-R)/\rho_t}$ from Equation (77). The length of the rod at this point, ℓ_c, is found by using v_c in Equation (81). Beyond this point the rod continues to penetrate as a rigid body with $\ell_f = \ell_c$. Since the length does not change, $\dot{\ell} = 0$ in Equation (78) and $u = v$ throughout this second stage with v interpreted as the speed of the center of mass or of either end and $Y = \tfrac{1}{2} \rho_t v^2 + R$ from Equation (76). Then Equation (77) becomes

$$\rho \ell_c \dot{v} = - (\tfrac{1}{2} \rho_t v^2 + R) \tag{85}$$

which is simply Equation (15) with $b = 0$, $m_o = \rho \ell_c A$, $a = AR$ and $c = \tfrac{1}{2} \rho_t A$ with A the cross-sectional area. If we take $v = \dot{z}$ and $\dot{v} = v \, dv/dz$ in Equation (85) and integrate from $z = 0$ and $v = v_c$ to final values $z = T$ and $v = 0$ we obtain Robertson's result, Equation (16), with $V_1 = 0$, namely

[27]G. I. Taylor, Proc. Roy. Soc. A194, 287, 1948.

$$T/\ell_c = \frac{1}{\mu^2} \ln [1 + (\frac{1}{2} \rho_t v_c^2)/R] = \frac{1}{\mu^2} \ln [1 + \mu^2 (\frac{1}{2} \rho v_c^2)/R] \qquad (86)$$

where T is now the extra depth of penetration in a semi-infinite target and depends logarithmically on the ratio of the rod's energy density at the beginning of its rigid body motion to the strength of the target. If we use $v_c^2 = 2 (Y-R)/\rho_t$ in Equation (86) we obtain $T = (\ell_c/\mu^2) \ln (Y/R)$.

If $R = Y$, then $A = 0$ and $u = v/(1 + \mu)$ in Equation (77) while

Equation (80) becomes $d\ell/\ell = (\rho/Y) (\frac{\mu}{1 + \mu}) v \, dv$ so

$$(\ell/L) = \exp \left[- \frac{\mu\rho}{2 Y (1 + \mu)} (V^2 - v^2)\right] \qquad (87)$$

and the final length $\ell = \ell_f$ when $v = 0$ depends exponentially on $(\frac{1}{2} \rho V^2)/Y$ and as before can never be zero for finite V. The depth of penetration

$$z = \int_o^t u \, dT = \frac{1}{1 + \mu} \int_o^t v \, dt. \text{ If we use Equation (79) to eliminate}$$

$dt = - \rho \, \dot{\ell} \, dv/Y$ and use Equation (87) for ℓ we obtain

$$z = (L/\mu) \left[1 - \exp \left\{- \frac{\mu\rho}{2 Y (1 + \mu)} (V^2 - v^2)\right\}\right] \qquad . \qquad (88)$$

If $\rho_t = \rho$ so $\mu = 1$, then $A = 0$ and the above formulas simplify further, although closed form solutions for z (v) cannot be found for the general case $R \neq Y$ unless $R = nY$ with n integer.

A model similar to Tate's has been proposed by Walters and Majerus[28]. These authors give a unified theory for zero obliquity penetration by shaped charge jets or kinetic energy projectiles. In particular, in their Appendix II for steady-state jet penetration neglecting viscosity they obtain in their Equation (II-1)

$$0 = [\sigma + \rho (v - u)^2] - [\sigma_I + \rho_t u^2] \qquad (89)$$

[28]W. P. Walters and J. N. Majerus, "Impact Models for Penetration and Hole Growth," ARBRL-TR-02069, May 1978. (AD #A056294)

which is the same as Equation (76) above provided $\sigma = 2Y$ and $\sigma_t = 2R$ and the jet is not stretching so that the speed of its rear is equal to the speed of the interface of its tip with a postulated interaction region. In the special case $R = Y$ above we found $u = v/(1 + \mu)$. If z_0 is the standoff distance and we use the form $v = (z_0 + z)/t$, then $u = dz/dt = v/(1 + \mu) = (1/(1 + \mu))(z_0 + z)/t$ so

$$z = z_0 \left[(t/t_0)^{\frac{1}{1+\mu}} - 1 \right] \tag{90}$$

which is the formula obtained by Allison and Vitali[29] and discussed by DiPersio, Simon and Merendino[30].

In their Appendix IIIA, Walters and Majerus consider penetration by a rigid rod $\ell = 0$, $u = v$ (the second stage of the case $R < Y$ considered above) and their Equation (III-1) with the height of their interaction region $H = \ell_c$ becomes

$$2 \rho \ell_c \dot{v} = - (\rho_t v^2 + \sigma_t) \tag{91}$$

which is Equation (85) provided $\sigma_t = 2R$. In their Appendix III-B they consider penetration by a non-stretching jet (or rod) with constant speed v and obtain as their Equation (III-9) for u

$$\dot{u} = a' + b' u + c' u^2 \tag{92}$$

with $\rho H a' = (\sigma - \sigma_t) + \rho v^2$, $\rho H b' = - (\frac{\pi H}{A} \mu_t' + 2 \rho v)$ and $\rho H c' = (\rho - \rho_t)$ where $A = \pi r_0^2$ is the cross sectional area of the cylindrical rod and μ_t' is the target viscosity. Since $\rho H A$ is the mass in the interaction region moving with velocity u, Equation (92) is the equation of motion for this region or for the entire rod if $H = \ell$. The coefficient b' is negative, but the coefficient c' is negative only if $\rho_t > \rho$, while the coefficient a' is negative only if $\sigma_t > \sigma + \rho v^2$. Equation (92) has the same form as Equation (15) with $a' = - a/m_0$, $b' = - b/m_0$ and $c' = - c/m_0$

[29] F. E. Allison and R. Vitali, "A New Method of Computing Penetration Variables for Shaped Charge Jets," BRL 1184, 1963. (AD #400485)

[30] R. DiPersio, J. Simon and A. Merendino, "Penetration of Shaped Charge Jets Into Metallic Targets," BRL Report 1296, 1965. (AD #476717)

(with u playing the role of v) and its solutions are formally the same so we can find u (t) and $\int^t$ u dt in closed form for any value of q = 4 a' c' - $(b')^2$ in Equation (22). Then from Equation (78) we can find

$$\ell = L - v t + \int^t u \, dt \tag{93}$$

in closed form. For example, for q = 0, the simplest case, we have by analogy with Equation (26)

$$\int_0^t u \, dt = - \frac{b'}{2c'} t + \left(\frac{m_0}{c'}\right) \ell n \left[1 + \left(\frac{c'}{m_0}\right)\left(\frac{b'}{2c'} + u_0\right) t\right] \tag{94}$$

which can be used in Equation (93) to obtain ℓ (t). Similarly equations analogous to Equations (24) and (28) could be used for q < 0 or q > 0 respectively. Since v is not really a constant in practical cases, especially toward the end of the motion in a semi-infinite target, we can expect Equation (93) to agree with experiment only approximately and only during the early part of the motion. Equation (93) requires ℓ to vanish in finite time for any q, contrary to experiments with semi-infinite targets, but the agreement is reasonable during the initial stages as noted by Walters and Majerus. Presumably numerical solutions of their more general equations will give predictions in better agreement with experiment at later times.

In their Appendix IV Walters and Majerus consider the case of a non-eroding rod ($\dot{\ell}$ = 0) for which they obtain Equation (15) for u = v with a = A σ_t, b = 2π H μ_t and c = A ρ_t where σ_t, μ_t and ρ_t are the yield stress, viscosity and density respectively for the target. The solutions have already been discussed above and by Zook[2].

Another erosion model for zero obliquity impact has been proposed by Recht[31]. This model was previously described at the Fourteenth Annual Meeting of the Society of Engineering Sciences at Lehigh University in 1977 and earlier at the Workshop on Mechanics of Impact and Penetration, December 1976, Aberdeen Proving Ground, Md. An outline of his model can also be found on pp 25-29 of the Backman and Goldsmith review article cited above[1]. When the projectile speed exceeds an assumed constant plastic wave speed C, a shockwave develops near the tip of the projectile, eroding it away. When the projectile speed falls below C, deformation of the tip takes place, shortening it because of lateral spreading. When this spreading exceeds some critical amount (postulated to be 25% in Recht's application to a case of a steel cylinder impacting a steel

[31]R. F. Recht, "Taylor Ballistic Impact Modeling Applied to Deformation and Mass Loss Determinations," Int. J. of Eng. Sciences, 16, 809, 1978.

plate), then the material which has spread beyond this distance is assumed to be sheared off as the motion proceeds.

In arriving at Equation (41) of his 1978 paper, Recht[32] considered that the main projectile changes its mass from m to $m + dm$ and changes the speed of its center of mass from v to $v + dv$ during the time interval dt. Here dm and dv are negative. The eroded mass $(-dm)$ was assumed to have the plate plug speed, v_p. More properly, at the end of the interval dt the plug speed is $v_p + dv_p$, although this will not matter as we will see shortly. If one makes the same free collision assumption that Recht and Ipson made in their 1963 paper cited above[5] with m_p already formed and constant throughout the motion, then the momenta before and after this collision would be equal, that is,

$$mv + m_p v_p = (m+dm)(v+dv) + m_p(v_p+dv_p) + (-dm)(v_p+dv_p). \qquad (95)$$

If we neglect the second order terms $dm\,dv$ and $dm\,dv_p$, we find

$$m\,dv = (-dm)(v-v_p) - m_p\,dv_p \qquad (96)$$

and if we let $(F\,dt) = m\,dv$ with $F = -\sigma A$, we obtain Recht's Equation (41) mentioned above, namely,

$$\sigma A\,dt + (-dm)(v-v_p) = m_p\,dv_p . \qquad (97)$$

More properly, when $dm \neq 0$, Newton's law requires

$$m\,dv + v\,dm = F\,dt = -\sigma A\,dt \qquad (98)$$

which gives us from Equation (96)

$$\sigma A\,dt + v_p\,dm = m_p\,dv_p \qquad (99)$$

instead of Equation (97). There seem to be at least three shortcomings in Recht's model. First of all, he makes the unrealistic assumption of a free collision in Equation (95). In his earlier paper with Ipson he was able to compensate for this by equating the catchall energy E to the change in energy of the mass m_o during the assumed free collision, requiring that the exit speed V_1 be equal to the speed V_{1f} after the free

[32]*Private communication to J. Dehn, 14 Dec 1978.*

59

collision, thus producing an expression for the shearing work W. In his erosion model above he does not employ energy balances to compensate for the unrealistic assumption of a free collision, so the error might be uncorrected. However, as we have noted, he does ignore the theoretical requirement that (F dt) = m dv + v dm, so that this error might compensate for the free collision assumption. It might also make it worse. Thirdly, it would be desirable to use more than a simple constant force F = -σA. Even his earlier model with Ipson produced a result similar in form to that of Robertson who used F = - (a$'$ A) - ($\frac{1}{2}$ γ ρ_t A) v^2. We have also seen the desirability of including terms dependent on v and on the depth of penetration, s.

Many physicists take the attitude that compensating errors are perfectly acceptable in a theory as long as they result in a definite prescription for calculations which agree with experiment. There is something to be said for this point of view just as there is something to be said for purely empirical interpolation models which also agree with experiment at least for limited conditions. However, there is also something to be said for the view that we should not be satisfied with a fortuitous compensation of errors if we expect to make any progress in achieving a broader understanding of the physical world. Dirac is one of the foremost proponents of this latter view.

"My early research work, in the early 1920's was based on Bohr orbits, and was completely unsuccessful. I was taking the Bohr orbits as physically real and trying to build up a mathematics for them.... One sees now how futile such work was.... The Bohr orbits were an unsound physical concept and should not be used as the basis for a theory."[33]

Dirac goes on to relate how his dissatisfaction with the Klein-Gordon equation led him to develop his own relativistic equation for the electron from which the concept of spin naturally followed. He also describes more recent efforts by physicists to solve the relativistic wave equation for interacting particles, efforts which have led to divergent integrals which are discarded by a renormalization of fundamental physical constants. Although most physicists are satisfied with this since their calculations agree with experiment, Dirac gives cogent reasons for not being content. He then says,

"For these reasons I find the present quantum electrodynamics quite unsatisfactory. One ought not to be complacent about its faults. The agreement with observation is presumably a coincidence, just like the original calculation of the hydrogen spectrum with Bohr orbits. Such coincidences are no reason for turning a blind eye to the faults of a theory."[33]

_____

[33]*P. A. M. Dirac, "The Mathematical Foundations of Quantum Theory," in Mathematical Foundations of Quantum Theory, Ed. by A. R. Marlow, N.Y. Academic Press, 1978.*

VII. A NEW MODEL OF MASS EROSION

A. Development of the Theory

Here erosion is being thought of as a continuous process which can be described by differential equations. We might expect at least the dissipative terms in our force field to depend on the instantaneous values of the mass (m) and /or its rate of change ($\dot{m}$). A dissipative term accounts for kinetic energy loss by a decrease in velocity in the constant mass case. When the mass itself is decreasing, additional energy loss should also be described by such a term. Let us presume that this is true and proceed to make particular assumptions about our dissipative terms.

The viscous loss coefficient b_1 has the dimensions of mass per unit time so a simple modification of this term might be

$$-(b_{1s} - a_{1s} \dot{m}) \dot{s} \tag{100}$$

where ϵ_{1s} is a positive, dimensionless constant. When the mass change rate is negative ($\dot{m} < 0$), then the dissipative coefficient b_{1s} is effectively increased, while for $\dot{m} > 0$ mass gains tend to offset velocity losses and the coefficient b_{1s} is effectively decreased. When $\dot{m}=0$ we have the constant mass case and return to the original form of this term. Examples involving $\dot{m}<0$ are target penetrators or space vehicle re-entry shields. Examples involving $\dot{m}>0$ might be rain or sleet in the atmosphere or crystallites precipitating from a chemical solution.

If we wish to modify the coefficient of the v^2 term we might consider a form like

$$- b_{2s} (m_o/m) (\dot{s})^2 \tag{101}$$

This gives us a reduction in retardation when $(m_o/m)<1$ and an increase for $(m_o/m)>1$ with a return to our original form when $(m_o/m)=1$, the constant mass case. We will not treat the v^2 term in this paper.

Since $d(m \dot{s})/dt = m \ddot{s} + \dot{m} \dot{s}$ is the kinematic expression when $m=m(t)$, we must solve the equation

$$m \ddot{s} + \dot{m} \dot{s} + (b_{1s} - \epsilon_{1s} \dot{m}) \dot{s} + b_{2s} (m_o/m) \dot{s}^2 + a_s + d_{1s} s + d_{2s} s^2 = 0 \tag{102}$$

where $m(t)$ and $s(t)$ ($s=x$, y or z) must both be determined.

Let $\phi = \phi(t)$ be an arbitrary transformation of the independent variable so that $\dot{s} = \dot{\phi}\ ds/d\phi$ and $\ddot{s} = \dot{\phi}^2\ (d^2s/d\phi^2) + \ddot{\phi}\ (d\dot{\phi}/d\phi)(ds/d\phi)$. Then Equation (102) becomes

$$M\left(\frac{d^2s}{d\phi^2}\right) + B_{1s}\left(\frac{ds}{d\phi}\right) + B_{2s}\left(\frac{ds}{d\phi}\right)^2 + a_s + d_{1s}\ s + d_{2s}\ s^2 = 0 \qquad (103)$$

where
$$M = m\dot{\phi}^2 \qquad (104)$$

$$B_{1s} = \left[m\ \frac{d\dot{\phi}}{d\phi} + b_{1s} + \left(1 - \varepsilon_{1s}\right)\dot{m}\right]\dot{\phi} \qquad (105)$$

$$B_{2s} = b_{2s}\ (m_0/m)\ \dot{\phi}^2 \qquad (106)$$

Now let us choose ϕ so that at least M and B_{1s} are constants and explore the implications of this choice. One implication is evident from the form of Equation (103), namely, that whatever solutions we found for $z(t)$ in Equation (44) can be used to write $s(\phi)$ here. Another implication is that Equation (104) becomes

$$M = m\dot{\phi}^2 = m_0\dot{\phi}_0^2 \qquad (104a)$$

where $\dot{\phi}_0$ is the value of $\dot{\phi}$ at $t=0$. We can also use Equation (104a) to obtain

$$\dot{m} = \dot{\phi}\ dm/d\phi = \dot{\phi}\left[-2M/\dot{\phi}^3\right]\left(d\dot{\phi}/d\phi\right) = -2m\ d\dot{\phi}/d\phi \qquad (107)$$

and use this to eliminate $(md\dot{\phi}/d\phi)$ in Equation (105) to obtain

$$B_{1s} = \left[b_{1s} - \left(\varepsilon_{1s} - \frac{1}{2}\right)\dot{m}\right]\dot{\phi} = \left[b_{1s} - \left(\varepsilon_{1s} - \frac{1}{2}\right)\dot{m}_0\right]\dot{\phi}_0. \qquad (108)$$

Now for the constant mass case $(\dot{m}_0 = 0)$, $B_{1s} = b_{1s}\ \dot{\phi}_0$ from Equation (108). However in this case we require $B_{1s} = b_{1s}$, so $\dot{\phi}_0 = 1$. This implies $M = m_0$ in Equation (104a). If we put Equation (104a) in Equation (106) we find $B_{2s} = b_{2s}\left(\frac{m_0}{m}\right)^2$ which is not constant. If we had used (m/m_0) instead of (m_0/m) in Equation (101), then $B_{2s} = b_{2s}$, also a constant.

62

Consequently, Equation (108) is the second relation we need to solve for $\phi(t)$ and so $m(t)$ and $s(t)$. Since $m = m_o/\dot\phi^2$ from Equation (104a) and $\dot{m} = -2\, (m_o/\dot\phi^2)\, d\dot\phi/d\phi$ from Equation (107), Equation (105) becomes

$$B_{1s} = b_{1s}\dot\phi + 2\left(\epsilon_{1s} - \frac{1}{2}\right)\left(m_o/\dot\phi\right) d\dot\phi/d\phi \tag{109}$$

which can be integrated to obtain

$$\dot\phi = \left[\left(1 - b_{1s}/B_{1s}\right) \exp\left\{-B_{1s}\ (\phi)/\left[2m_o\left(\epsilon_{1s} - \frac{1}{2}\right)\right]\right\} + b_{1s}/B_{1s}\right]^{-1} \tag{110}$$

where we have used $\dot\phi_o = 1$ and let $\phi_o = t_o = 0$ for convenience. Equation (110) can be integrated once more to obtain

$$\left(b_{1s}/B_{1s}\right)\phi + \left[2\,m_o\left(\epsilon_{1s} - \frac{1}{2}\right)/B_{1s}\right]\left(1 - b_{1s}/B_{1s}\right)\left[1 - \exp\left\{-\phi/\right.\right.$$
$$\left.\left.\left[2\,m_o\left(\epsilon_{1s} - \frac{1}{2}\right)/B_{1s}\right]\right\}\right] = t \tag{111}$$

which gives us a relation between ϕ and t. The left side of Equation (111) is a transcendental function of ϕ and becomes algebraic only in certain simple cases such as $b_{1s} = B_{1s}$ (the constant mass case for which $\phi = t$) or $b_{1s} = 0$ for which

$$\phi = \left(\dot{m}_o/2\,m_o\right) \ln\left[1 + \left(\dot{m}_o/2\,m_o\right) t\right] \tag{112}$$

when we use Equation (108). The general form, Equation (111), gives the transformation which is required to make M and B_{1s} in Equation (103) constant. By using Equation (110) in Equation (104a) we also obtain

$$m = m_o\left[\left(1 - b_{1s}/B_{1s}\right) \exp\left\{-\phi/\left[2\,m_o\left(\epsilon_{1s} - \frac{1}{2}\right)/B_{1s}\right]\right\} + b_{1s}/B_{1s}\right]^2 \tag{113}$$

If $b_{1s} = B_{1s}$, then $m = m_o$, the constant mass case. If $b_{1s} = 0$, then

$$m = m_o\ e^{\dot{m}_o\phi/m_o} = m_o\left[1 + \left(\dot{m}_o/2\,m_o\right) t\right]^2. \tag{114}$$

In summary, instead of assuming a form for m(t), we have made reasonable assumptions about modifications to the coefficients in our force terms, we have transformed the independent variable in order to obtain another equation with constant coefficients neglecting the v^2 term and have derived a relation for $m\left[\phi(t)\right]$. This enables us to write closed form expressions for the displacement components $s\left[\phi(t)\right]$, provided we require

$$b_{1x} \left/ \left(\epsilon_{1x} \frac{-1}{2}\right)\right. = b_{1y} \left/ \left(\epsilon_{1y} \frac{-1}{2}\right)\right. = b_{1z} \left/ \left(\epsilon_{1z} - \frac{1}{2}\right)\right. \tag{115}$$

and

$$B_{1x} \left/ \dot{b}_{1x}\right. = B_{1y} \left/ \dot{b}_{1y}\right. = B_{1z} \left/ \dot{b}_{1z}\right. \tag{116}$$

so that $\dot{m}$ and $\dot{\phi}$ will be the same for all components in Equation (108). Equations (115) and (116) then guarantee that

$$B_{1x} \left/ \left(\epsilon_{1x} - \frac{1}{2}\right)\right. = B_{1y} \left/ \left(\epsilon_{1y} - \frac{1}{2}\right)\right. = B_{1z} \left/ \left(\epsilon_{1z} - \frac{1}{2}\right)\right. \tag{117}$$

so that ϕ and m in Equation (111) and Equation (113) will be the same in all three component Equations (103) neglecting the v^2 term. Such a transformation might be called a constant mass frame transformation, since, in the new time frame ϕ, $M=m_o$ is constant and is acted upon by force terms containing constant coefficients one of which multiplies the transformed speed $ds/d\phi$. The utility of such a transformation can only be judged by comparison with experiment.

First let us examine the qualitative behavior of our solution for m. If we use Equation (111) and Equation (113) in Equation (107), we obtain

$$\dot{m} = \dot{m}_o \exp \left\{ -\phi \left/ \left[2 \, m_o \left(\epsilon_{1s} - \frac{1}{2}\right) \left/ B_{1s}\right.\right]\right.\right\} \tag{118}$$

where we have also used Equation (108). We see that $\epsilon_{1s} = \frac{1}{2}$ corresponds to the constant mass case since it makes $\dot{m} = o$ for all $\phi = t > 0$ $(\dot{b}_{1s} = B_{1s})$ in Equation (111). Here we are interested in the case m<0 for which it is convenient to write Equation (108) as $B_{1s} = \dot{b}_{1s} + (\epsilon_{1s} - \frac{1}{2}) \, (-\dot{m}_o)$.

When $\varepsilon_{1s} > \frac{1}{2}$, then $B_{1s} > b_{1s} > 0$ and the right side of Equation (111) is positive and increases without limit. If ϕ is also positive, then both terms on the left of Equation (111) are positive with the second term approaching a maximum value while the first increases without limit so that for late times ϕ becomes approximately proportional to t. Negative ϕ is not allowed since both terms on the left of Equation (111) would then be negative. For $\phi > 0$, Equation (118) says that $|\dot{m}|$ decreases as ϕ (or t) increases. Consequently a plot of m versus t will be concave upward with m decreasing to the limiting value $m_0 (b_{1s}/B_{1s})^2$ as t increases without limit. In this case, m will truly vanish only when $b_{1s} = 0$.

When $\varepsilon_{1s} < \frac{1}{2}$, then $B_{1s} \gtrless 0$. If $B_{1s} > 0$ because $b_{1s} > |\varepsilon_1 - \frac{1}{2}| (- \dot{m}_0)$, then $b_{1s} > B_{1s} > 0$ and Equation (111) has a solution only for the finite $0 \leqslant t \leqslant t_{MAX}$ with $\phi > 0$. Negative ϕ is not allowed since the first term on the left of Equation (111) would be negative and eventually dominate the second term. At t_{MAX}, $dt/d\phi = \frac{1}{\dot{\phi}} = (m/m_0)^{1/2}$ from Equations (111), (110) and (104a) and vanishes for

$$\phi_{MAX} = [- 2 m_0 (\varepsilon_{1s} - \frac{1}{2})/B_{1s}] \, \ell n \, [1/(1 - B_{1s}/b_{1s})] \quad (119)$$

or

$$t_{MAX} = [2 m_0 (\varepsilon_{1s} - \frac{1}{2})/B_{1s}]\{1 - (b_{1s}/B_{1s}) \, \ell n \, [1/(1 - B_{1s}/b_{1s})]\}. \quad (120)$$

From Equation (118), $|\dot{m}|$ increases as ϕ (or t) increases so that a plot of m versus t is concave downward with m vanishing at $t = t_{MAX}$. If $B_{1s} = 0$ because $b_{1s} = |\varepsilon_{1s} - \frac{1}{2}| (- \dot{m}_0)$, then, since

$$\lim_{B_{1s} \to 0} \left[\frac{1 - \exp\left\{ - B_{1s} \, \phi/[2 m_0 (\varepsilon_{1s} - \frac{1}{2})] \right\}}{B_{1s}} \right] = \phi/[2 m_0/(\varepsilon_{1s} - \frac{1}{2})], \quad (121)$$

Equation (111) reduces to

$$\phi = [2 m_0/(- \dot{m}_0)] [1 - \sqrt{1 - (- \dot{m}_0/m_0) \, t}] \quad (122)$$

65

so $t_{MAX} = [m_o/(-\dot{m}_o)]$ and $\phi_{MAX} = 2\, t_{MAX}$ when m vanishes. In this case, from Equation (118), $\dot{m} = \dot{m}_o$ and m decreases linearly with time as follows

$$m = m_o [1 - (- \dot{m}_o/m_o)t] . \qquad (123)$$

If $B_{1s} < 0$ because $b_{1s} < |\varepsilon_{1s} - \frac{1}{2}| (- \dot{m}_o)$, then ϕ must again be positive and a solution exists only for a finite time as before expressed by Equation (120). Now however from Equation (118) we see that $|\dot{m}|$ decreases as ϕ (or t) increases so that a plot of m versus t is concave upward with m vanishing at $t = t_{MAX}$.

In summary, for $\dot{m} < 0$, we can obtain two types of mass loss with time, depending on whether ε_{1s} is greater or smaller than 0.5. If $\varepsilon_{1s} > 0.5$, then m will not vanish even in a semi-infinite target provided $b_{1s} \neq 0$. However, for sufficiently small b_{1s}/B_{1s} it might appear to vanish. Erosion decreases as the speed decreases. If $\varepsilon_{1s} < 0.5$, then m must vanish in finite time, presuming the target is thick enough, with the erosion rate increasing, decreasing or remaining constant during the motion. Thus the model offers a variety of possibilities. The case $\varepsilon_{1s} = 0$, that is no modification of the coefficient b_1 in Equations (100) and (102), is a particular case of $\varepsilon_{1s} < 0.5$ and so cannot be used to describe penetration in a semi-infinite target since m does not always vanish in such a target.

A similar analysis can be made for $\dot{m} > 0$.

B. A Classical Application: The Oscillator with Diminishing Mass

A well-known classical problem is the constant mass harmonic oscilla-tor in a forcing field and a wide variety of electrical and mechanical problems have been solved by applying the solution of the basic differen-tial equation. Suppose the oscillator mass is not constant but changes during the motion. How does the solution change? An answer has been given in the previous section which we will now apply to a particular case which can be easily tested in the laboratory.

Consider a liquid-filled vessel of constant interior cross-sectional area A, height h_o, and mass $m_{To} = m_v + m_o$ suspended in the earth's gravitational field by a spring of negligible mass and friction and with spring constant k. Here m_v is the constant mass of the vessel while m_o is the initial mass of the liquid so m_{To} is the initial total mass. At time zero the vessel is released from its position a distance S below its equilibrium position and simultaneously a hole of cross-sectional

66

area a < A is opened in the bottom of the vessel. The mass of the liquid at any time is $m = \rho A h$ where ρ is its constant density and h is the height of the liquid at time $t > 0$. The speed of recession of the liquid surface relative to the vessel is $v = -\dot{h} = -\dot{m}/(\rho A)$. From Bernoulli's principle the exit speed, v_E, is related to v by

$$\frac{1}{2} \rho (v_E^2 - v^2) = \frac{1}{2} \rho v_E^2 [1 - (a/A)^2] = \rho gh = \rho g (m/\rho A) \quad (124)$$

since $v = (a/A) v_E$ by the equation of continuity. Since the total mass is $m_T = m_V + m$ so $\dot{m}_T = \dot{m} = -\rho A v = -\rho a v_E$, then

$$\dot{m} = -\sqrt{\frac{2 \rho g A (a/A)^2}{[1 - (a/A)^2]}} \; m^{1/2} = -\sqrt{\frac{m_o \; 2g \; (a/A)^2}{h_o[1 - (a/A)^2]}} \; m^{1/2}. \quad (125)$$

If we integrate this equation we obtain

$$m_T - m_V = m = m_o \left[1 - \frac{1}{2 \, m_o} \sqrt{\frac{2 \, g \, (a/A)^2 \, (\rho A h_o)^2}{h_o \, [1 - (a/A)^2]}} \; t \right]^2 \quad (126)$$

which has the same form as Equation (114) above with

$$\dot{m}_o = -\sqrt{\frac{2 \, g \, (a/A)^2 \, (\rho A h_o)^2}{h_o \, [1 - (a/A)^2]}} = -m_o \sqrt{\frac{2 \, g \, (a/A)^2}{h_o \, [1 - (a/A)^2]}} = -2 \, K \, m_o \quad (127)$$

which defines the constant K. From Equation (127) we can determine $(-\dot{m}_o)$, knowing m_o, g, a, A and h_o. A specialized form of Equation (102) can be used to describe the system we are considering, namely, an undamped ($b_{1s} = b_{2s} = 0$), harmonic ($d_1 = k$, $d_{2s} = 0$) oscillator with diminishing mass ($\dot{m}_T = \dot{m} < 0$) in the earth's gravitational field ($a_s \to mg$). Thus we have

67

$$m_T \ddot{s} + (1 - \varepsilon_1) \dot{m}_T \dot{s} + k s = (- m_T g).$$ (128)

If we let $\phi = \phi(t)$ be an arbitrary transformation of the independent variable t as before, we obtain

$$m_T \dot{\phi}^2 \frac{d^2 s}{d\phi^2} + m_T \dot{\phi} \frac{d\dot{\phi}}{d\phi} \frac{ds}{d\phi} + (1 - \varepsilon_1) \dot{m}_T \dot{\phi} \frac{ds}{d\phi} + k s = - m_T g$$ (129)

or

$$M \frac{d^2 s}{d\phi^2} + B_1 \frac{ds}{d\phi} + k s = (- m_T g)$$ (130)

where Equations (104) and (105) for the constants M and B_1 are in this case $M = m_T \dot{\phi} = m_{To} \dot{\phi}_o^2 = m_{To} = m_o + m_v$ and $B_1 = [m_T \, d\dot{\phi}/d\phi + (1 - \varepsilon_1) \dot{m}_T] \dot{\phi} = - (\varepsilon_1 - \frac{1}{2}) \dot{m}_{To}$, by Equations (105) and (108). In this case we have from Equations (111) and (127)

$$\phi = (1/K) \ln (1 - Kt)^{-1}$$ (131)

and by Equations (114), (126) and (127)

$$m_T - m_V = m = m_o e^{-2 K\phi} = m_o (1 - Kt)^2$$ (132)

then Equation (130) becomes

$$M \frac{d^2 s}{d\phi^2} + B_1 \frac{ds}{d\phi} + k s = - g (m_V + m_o e^{-2 K\phi}).$$ (133)

The general solution is the sum of the solution of the homogeneous equation (right side of Equation (133) set equal to zero) (given by Equation (45) with $\delta = 0$) and a particular solution. In other words, our solution has the form

$$s = C_1 e^{\gamma^+ \phi} + C_2 e^{\gamma^- \phi} + (C_3 + C_4 e^{-2K\phi})$$ (134)

68

If we substitute Equation (134) into Equation (133) and require the coefficients of the exponentials to vanish we find

$$\gamma^{\pm} = -\frac{B_1}{2M} \pm \sqrt{\left(\frac{B_1}{2M}\right)^2 - k/M} = -\alpha \pm i\omega \qquad (135)$$

$$C_3 = -m_V\, g/k \qquad (136)$$

$$C_4 = -m_0\, g/[4\,M\,K^2 - 2\,K\,B_1 + k] \qquad (137)$$

with C_1 and C_2 to be determined from initial conditions.

If we hang the empty vessel on the spring it will extend a distance $(-C_3)$ which determines k in Equation (136) once we measure m_V and g. If we fill it with a liquid mass m_0 and keep the hole closed so a = K = 0 it will extend an additional distance $m_0\, g/k$ which gives us a second measure of k once we measure m_0. If we open the exit hole and observe the relaxation of the system, the motion is described by the particular solution

$$s = C_3 + C_4\, e^{-2K\phi} = -(g)[m_V/k + m_0\,(1 - Kt)^2/(4\,M\,K^2 - 2\,K\,B_1 + k)]. \qquad (138)$$

At the end of the relaxation time, $1/K$, or $\phi = \infty$ the vessel is empty and motionless at $s = -g\,m_V/k$. If we measure s at various times during the motion, we can determine $B_1 = (\epsilon_1 - \frac{1}{2})\,(-\dot{m}_0) = (\epsilon_1 - \frac{1}{2})\,2\,m_0\,K$, that is, determine ϵ_1, since we know m_0 and K. Now we know C_3 and C_4.

If we refill the vessel as before and pull it down an additional distance $(-S)$, then release it as we simultaneously open the exit hole, an oscillatory motion is superimposed on the relaxation motion. The initial conditions are

$$s_0 = C_1 + C_2 + (C_3 + C_4) = -S + (C_3 + C_4) \qquad (139)$$

and $\dot{s}_0 = \dot{\phi}_0(ds/d\phi)_0 = (ds/d\phi)_0 = 0$, which gives

69

$$0 = C_1 \gamma^+ + C_2 \gamma^- - 2 K C_4.$$

(140)

From Equations (139) and (140) we find

$$C_1 = (2 K C_4 + \gamma^- S)/(\gamma^+ - \gamma^-)$$

(141)

$$C_2 = (2 K C_4 + \gamma^+ S)/(\gamma^+ - \gamma^-)$$

(142)

so Equation (134) becomes

$$s = e^{-\alpha\phi}[\{(2 K C_4 - \alpha S)/\omega\} \sin \omega\phi - S \cos \omega\phi]$$
$$+ C_3 + C_4 e^{-2 K\phi}$$

(143)

where C_3 is given by Equation (136) and C_4 is given by Equation (137). This describes the motion until the liquid is gone. Again, when the liquid is gone at $t = 1/K$ sec or $\phi = \infty$, $s = - m_V g/k$ by Equation (143) and the motion ceases. For $t < 1/K$ the decay of the amplitude is described by

$$e^{-\alpha\phi} = (1 - Kt)^{\alpha/K}$$

where

(144)

$$\frac{\alpha}{K} = \frac{B_1}{2 m_{To} K} = \frac{(\varepsilon_1 - \frac{1}{2})(- \dot{m}_o)}{2(m_o + m_V)K} = \left(\frac{m_o}{m_o + m_V}\right)(\varepsilon_1 - \frac{1}{2})$$

(145)

so observing the amplitude as a function of time would also give a measure of ε_1. If $\varepsilon_1 = 1.5 + m_V/m_o$, then $\alpha/K = 1$ and the amplitude decays linearly with time at a constant rate $(- K)$. If $\varepsilon_1 > 1.5 m_V/m_o$, a plot of amplitude versus time will be concave upward with the decay rate initially of greater magnitude but approaching zero as $t \to 1/K$. If the hole is not opened, so $K = \alpha = \dot{m}_o = 0$, then $\phi = t$ and from Equation (143)

$$s = - S \cos \omega_t t - m_{To} g/k$$

(146)

where $\omega_t = \sqrt{k/m_{To}}$, describing undamped harmonic motion of a constant mass with constant offset $(- m_{To} g/k)$. A measurement of $\omega_t = 2\pi\nu = 2\pi/\tau$

where ν is the frequency and τ is the period in real time will give another measure of k.

When the hole is opened at $t = \phi = 0$, ω is a constant only in the transformed time ϕ. We can determine the turning points of the motion by setting $\dot{s} = \dot{\phi}\, ds/d\phi = 0$ (or $ds/d\phi = 0$ since $\dot{\phi} = \frac{1}{(1-Kt)} \neq 0$). In the s-$\phi$ plane the period $\tau_\phi = 2\pi/\omega$ where $\omega = \sqrt{k/m_{To} - [B_1/(2\,m_{To})]^2}$ is constant and successive minima occur for $\phi_n = n\,\tau_\phi = n\,(2\pi/\omega)$ while real time successive minima occur at

$$t_n = (1 - e^{-K\phi})/K = (1 - e^{-nK2\pi/\omega})/K \qquad (147)$$

with $n = 0, 1, 2 \ldots$, using Equation (131). As can be seen the difference $t_{n+1} - t_n$ becomes smaller as time increases. As expected, the oscillation becomes more rapid as the mass decreases.

This latter point was checked experimentally by suspending a 16 gm vessel (waxed cardboard carton) of cross sectional area A = 50 cm^2 and height h_o = 9.8 cm from a spring with constant k = 1.5 x 10^5 dyne/cm determined by hanging various weights upon it and observing its extension. This vessel was filled with 490 gm of soapy water (to improve the flow) and a real time period determined by recording the time at which every fortieth minimum occurred and averaging over ten such measurements. The time was measured to the nearest 0.01 second using the crystal controlled timer built into the Hewlitt-Packard Model 55 hand held electronic calculator. The memory was used to record and average the times, giving an average period of 0.413 ± .002 sec with the actual difference between high and low values being 0.2/40 = 0.005 sec. If $\omega_t = \sqrt{k/m_{To}}$ then

$k = m_{To}\,\omega_t^2 = 506\,(2\pi/.413)^2 = 506\,(231.451) = 1.17$ x 10^5 which is 22% lower then the value measured by extension. The difference is due to friction which we have been neglecting. Actually $\omega_t = \sqrt{k/m_{To} - [b_1/2m_{To}]^2}$,

implying that b_1 the friction coefficient, is $2\,m_{To}\sqrt{k/m_{To} - \omega_c^2} =$

8.16 x 10^3 gm/sec using k = 1.5 x 10^5 dyne/cm so that b_1 is not negligible and must be known if we wish to calculate the observed decay in amplitude. For this system with m_{To} = 506 gm, oscillations could be observed for more then five minutes, but the system appeared *stationary*

after 7 minutes. A solid brass weight of 500 gm was observed to oscillate for about 10 minutes on the same spring, indicating a damping contribution from the liquid motion. Still, we don't need to know b_1 in order to check the fact that ω_t is constant for a constant mass. In this case $\omega_t = 2\pi/(.413) = 15.21 \text{ sec}^{-1}$.

A circular hole was opened in the bottom center of the vessel and the drain time (until dripping began) was found to be $1/K = 250$ sec, so $K = .004 \text{ sec}^{-1}$. Thus the effective diameter was 0.19 cm and the effective area of the hole was 0.028 cm^2 which is only 35% of the actual area of 0.079 cm^2 (actual diameter 0.3175 cm) because of the well-known vena contracta effect. The filled vessel was pulled down a distance $S = 1$ cm and released at time zero while the hole was opened simultaneously. As before, the time at which every fortieth minimum occurred was measured, giving the values in Table II.

Table II. Times (sec) for Minima of Decreasing
Mass Oscillator

n	0	40	80	120	160	200	240	280	320	360
t_n (obs)	0	15.98	31.33	45.77	59.38	71.82	83.90	95.36	106.59	117.41
$t_n - t_{n-40}$	-	15.98	15.35	14.44	13.61	12.44	12.08	11.46	11.23	10.82
$(t_n - t_{n-40})/40$	-	.400	.384	.361	.340	.311	.362	.286	.281	.270
t_n (calc)	0	16.25	31.44	45.64	58.93	71.34	82.96	93.81	103.96	113.45

If we extrapolated $(t_n - t_{n-40})/40$ to time zero we would obtain 0.413 which is the time for one vibration with the constant mass system. The observed increase in vibration frequency agrees at least qualitatively with the model. If we wish to calculate ω in Equation (147), namely,

$$\omega = \sqrt{k/m_{To} - [\{b_1 + (\varepsilon_1 - \frac{1}{2})(- \dot{m}_o)\}/(2\ m_{To})]^2} \qquad (149)$$

we can use $b_1 = 8.16 \times 10^3$ gm/sec as above. Since $(- \dot{m}_o) = 2\ K\ m_o = 3.92$ gm/sec, ε_1 must be considerably larger than 1/2 to have much effect on the value of ω. In order to measure ε_1 we would need precise equipment since $k >> 2\ K\ B_1$ in Equation (133) for $\varepsilon_1 < 10^6$. If we assume $\varepsilon_1 = 100$, then $\omega = 15\ \text{sec}^{-1}$ in Equation (149) which is not much less than $\omega_t = 2\pi/(.413) = 15.21\ \text{sec}^{-1}$. If we use $\omega = 15\ \text{sec}^{-1}$ and $K = .004$

72

sec^{-1} in Equation (147) we can calculate the t_n values given in the last line of Table II. These are in reasonable agreement with the observed values, although the agreement becomes worse as the motion damps out. A slightly different choice for ε_1 could have made the observed and calculated values agree initially. If the spring were weaker or the mass heavier, better agreement might be expected for a longer time.

Even the classical damped harmonic oscillator with constant mass requires a theoretically infinite time for its amplitude to decay to zero and so does not perfectly describe real mechanical (or electrical) oscillators which cease their motion in finite time because of factors not adequately represented by the simple equation used. Similarly, we cannot expect a perfect description of a variable mass oscillator by a simple amendment of the constant mass equation.

We have given this illustration to show that the proposed amendment to the classical equation, namely the added damping factor $(- \varepsilon_1 \dot{m})$, can provide a reasonable description in at least one simple case up to 360 oscillations. Our intention here is to use this amendment to describe an eroding penetrator for which the motion should be completed in less than one cycle. Thus, our expectation is that the model will be good enough for the practical calculations we have in mind. Of course only comparisons with experimental projectile-target data will tell us how close this agreement will be. We will make such comparisons in the next subsection.

C. Applications to Target Penetration

Tate[34] has given time-dependent data for the penetration and erosion of dural and aluminum rods striking a semi-infinite polyethylene target at zero obliquity. The 5.45 gm rods were 6.35mm in diameter and 63.5mm long while the striking speed was 1.646 km/s. Figure 5a gives the position of the tip of the dural rod as a function of time. Tate's data also gave the position of the rear of the rod as a function of time, but this is not shown to avoid crowding. Instead the difference between the tip and rear which is the remaining length is shown in Figure 5b. For the dural rod the final depth of penetration of the tip was about 155mm while the remaining length was 18mm. Figures 6a and 6b show similar data for an aluminum rod which had a final depth of penetration of about 120mm and a final length close to zero (unobservable). Tate's comment was, "The whole of the aluminum rod is used up in the penetration process".

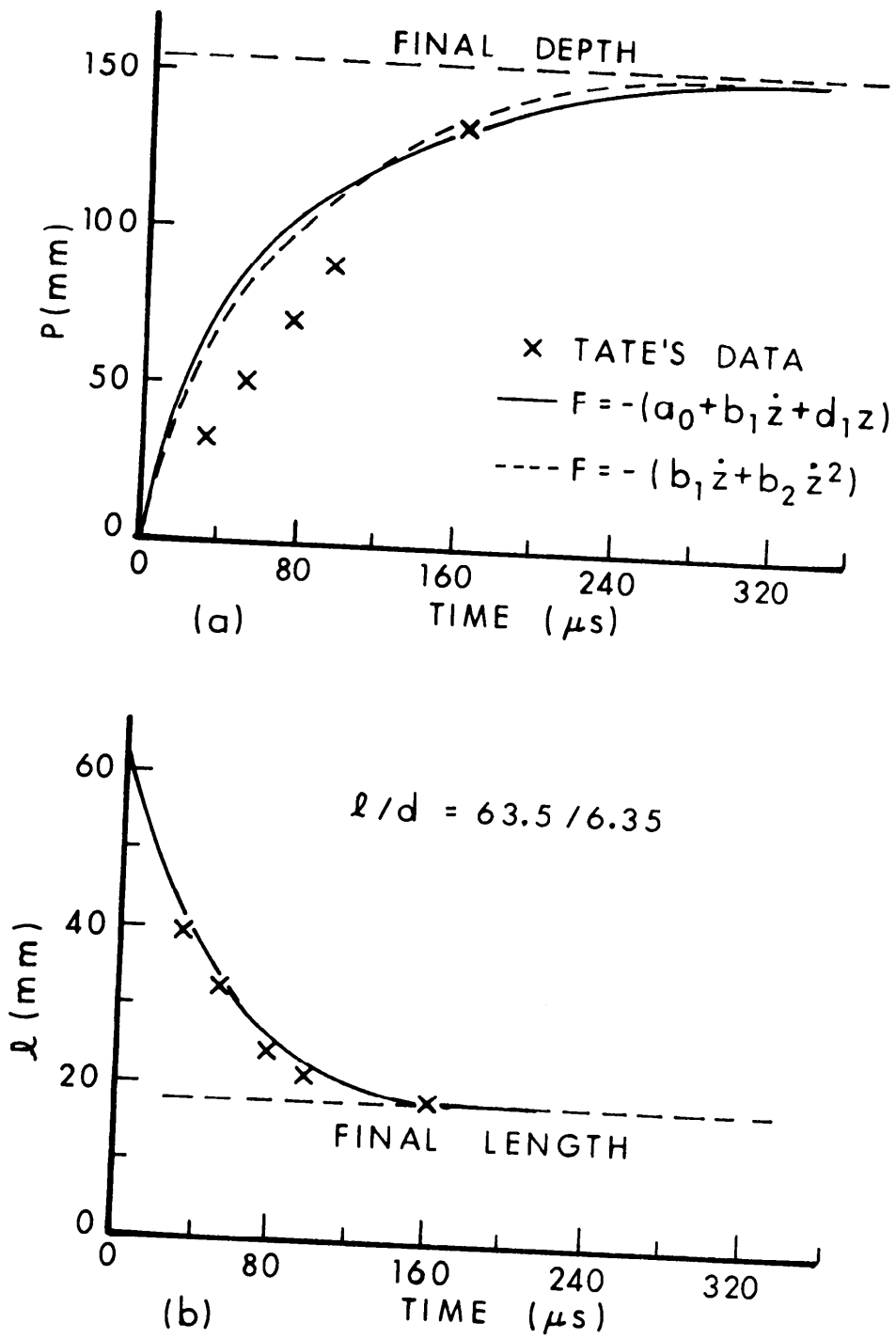[34]A. Tate, "A Theory for the Deceleration of Long Rods After Impact," J. Mech. Phys. Solids 15, 387, 1967.

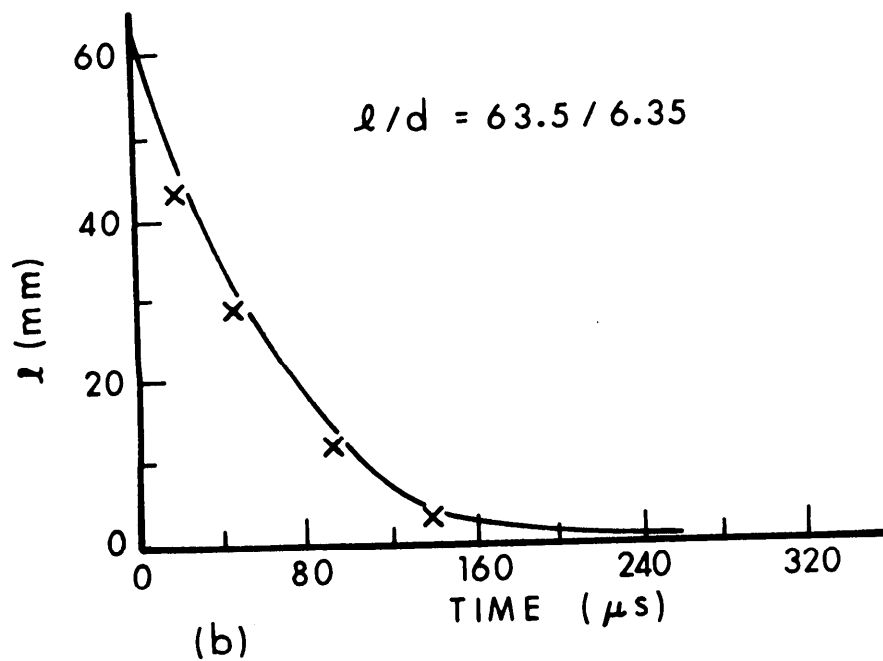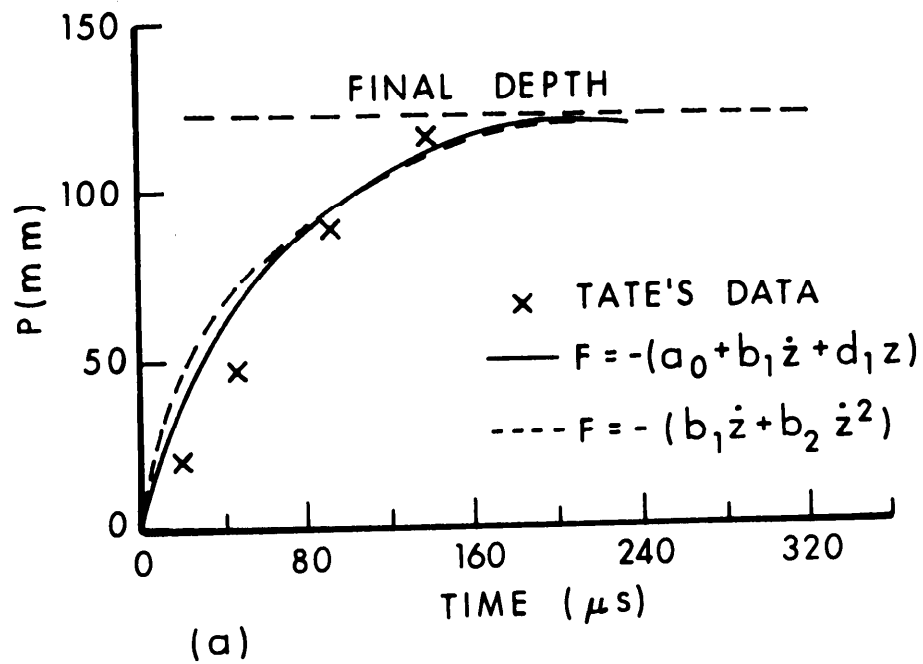Figure 5. Dural rod penetrating polyethylene: measured and calculated values.

Figure 6. Aluminum rod penetrating polyethylene: measured
and calculated values.

Let us apply our model to Tate's data. We recall that $d_{2z} = 0$ for a cylindrical rod. In addition we will neglect the v^2 force term (assuming $b_{2z} v \ll B_{1z}$). The displacement of the center of mass is (omitting the subscript z)

$$z = \frac{1}{2\beta} e^{-\alpha\phi} [\{v_o + \delta(-\alpha-\beta)\} e^{\beta\phi} - \{v_o + \delta(-\alpha+\beta)\} e^{-\beta\phi}] + \delta$$

(150)

from Equation (46) with $\phi(t)$ instead of t given by Equation (111). If the rod density and cross section are constant during the motion we have from Equation (113)

$$m/m_o = \ell/\ell_o = [(1 - b_1/B_1) \exp\{-\phi/[2 m_o (\varepsilon_1 - \tfrac{1}{2})/B_1]\} + b_1/B_1]^2.$$ (151)

We recall that $B_1 = b_1 + (\varepsilon_1 - \tfrac{1}{2})(-\dot{m}_o)$ and will take $\varepsilon_1 > \tfrac{1}{2}$ so $B_1 > 0$. If we assume that the viscosity of polyethylene is $\nu = 0.5$ m^2/s $= .005$ cm^2/μs as was done by Walters and Majerus[28] based on analogous Russian measurements[20]

$$b_1 \sim 6\pi R\rho\nu = 6\pi(.635/2)(2.7)(.005) \sim .08 \text{ gm}/\mu s .$$ (152)

As before in our application to the constant mass data of Backman and Finnegan we will take b_1 to be less than the estimated value, namely, $b_1 = .04$ gm/μs. From Figures 5 and 6 we can estimate $\dot{m}_o = -.07$ gm/μs and the final position of the center of mass $\delta = 155-18/2 = 146$mm for the dural rod or $120-0/2 = 120$mm for the aluminum rod. The depth of penetration of the tip will be $P = z + \ell/2$ in either case. For the dural rod we will take $\varepsilon_1 = 1$ and $d_1 = 10^{-5}$ gm/$(\mu s)^2$, while for the aluminum rod, $\varepsilon_1 = 4$ and $d_1 = 3.5 \times 10^{-4}$ gm/$(\mu s)^2$.

The solid lines in Figures 5 and 6 give the calculated results which compare reasonably well with experiment. The overestimate of P at early times may be due to our neglect of the v^2 force term which would be more important at retarding penetration during the early stages when the speed is high. It is of course desirable to include this term (though not the $d_{2z} s^2$ term) and future work will discuss methods of doing this. For the present we will compare the solution for the force - $(a_o + b_1 v + d_1 s)$ given by Equation (150) with the solution for the force - $(b_1 v + b_2 v^2)$ given by

76

$$z = \frac{m_o}{b_2} [\ln \{(1 + \frac{b_2}{b_1} v_o) \exp (b_1 \phi/m_o) - b_2 v_o/b_1\} - b_1 \phi/m_o] \qquad (153)$$

where we must take $a_o = 0$ to describe embedment as explained above. From Equation (153) we see that as $t \to \infty$, $\phi \to \infty$

$$z \to z_{MAX} = \frac{m_o}{b_2} \ln (1 + b_2 v_o/b_1). \qquad (154)$$

From Equation (154) we see that $\lim_{b_2 \to 0} z_{MAX} = m_o v_o/b_1$ so that

$b_1 < m_o v_o/(z_{MAX})$ observed to keep $b_2 > 0$. For the dural rod for example, $b_1 < 5.45$ gm x 1.646mm/μs/146mm = .06 gm/μs while for the aluminum rod, $b_1 < 5.45$ gm x 1.646mm/μs/120mm = .075 gm/μs. In either case $b_1 = .04$ gm/μs as above is small enough. If we use this value for b_1 and the same values for ϵ_1 as before, namely, $\epsilon_1 = 1$ for dural and $\epsilon_1 = 4$ for aluminum, then (since $\dot{m}_o$ is the same) it is clear from Equation (151) that the calculation of ℓ will not be different than before since it is independent of a_o, d_1 or b_2. The same is true for ϕ as is clear from Equation (111). Only z and therefore P will change. The dashed line in Figure 5 gives the result calculated from Equation (153) when we use $b_2 = .03$ gm/mm, while the dashed line in Figure 6 does the same for aluminum with $b_2 = .052$ gm/mm. There is little to recommend one force over the other for embedment.

The values of the parameters b_1, $\dot{m}_o$, m_o, v_o and $\delta = - a_o/d_1$ were fixed by experiment, that is, α, v_o and δ were fixed in Equation (150) as were ℓ_o or m_o and b_1 in Equation (151). The parameter ϵ_1 (and so B_1) was adjusted in Equations (111) and (151) to give reasonable agreement with experimental ℓ vs. t values. The parameter d_1 (and so β) was adjusted to give reasonable agreement for z (or P) vs. t. Similarly b_2 was adjusted in Equation (153). In neither case was there an effort made to obtain a best fit since our purpose here is merely to illustrate the potential of the method. Future work should include fitting a variety of data and codification of the parameters.

Studies of penetration into a semi-infinite target are not commonly made by those who study KE penetrators in this country (in contrast to those who study shaped charge jet penetrators). Usually projectiles are fired through a plate target of fixed thickness and their residual speed and mass is determined as a function of striking speed. For example, Herr and Grabarek[22] have observed that for both steel and tungsten rods striking steel armor plates end on at zero obliquity the residual mass increases as the striking speed increases in the ordnance range. This is illustrated in their Figure 16 for a 7.78 gm steel rod with a length of 50mm and a diameter of 5mm perforating a 6.35mm thick steel plate. This behavior is entirely reasonable for erosion since for higher v_o, less time is spent in the target. If the initial erosion rate is not a strong function of v_o and declines with time, then less erosion will occur as less time is spent in the target.

Let us use the force - $(a_o + b_1 \dot{z} + d_1 z)$ to describe their data. We can determine the amount of time or transformed time ϕ spent in the target by setting $z = T$ in Equation (150) for a given $v_o \geq v_{oPL} = 0.64$ mm/μs measured by Herr and Grabarek. We recall that at the perforation limit speed $z = \delta = T$ and $\dot{z} = 0$ as $\phi \to \infty$. The ricochet limit speed was not measured but was taken to be $v_{oRL} = 0.55$mm/μs. In addition b_1 was estimated to be $\sim 6\pi R\rho\nu = 6\pi(.635/2) \times 7.8 \times 5.5 \times 10^{-2} \sim 2.5$ gm/μs using the Russian[20] value for steel of $\nu = 5.5$ M^2/s $= .055$ cm^2/μs. Instead of cutting b_1 by half as we did for aluminum targets, it seems more appropriate to divide by five and take $b_1 = 0.5$ gm/μs. This may be due to the approximate nature of our model (in particular to our neglect of v^2 terms) or perhaps partly due to a lack of Stokes' law transfer from the explosive plate measurement technique used by the Russians and long rod penetration of steel plates. Such questions require much more investigation and will be left for future work. The actual values used for the parameters were $b_1 = 0.5$ gm/μs, $d_1 = 7.78 \times 10^{-3}$ gm/$(\mu s)^2$, $c_1 = 1$ and $\dot{m}_o = -0.4$ gm/μs. Once ϕ is determined for a given v_o, then Equation (151) is used to calculate the residual mass and the derivative of Equation (150) is used to calculate the residual speed, namely,

$$\dot{z} = \dot{\phi} \, dz/d\phi$$

$$= \sqrt{\frac{m_o}{m}} \; \frac{1}{2\beta} \left[- \{v_o - \delta(\alpha+\beta)\}(\alpha-\beta)e^{-(\alpha-\beta)\phi} + \{v_o - \delta(\alpha-\beta)\}(\alpha+\beta)e^{-(\alpha+\beta)\phi} \right]$$

$$(155)$$

78

where we have used Equation (104a) for $\dot{\phi}$. The results of these calculations are compared with the data of Herr and Grabarek in Figures 7a and 7b. Table III also shows how ϕ decreases as v_0 increases in agreement with the idea that less time in the target means less erosion. Real time t behaves in a similar way and can be found from Equation (111) although there is no need to do this in order to carry out the calculation.

Since we are dealing with a case of rectilinear motion in the perforation regime only, we can also describe the data by using the force $-(a_0 + b_1 \dot{z} + b_2 \dot{z}^2)$ provided we require a_0 to vanish when $v_0 = v_{oPL}$. Let us take $a_0 = a_1 T (v_0/v_{oPL} - 1)$ with a_1 small. Now we determine ϕ for given v_0 by letting $z = T$ in

$$z = \left(\frac{m_0}{b_2}\right) \ell n \left[(1 - Ae^{-B\phi})/(1 - A) + \left(\frac{h^+}{2b_2}\right) \phi\right] , \qquad (156)$$

the analog of Equation (24) where $(-q) = b_1^2 - 4a_0 b_2$, $h^{\pm} = - b_1 \pm \sqrt{-q}$, $A = (2b_2 v_0 - h^+)/(2b_2 v_0 - h^-)$ and $B = \sqrt{-q}/m_0$. Once ϕ is determined then Equation (151) is used to calculate the residual mass and the derivative of Equation (156) is used to calculate the residual speed, namely,

$$\dot{z} = \dot{\phi} \, dz/d\phi = \sqrt{\frac{m_0}{m}} \, (-\frac{1}{2b_2}) \, (h^+ - A h^- e^{-B\phi})/(1 - A e^{-B\phi}). \quad (157)$$

If we choose $a_1 = .001$ gm/$(\mu s)^2$, $b_1 = 0.3$ gm/μs, $b_2 = .01$ gm/mm, $\varepsilon_1 = 1$ and $\dot{m}_0 = - 0.4$ gm/μs we obtain the dashed lines in Figure 7. The calculation for the residual mass is so close to the previous calculation that the solid and dashed curves are indistinguishable. Again no attempt has been made to optimize agreement with experiment. We note that an even lower value of b_1 seems appropriate when a v^2 term is included. If we limit ourselves, to zero obliquity perforations as studied by Tate or by Herr and Grabarek, there is little to recommend the component force $-(a_0 + b_1 \dot{z} + d_1 z)$ over the force $-(a_0 + b_1 \dot{z} + b_2 \dot{z}^2)$. However, if we wish to include richochet, embedment and perforation in one unified theory, then the former force is preferable as we have seen.
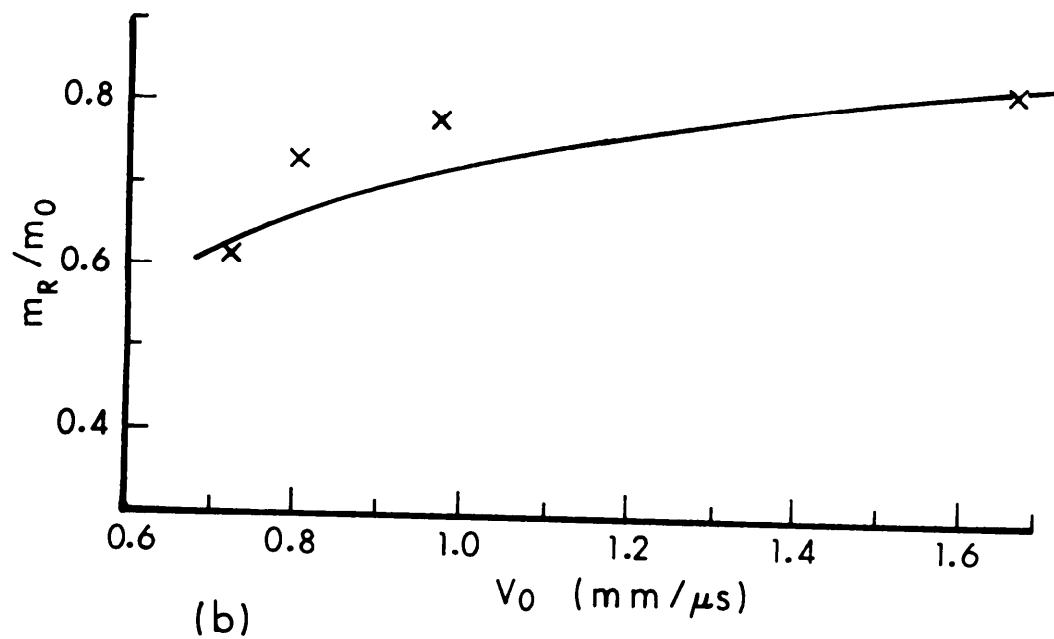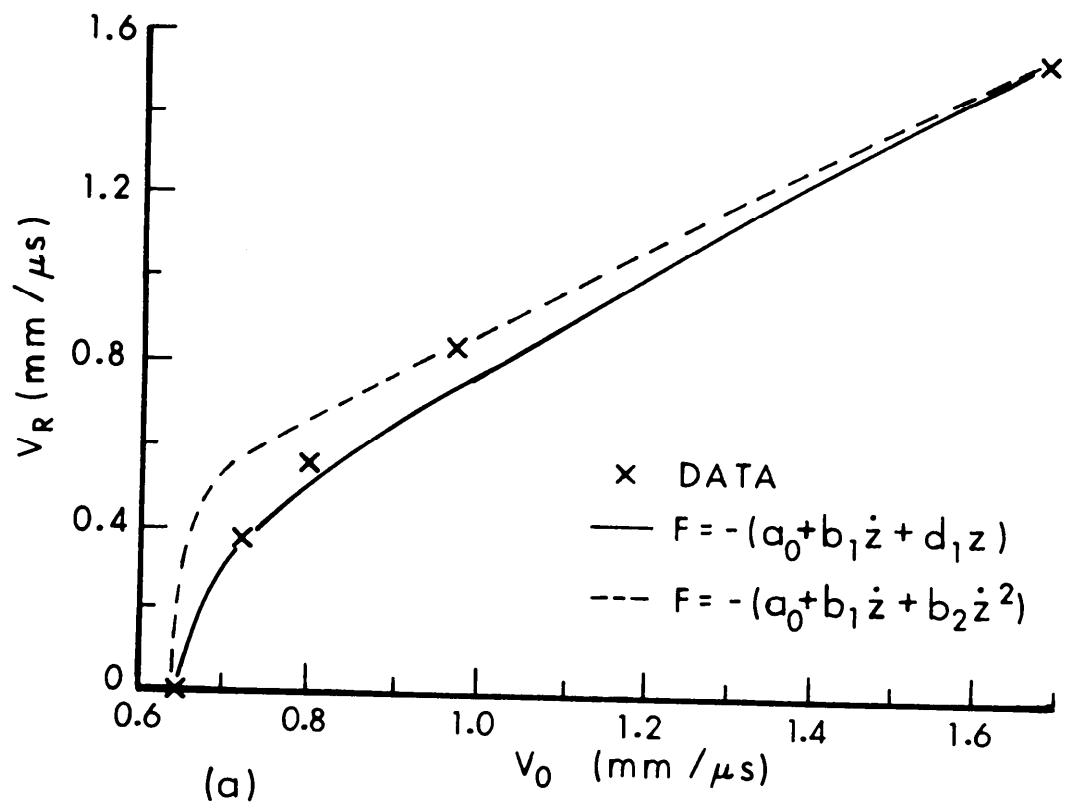
Figure 7. Residual speed and mass versus striking speed for a long steel rod penetrating a steel plate: measured and calculated values.

Table III. Calculated Values for Rod Mass and Speed
Using the Force $-(a + b_1 \dot{z} + d_1 z)$

v_o mm/μs	.64	.7	1.0	1.3	1.6
ϕ μs	∞	15.05	7.85	5.56	4.34
m/m_o	.51	.62	.73	.78	.82
v_1 mm/μs	0	.29	.76	1.13	1.47

In Herr and Grabarek's report there are some indications that for some materials, perhaps tungsten rods versus steel, the residual mass might first increase and then decrease somewhat as v_o increases. The data is not good enough to say that this occurs. If a case is found in which this behavior occurs, then the above model can be modified by the addition of a simple ad hoc postulate to include such a case. For given materials we might expect $\dot{m}_o$, the initial erosion rate, to depend somewhat on v_o, the striking speed. A simple representation of this might be

$$\dot{m}_o = - \sigma \, (v_o - v_E)^n \tag{158}$$

where σ and n are constants and v_E is a critical striking speed below which no erosion occurs. When Equation (158) is put into Equation (118), we see that the slope in an m versus ϕ (or t) plot, namely $\dot{m}$, becomes more negative for higher v_o. This behavior is shown in Figure 8 by the two curves marked v_{o1} (low) and v_{o2} (high). For the low striking speed v_{o1} the time to perforation, t_1, will be greater than the time to perforation, t_2, corresponding to the higher striking speed v_{o2}. The intersections of vertical lines through t_1 and t_2 with the mass curves give the residual masses at perforation. In Figure 8 we have shown the case for which the residual mass is the same for both striking speeds (that is, the dashed line is horizontal). However, it is easy to see that a more negative slope on the v_{o2} curve would lead to a lower residual mass after perforation than for the lower v_{o1} if t_2 remained the same. Similarly a less negative slope on the v_{o2} curve would lead to a higher residual mass than for v_{o1} if t_2 were the same. Trial calculations have been made and these have confirmed the ability of such a modification to represent the occurrence of a maximum in the residual mass versus striking speed curve with leveling off to a
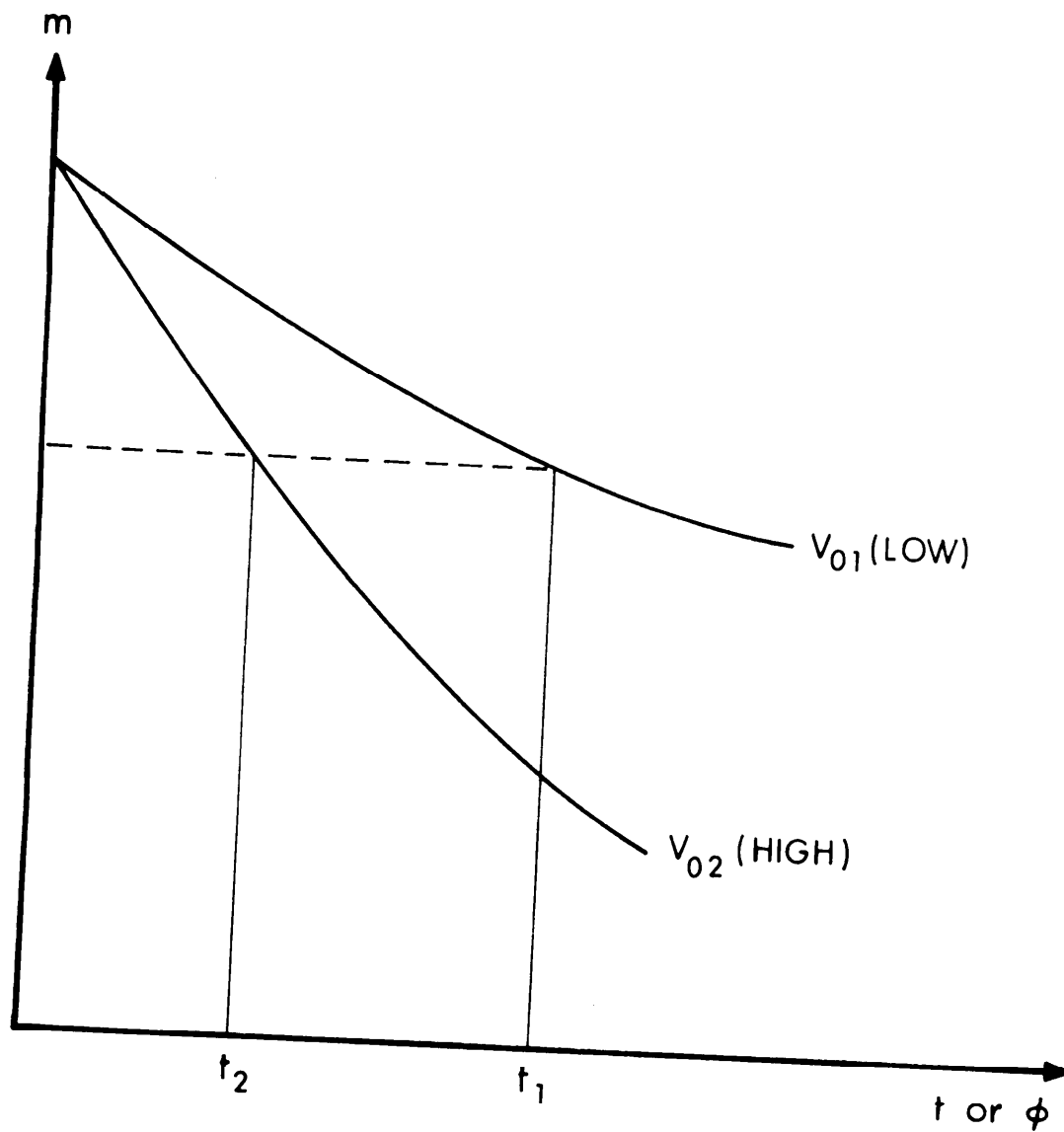
Figure 8. Sketch of possible mass loss behavior for an initial erosion rate dependent on striking speed.

constant value at higher striking speeds. However, these calculations will not be presented here since we have no convincing evidence that such a phenomenon occurs.

VIII.   A MODEL OF PROJECTILE BREAKUP

Here we are thinking of breakup as a discrete or discontinuous process in contrast to the continuous process of erosion. In recent years microscopic fracture theories have been advanced and linked to continuum fracture mechanics by constructing statistical distribution functions which represent molecular bond-breaking or flaw activation rates.[35] In this way more physics can be incorporated into a theory which, however, remains basically statistical in nature. This is partly necessitated by the enormous complexity involved in giving a deterministic description to each component of a large ensemble. There is also a virtue in this necessity since the behavior of large ensembles seems to follow rather simple laws which are of more interest than the behavior of the individual components. Gredenko has expressed this very well in discussing the molecular structure of matter:

"The problem here is not in fact, that of investigating the motion of individual particles but that of determining the laws to which aggregates of a large number of interacting particles are subject. However, the laws that arise in consequence of the mass character of the participating components have their own peculiarities and do not amount to a simple summation of the individual motions. Furthermore, within certain limits, these laws are found to be independent of the individual properties of the particles that give rise to them."[36]

Early models of fragmentation such as that proposed in England by Mott and Linfoot[37] were also statistical. At the suggestion of B. L. Welsh these authors proposed that the number of bomb or shell fragments with masses between m and m + dm could be represented by the distribution

$$dn = c^1 \, e^{-am^{1/3}} \, d\left(m^{1/3}\right) = \frac{c^1}{3 \, m^{2/3}} \, e^{-am^{1/3}} \, dm \qquad (159)$$

where c^1 and a are constants and dn is the number in the mass interval dm. The fact that this distribution fit experimental observations

---

[35]D. R. Curran, L. Seaman and D. A. Shockey, "Dynamic Failure in Solids" Physics Today, Jan 1977, pp 46-55.

[36]B. V. Gnedenko, The Theory of Probability, Trans. by B. D. Seckler, NY, Chelsea Publ. Co., 1962.

[37]N. F. Mott and E. H. Linfoot, "A Theory of Fragmentation," Advisory Council on Scientific Research and Technical Developments, A. C. 3348, Jan 1943.

reasonably well suggested the following idea to Mott and Linfoot. If the number of fragments with characteristic length x in the interval between x and x + dx were $c^1 e^{-x/x_0}$ dx and the length x were proportional to the cube root of the mass for a three-dimensional body, then Equation (159) would result. They pointed out the fact that similar distributions had been used to describe the weight or diameter distributions of crushed minerals or sand particles[38] and discussed the one- and two-dimensional analogues of Equation (159) which might be thought of if linear or planar breakup were involved.

Soon after, also in England, Ursell[39] suggested that the chance that the number of fractures be n ought to be given by a Poisson distribution $e^{-\lambda \ell}$ $(\lambda \ell)^n/n!$ for a rod of length ℓ with the expectation of fractures being $\lambda \ell$. Transatlantic communications must have been excellent for in less than six months Thomas published a report in the United States showing that the results of Mott, Linfoot and Ursell could be obtained from more general considerations which did not require random planes traversing a volume[40]. He pointed out that Equation (159) (or its one- and two-dimensional analogs) does not depend on particular breaking mechanisms such as the simultaneous formation of all fragments, but allows for example, smaller fragments to be formed at a later stage from larger fragments already formed.

Thomas' observation on the generality of Equations of the type of Equation (159) has been enlarged upon by Molitz[41] who used a Weibull[42] distribution to describe fragment masses from shells. This has a density function

$$dn = C \, m^{\lambda-1} \, e^{-a(m^\lambda)} \, dm \qquad (160)$$

which reduces to Equation (159) when $\lambda = 1/3$ (or to the "two- or one dimensional" analogs when $\lambda = 1/2$ or 1). Of course, the "one-dimensional"

[38]*Lienau, J. Franklin Inst., (1935) p 485*

[39]*H. D. Ursell, "Fragmentation Data and Theories of Fragmentation," A.C. 3817, April 1943.*

[40]*L. H. Thomas, "Comments on Mott's Theory of the Fragmentation of Shells and Bombs", BRL R 398, Sept 1943. (ATI #36152)*

[41]*H. Molitz, "Einige Bemerkungen zu den Verteilungsfunktionen der Splitter grössen, Explosivstoffe 2 Mar/Apr 1973, p 33.*

[42]*W. Weibull, Statistical Evaluation of Data from Fatigue and Creep-rupture Tests. Fundamental Concepts and General Methods". WADC Tech.Rept 59-400, Part I, 1959.*

analog with $\lambda=1$ is the exponential distribution while the case $\lambda=2$ is called Rayleigh's distribution.

Gredenko[43] showed in the asymptotic theory of extreme values that only three types of limiting distributions exist with Weibull's formula being the third asymptotic distribution of the smallest values[44]. In short, Equation (160) is a generalization (with λ as an adjustable parameter) which does not depend on the details of any physical model of breakup. In fact, it has been applied to a wide variety of physical and social phenomena[45].

Since practical fragmentation experiments require a non-zero (measurable) lower mass limit, we can introduce a cutoff mass, m_c, and write Equation (160) as

$$dn = C \ (m-m_c)^{\lambda-1} \ e^{\ -a(m-m_c)^{\lambda}} \ \ dm \tag{161}$$

which is the usual generalization to include a shift in the origin. Here λ is an adjustable parameter which at least for shell fragmentation by high explosives experience indicates is less than unity (near 1/2 or 1/3).

In view of the above considerations about the generality of Equation (160), it seems reasonable to apply it to projectile breakup under impact as well as to shell fragmentation by high explosives. When a projectile shatters or breaks into many small pieces during a high speed impact, then Equation (160) might be sufficient. However, for impacts at ordnance speeds, projectiles tend to break up into relatively few pieces of size comparable to each other and the original projectile. In this case a discrete distribution function related to Equation (160) should be more appropriate. Let us trace a connection between certain discrete and continuous distributions which will be suitable for our purpose.

---

[43]B. V. Gredenko, "Limit Theroms for the Maximum Term of a Variational Series", Doklady Akad. Nauk, USSR 32, 1941.

[44]E. J. Gumbel, "Statistical Theory of Extreme Values (Main Results)" c.6 in Contributions to Order Statistics, Ed. by A. E. Sarkan and B. G. Greenberg (NY: John Wiley & Sons, Inc., 1962.

[45]W. Weibull, "A Statistical Distribution Function of Wide Applicability", J. Appl. Mech., Sept 1951, p 293.

Consider an interval y and divide it into k parts each of size $\varepsilon=y/k$ with k large enough so that subinterval ε contains on the average only one random event. Let r be the constant average rate of occurrence of events in the interval y. Then the probability of one such event occurring in the subinterval ε is $p = r\varepsilon = ry/k$. The probability of of no events occurring in the subinterval ε is $(1-p)$. If these events are randomly distributed, the probability of finding exactly s of them in k intervals (k trials) is given by the binomial distribution.

$$q(s; k, ry) = \frac{k!}{s!\,(k-s)!}\, (ry/k)^s\, (1-ry/k)^{k-s} \tag{162}$$

where $s = 0,1,2\ldots k$ and $q = 0$ for all other s. Now consider the limit as $k \to \infty$, namely,

$$\lim_{k\to\infty} q = \frac{(ry)^s}{s!} \left[\lim_{k\to\infty} \frac{k!}{(k-s)!\,k^s}\right]\left[\lim_{k\to\infty}(1-ry/k)^k\right]\left[\lim_{k\to\infty}(1-ry/k)^s\right]$$

$$= P(s;ry) = \frac{(ry)^s}{s!}\, [1]\left[e^{-ry}\right][1] \tag{163}$$

which is the Poisson distribution. After division of the numerator by the demominator the first limit in Eq (163) becomes

$$\lim_{k\to\infty} \frac{k(k-1)(k-2)\ldots(k-s+1)}{k^s} = \lim_{k\to\infty} 1\left(1-\frac{1}{k}\right)\left(1-\frac{2}{k}\right)\ldots\left(1-(s-1)/k\right) = 1 \tag{164}$$

while the third limit is obviously unity. If we let $z = -(ry)/k$, the second limit becomes the (-ry) power of the limit which defines the base of the natural logarithm, namely,

$$\lim_{z\to 0}\left[(1+z)^{1/z}\right]^{(-ry)} = e^{-ry} \tag{165}$$

Finally consider the probabily that one or more events will occur in the interval y, namely,

$$\sum_{s=1}^{\infty} P(s;ry) = \sum_{s=0}^{\infty} P(s;ry) - P(0;ry) = 1 - e^{-ry} \tag{166}$$

by equation (163) and the fact that

$$\sum_{s=0}^{\infty} e^{-ry}\frac{(ry)^s}{s!} = e^{-ry}\sum_{s=0}^{\infty}\frac{(ry)^s}{s!} = e^{-ry}\ e^{ry} = 1 \qquad (167)$$

From Equations (166) and (163) it is clear that e^{-ry} is the probability that no events will occur in the interval y. If we look upon ry as a continuous random variable it is obvious that the cumulative probabilities e^{-ry} and $1-e^{-ry}$ have as their density function

$$d(n/N) = dn/N = e^{-(ry)}\ d(ry) = r\ e^{-ry}\ dy \qquad (168)$$

which is the usual exponential distribution giving the probability that an event will occur in the interval from ry to $ry+rdy$. Here dn is the number of such events in the interval dy or rdy and N is the total number of such events. If we integrate Equation (168) over (ry) from 0 to ry we obtain Equation (166), while if we do the same from ry to ∞, we obtain e^{-ry}. The mean value of $\bar{y}$ is $1/r$ while the median value $\tilde{y}$ is $(\ln 2)/r = .7r$.

In summary, we have seen that the Poisson distribution is a limiting form of the binomial distribution for small p (in particular for $k \gg ry \gg p = ry/k$). We have also seen that sums over the discrete Poisson distribution which divide the set of possible outcomes into that of no event occurring and its complement, that of one or more events occurring, have the form of a cumulative exponential distribution with continuous density function given by Equation (168).

The above analysis has been deliberately general to emphasize the point that probability distributions of random variables are not restricted to any particular phenomenon much less to a particular mechanism envisioned for the phenomenon. They are rather simple, approximate expressions of laws which a variety of large aggregates seem to follow rather well. For example, the above analysis is commonly employed in discussions of reliability or "time-to-first-failure" problems. The interval y is taken to be a time and r is a failure rate with ry being the expected number of failures in time y. Similarly, y might be a time and r an arrival rate of trucks at a loading dock with ry the expected number of arrivals in time y. In another application the interval y is taken to be a volume. For example, if microorganisms are distributed randomly in a body of water and a sample drop is examined under a microscope, we expect to find ry organisms if r is the density or number per unit volume. In view of the great variety of applications for such formulas it does not seem necessary or appropriate to put much weight on discussions of dimensionality.

If we let $y = (m/\rho)^\lambda$ in Equation (168) it becomes

$$dn = N\, e^{-r(m/\rho)^\lambda}\, d\left[r(m/\rho)^\lambda\right] = \frac{Nr\lambda}{\rho^\lambda}\, m^{\lambda-1}\, \exp\left[-rm^\lambda/\rho^\lambda\right]\, dm \quad (169)$$

which is Equation (161) with $C = N\lambda(r/\rho^\lambda) = N\lambda a$. When $\lambda = 1/3$ Equation (169) becomes Equation (160) with $C^1 = Na = N(\rho^{1/3}/r)^{-1} = N\mu^{-1/3}$ if we define $\mu = \rho/r^3$. In other words, Mott's formula is a particular case of Equation (161) which in turn is a particular case of Equation (168) which is an exponential distribution of the random variable y. If m is a mass and ρ is a mass per unit volume then x can be interpreted as a characteristic dimension of the volume in question. If the original volume is cubical and breaks into cubes then x is the length of an edge and λ is $1/3$.

If the volume is not a cube or does not break into cubes but the fragments are chunky then an effective value for λ should not be far from $1/3$. If the volume and/or fragments are rods, plates, shells or some arbitrary shapes, then the a priori value of λ is not obvious. If Equation (169) is to be applied to such a volume it seems better to treat λ as an adjustable parameter to be determined by sample experiments.

As we have noted, Equation (168) is the density function for certain sums over the Poisson distribution. It is instructive to return to Equation (162) and repeat the analysis for the particular application of material breakup. In this case k is the very large number of defects which are found in real materials, while s is the number which are activated or converted into breaks in a given stressful situation. Now r is the average rate of occurrence of activated defects or breaks which are assumed to be randomly distributed over the interval y which is a characteristic dimension of some type. Since an event in this description is a break, then N in Equations (168) and (169) is the number of breaks which occur in the interval. The number of pieces will be $N+1$ which is practically equal to N for $N \gg 1$. Here r or ry is a function of the stress applied to the body in question and will depend on the manner in which it is applied as well as on its magnitude. In addition, it will depend on the material properties of the body as well as its geometry. In the case of an explosive-filled shell, N is usually taken to be equal to the large number of fragments collected, λ is taken to be $1/2$ or $1/3$, and μ is treated as an adjustable parameter. Various schemes for estimating μ for certain geometries and materials have also been proposed, starting with a report by Mott[46]. If we integrate Eq (169) from m_1 to m_2 we

---

[46] N. F. Mott, "Fragmentation of HE Shells; a theoretical Formula for the Distribution of Weights of Fragments", A.C. 3642 (1943).

obtain the number of fragments predicted to be in this mass range for given N, λ and $\mu^{-\lambda} = \left(\rho r^3\right)^{-\lambda}$. If we let $m_1 = 0$ we obtain the number of fragments which should have mass less than m_2 or variable less than $w_2 = ry$ $= r(m_2/\rho)^{\lambda}$, namely,

$$N(m < m_2) = \int_0^{m_2} N \, e^{-r(m/\rho)^{\lambda}} \, d\left[r(m/\rho)^{\lambda}\right] = \int_0^{w_2} N \, e^{-w} \, dw$$
$$= N\left[1 - \exp\left\{-r\left(\frac{m_2}{\rho}\right)^{\lambda}\right\}\right] = N\left[1 - e^{-w_2}\right] \qquad (170)$$

with $N(m < m_2)/N$ giving the chance that an individual fragment will have mass less than m_2. The complementary probability, namely, the chance that a fragment will have a mass greater than m_2, is of course

$$N(m > m_2)/N = \int_{w_2}^{\infty} e^{-w} \, dw = \exp\left\{-r(m_2/\rho)^{\lambda}\right\} = e^{-w_2} \qquad (171)$$

Here m_2 obviously cannot exceed the original mass of the body before breakup (m_0) so taking the upper limit of the integral to be ∞ is an approximation. However the error involved for explosive fragmentation is usually small and quite acceptable since even the largest fragment produced is very much smaller than m_0. The error is also acceptable in view of the simplicity of the formula and the experimental accuracy which can be achieved. In equating N to the total number of fragments collected we are effectively defining r to be infinite for $m \geq m_0$ so that Equation (171) vanishes if $m_2 > m_0$ and $N(m < m_0) = N$ in Equation (170). Other formulations can be found to handle both a cutoff mass for particles too small to measure and a maximum (unbroken) mass equal to m_0. These will be the subject of a future report since they are more concerned with experiments in which breakup becomes shatter, that is, with the high explosive fragmentation of shells into a large number of pieces or with projectile breakup upon impact in the hypervelocity regime.

The median value of y, namely $\tilde{y}$, is found by setting $N(m < m_2)/N = 0.5 = N(m > m_2)/N$ in Equations (170) and (171) and solving for $y_2 = \tilde{y}$. Thus $y = (\ln 2)/r$ as before so the median value of the mass is

$$\tilde{m} = \rho \, (\tilde{y})^{1/\lambda} = \rho \left[(\ln 2)/r\right]^{1/\lambda} = (\ln 2)^{1/\lambda} \, (\rho/r^{1/\lambda}) \qquad (172)$$

The mean value of y, namely $\overline{y}$, is found from

$$\overline{y} = \int_0^\infty y\ e^{-(ry)}\ d(ry) = r^{-1} \tag{173}$$

which is consistent with the meaning of r as the average number of breaks per unit interval. Then the average value we expect for the mass is

$$\overline{m} = \rho(\overline{y})^{1/\lambda} = \rho/r^{1/\lambda} = \mu \tag{174}$$

by our previous definition of μ if $\lambda = 1/3$. By comparing Equations (172) and (174) we see that the mean and median values of the mass differ by the factor $(\ln2)^{1/\lambda}$ which is about 1/3 for $\lambda = 1/3$. Having $\tilde{m} < \overline{m}$ is characteristic of a distribution positively skewed (to the right).

In this report we are interested in projectile breakup during impact at ordnance speeds where the number of breaks is not much different from unity and the mass of each piece is not very much smaller than the striking mass m_o. Consequently, we cannot afford to set the number of pieces equal to the number of breaks, nor can we let the upper limit of any mass integral be effectively infinite. We can however, use the Poisson distribution since the number of defects or unactivated breaks, k, is still very large (effectively infinite) in any real material so that the limiting process of Equation (163) is still applicable.

Equation (163) is a probability distribution for the discrete variable s, given the continuous parameter (ry). As is well-known, the mean value of s is

$$\overline{s} = ry = \overline{N}_B \tag{175}$$

which is the average number of breaks we expect in the interval y under stress conditions specified by ry. Here ry is not necessarily an integer, and P is not necessarily maximum at $\overline{s}$. If we form the ratio $P(s)/P(s-1) = (ry)/s \gtrless 1$ from Equation (163), we see that for s<ry, P increases as s increases, while for s>ry, P decreases as s increases. If ry happens to be an integer, then P has two equal maxima at the modes $\hat{s} = ry$ and $\hat{s} = ry-1$. Otherwise P has one maximum at $\hat{s}$ equal to the largest integer which is less than ry so that $\hat{s}$ is not greatly different from $\overline{s}$. The median value of s, namely $\tilde{s}$ can be found by calculating the cumulative probabilities or partial sums $S(\ell;ry) = \sum_{s=0}^{\ell} P(s;ry)$ for $\ell=0,1,2,..$ until we find a sum which just exceeds 0.5 with $S(\ell-1;ry) <0.5$. The value of ℓ for which this is true is defined as $\tilde{s}$.

Since the number of pieces is the number of breaks plus one we have for the average mass

$$m_{AV} = m_o/(\overline{s}+1) = m_o/(ry+1) = m_o/(\overline{N}_B+1) \tag{176}$$

91

from Equation (175). In order to estimate m_{AV}, let us make some reasonable assumptions about ry=$\overline{N}_B$. In particular let us assume that $\overline{N}_B$ is proportional to an energy per unit volume carried by the projectile divided by the energy per unit volume needed to fracture the projectile, namely,

$$ry = \overline{N}_B = K \left[\frac{1}{2} \rho \; (v_o^2 - v_c^2) \right] \; /\sigma_y \qquad (177)$$

where the density, ρ, the striking speed, v_o, a critical speed, v_c, below which $\overline{N}_B=0$ and the yield stress, σ_y, can all be determined experimentally. Here K is the constant of proportionality which measures that fraction of the excess striking energy density which is converted to internal energy of the projectile and is responsible for any breaks which may appear. To account for obliquity it is reasonable to assume that K is proportional to the line of sight thickness $T/\cos \theta_o$ so

$$K = F/\cos \theta_o \qquad (178)$$

where F is a fraction dependent on factors like projectile shape, pitch and yaw as well as target hardness. Instead of σ_y, which is readily available for most materials of interest, it might be more satisfactory to use $\sigma_F \epsilon_F$, where σ_F and ϵ_F are the true stress and strain at fracture in an appropriate experiment which combines tensile and compressive forces. However, in view of the fact that σ_F and ϵ_F are not readily available for all materials of interest even in simple quasi-static tension experiments, we will use σ_y, assuming that σ_y and $\sigma_F \epsilon_F$ are related for particular materials of interest.

In summary, from Equations (177) and (178) we can calculate the number of breaks we expect, $\overline{N}_B$, and the number of pieces we expect, $\overline{N}_B+1$. Then we can find the average mass from Equation (176) and estimate the variance (or square of the standard deviation) we expect from this average mass from the well-known fact that the variance of the Poisson distribution is equal to the mean, namely, ry. Alternatively, we can calculate the median value from the cumulative probability $S(\ell;ry)$ or even the mode by rounding ry to the nearest integer less than or equal to ry.

Let us illustrate the above model by applying it to some data contained in the Holloway, et al. report cited above[4]. Consider a tungsten sphere of mass 0.45 gm and diameter 0.36 9cm striking a mild

92

steel plate at zero obliquity. All of the zero obliquity data for this case is plotted in Figure 9, a total of 39 points. For 24 of these points the target thickness was 0.16 cm, for 14 of them it was 0.32 cm and for one it was 0.64 cm. All but three involved spheres nominally 0.45 gm, while three were nominally 0.26 gm. This information is represented by the different symbols used in the figure. From the figure we can take $v_c=500$ m/s $= .5 \times 10^5$ cm/sec while the density is $\rho=17.1$ gm/cm^3 and $\sigma_y=6$ kilobars $= 0.6 \times 10^{10}$ dyne/cm^2.

If we assume $K=F=0.1$ in Equation (178) we can calculate $(\bar{N}_B)$ as a function of v_o namely, $\bar{N}_B = .1 \left[\frac{1}{2}(17.1)(v_o^2 - .5^2) \times 10^{10} \right] / .6 \times 10^{10} =$

$1.425(v_o^2 - .25)$. The results are given in Table IV with the ratio m_{AV}/m_o from Equation (176) plotted in Figure 9 as the dashed line.

Table IV

v_o(km/s)	≤ 0.5	.75	1.00	1.25	1.50	1.75	2.00	∞
$\bar{N}_B$	0	.445	1.069	1.870	2.850	4.008	5.344	∞
$\bar{N}_B+1$	1	1.445	2.069	2.870	3.850	5.008	6.334	∞
m_{AV}/m_o	1	.692	.483	.348	.260	.200	.158	0

Here we are neglecting mass loss by erosion. Below $v_o=.5$ km/s erosion is quite small experimentally and from considerations given in the previous section it should be even smaller for higher v_o. For comparison we have also plotted in Figure 9 the residual mass curve given by the Thor Equation in the Holloway report[4] namely,

$$m_1 = m_o - 10^{-4.3516}(T)^{.1455}(k)^{.7191}(\sec \theta_o)^{.4048}(m_o)^{1.3324}(v_o)^{.9911} \quad (179)$$

which in the present case becomes the mass ratio

$$m_1/m_o = 1 - .315(v_o)^{.9911} \quad (180)$$

with v_o expressed in k m/s where we have used $k=20$, $\theta_o=0$, $m_o=.45$ gm and $T=1.6$ mm. For $T=3.2$ mm the factor .315 becomes .348. For all practical purposes Equation (180) is a straight line and predicts that m_1/m_o vanishes for v_o near 3.2 km/s which is not reasonable. In
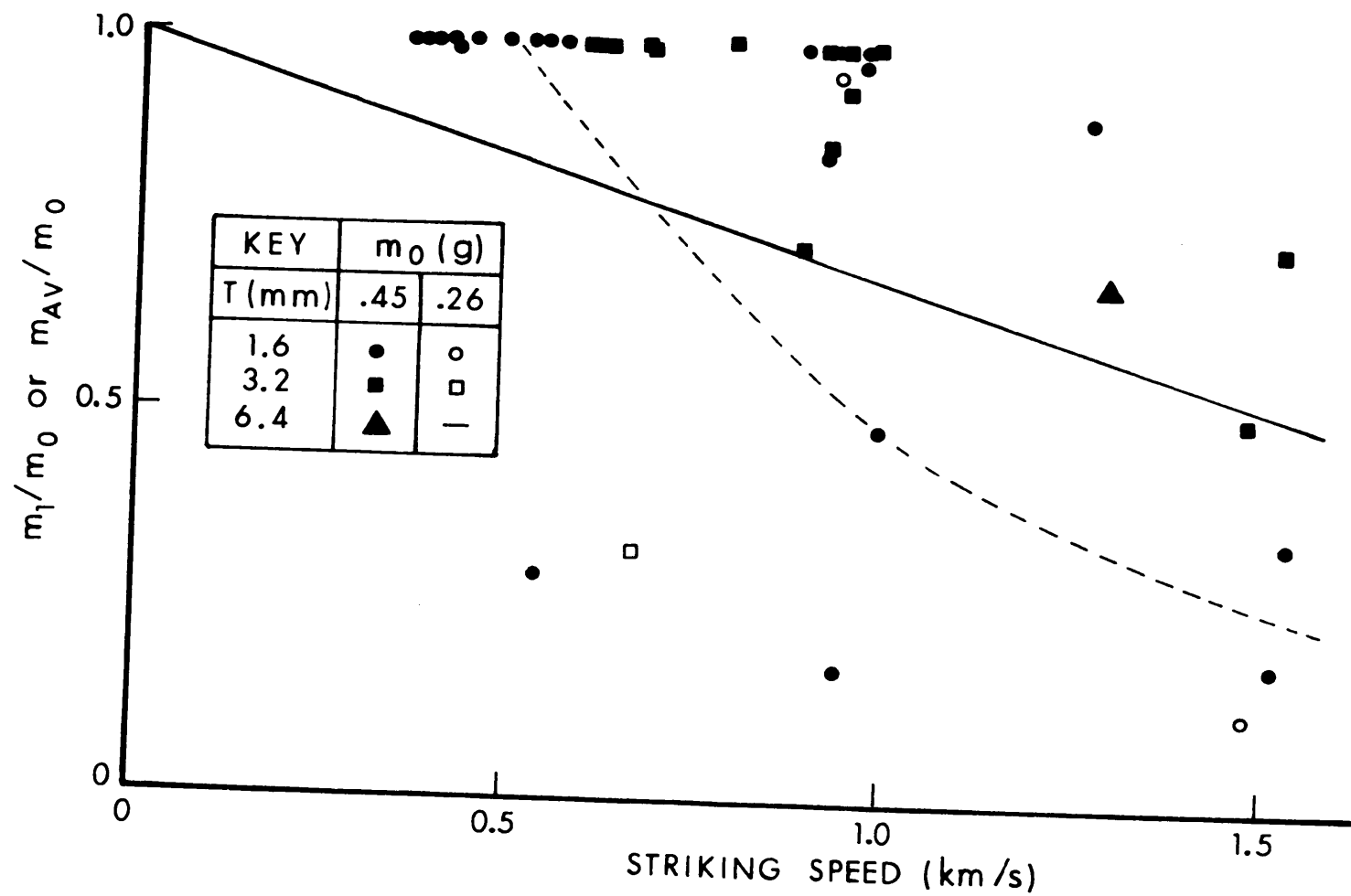
Figure 9. Residual mass fraction versus striking speed for tungsten spheres perforating steel plates at $\theta_0 = 0°$: largest piece found and average piece expected.

contrast Equation (176) vanishes only as $V_o \to \infty$. As noted before, Equation (179) also makes the unreasonable prediction that m_1 will decrease and eventually turn negative if m_o is increased while all other parameters are held constant, since the exponent 1.3324 exceeds unity. Equation (176) does not have this problem since the average residual mass is always proportional to the striking mass.

If we change one parameter, namely, $\theta_o = 45^o$, then we have the data plotted in Figure 10. If we keep F=.1 so K=.1/.707=.1414 instead of .1, then $\bar{N}_B$ is multiplied by 1.414 in Table IV and we have Table V.

<div align="center">TABLE V</div>

V_o(km/s)	≤ 0.5	.75	1.00	1.25	1.50	1.75	2.00	∞
$\bar{N}_B$	0	.629	1.512	2.644	4.030	5.667	7.556	∞
$\bar{N}_B+1$	1	1.629	2.512	3.644	5.030	6.667	8.556	∞
m_{AV}/m_o	1	.614	.398	.274	.199	.150	.117	0

the mass ratio in Table V is given by the dashed curve in Figure 10 which is lower than the dashed curve of Figure 9, following the trend of the data for the largest pieces. Equation (179) with $\theta_o = 45^o$ leads to

$$m_1/m_o = 1-.431(V_o)^{.9911} \qquad (181)$$

which is plotted as the solid line in Figure 10 and predicts negative m_1 beyond $V_o = 2.34$ km/s.

Since we have a Poisson distribution for the number of breaks, we can find the median value $s=\tilde{s}$ by calculating partial sums. For example, if we use $ry=\bar{N}_B=1.512$ for $V_o=1.0$ km/s in Table V we find the first partial sum ($\ell=0$) is .220, while for $\ell=1$ the cumulative sum is .553. Consequently, the median number of breaks is $\tilde{s}=1$ and the median number of pieces is 2. Thus half the time we should find fewer than 2 pieces and half the time more than 2 pieces with an average mass fraction $m_{AV}/m_o=.398$. If we count the number of data points above and below the dashed line in Figure 10 for the range $0.9 \leqslant V_o \leqslant 1.1$ km/s, we find ten below and ten above if we include the three eroded masses with $m_1/m_o \backsim 0.98$. This is fortuitous since each data point represents the mass fraction of the
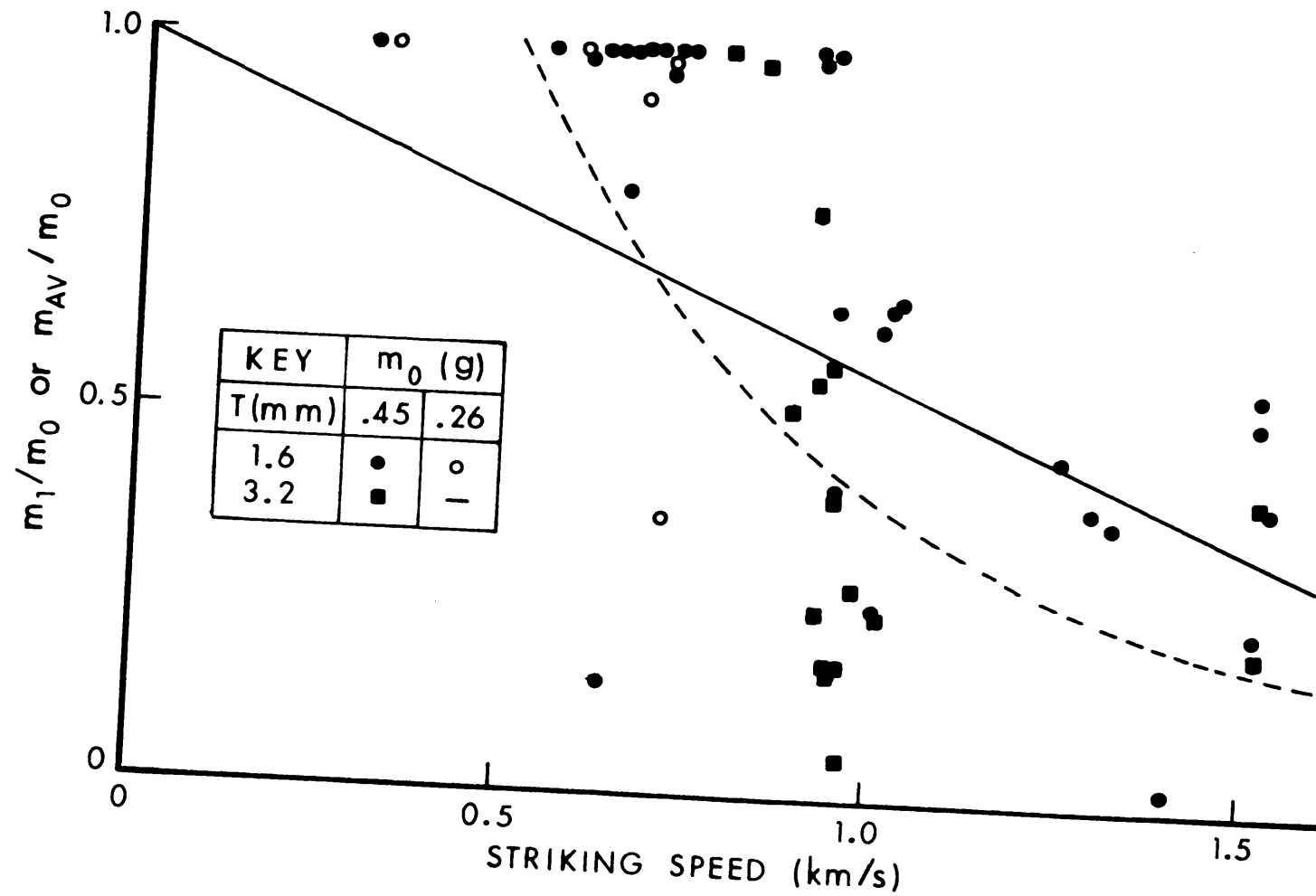
Figure 10. Residual mass fraction versus striking speed for tungsten spheres perforating steel plates at $\theta_o = 45°$: largest piece found and average piece expected.

largest piece found, and we cannot expect a 50/50 distribution about the average mass. If we consider v_o=1.5 km/s in Table V with $ry=\bar{N}_B$=4.03, the partial sums are .018, .089, .233, .426 and .621 so the median number of breaks is $\tilde{s}$ = 4 and half the time we expect to find more or less than 5 pieces with average mass fraction .199. All six of the data points near v_o=1.5 km/s in Figure 10 lie above the dashed line. This is consistent with the fact that the variance of the Poisson distribution is also equal to ry so the distribution spreads out as ry increases and the largest pieces are all likely to be above average in size. Similarly the smallest pieces are more likely to be much smaller than the average, although no data was reported to confirm or deny this prediction.

In the report by Herr and Grabarek[22] an effort was made to observe the masses of all the projectile pieces as well as target debris down to a cutoff size of 0.019 gm. For example, on pp 103-4 of their report they give particle data behind steel targets 6.35 mm thick struck at zero obliquity by tungsten alloy rods with $\dot{m}_o$=3.89 gm and L/D=49.2 mm/ 2.46 mm = 20. For v_o=.776 km/s the projectile was intact with a residual mass of 1.782 gm, indicating an erosion loss of 2.108 gm. They also reported a target plug of 0.991 gm and nine fragments with average mass of 0.075 gm totalling 0.673 gm. If these were all projectile fragments, then (2.108-0.673)=1.435 gm was either out of the field of view or distributed as fragments smaller than the cutoff mass. At v_o = .869 the projectile broke into three pieces of .311 gm, .739 gm and 1.238 gm, totalling 2.288 gm with average mass of 0.76 gm, indicating a possible erosion loss of 1.602 gm, less than the 2.108 gm erosion loss at the lower v_o as expected. They also reported a target plug of 0.765 gm and 15 fragments with average mass 0.062 gm, totalling 0.925 gm. If these were all projectile fragments, then (1.602-0.925)= 0.677 gm was not measured. At v_o = 1.384, the projectile broke into four pieces of .285 gm, .408 gm, .460 gm and 2.313 gm with average mass 0.867 gm, totalling 3.466 gm, indicating an erosion loss of only 0.424 gm. They also reported a target spall fragment of 0.143 gm and 20 other fragments with average mass 0.0476 gm and maximum mass 0.058 gm totalling 0.953 gm. Obviously not all of these fragments could be projectile fragments since their total mass exceeds the erosion loss of the projectile. At least half of them and probably most of them are target fragments, which may also be true for the lower speeds. This is the type of data we need both for estimating vulnerability/lethality and for judging the validity of any model we propose. Of course, for both purposes we need a great deal more data.

This case resembles the previous case in that tungsten projectiles strike steel plate targets at zero obliquity. However, the target here is thicker by a factor of 2 to 4 while the projectile is a long, thin rod rather than a sphere. Let us assume that the dominant

97

difference is the projectile shape. Since such a rod striking at a slight yaw of 2 to 3 degrees is more likely to fracture than a sphere, let us increase the value of F or K in Equation (178) by one third so that $\overline{N}_B = 1.333$ times larger or $\overline{N}_B = 1.9(v_o^2 - .25)$. This gives us the values in Table VI.

Table VI

v_o	$\overline{N}_B$	$\overline{N}_B + 1$	m_{AV}/m'_o	m'_o(obs)	m_{AV}(calc)	m_{AV}(obs)	$\tilde{s}$	$\tilde{s}+1$	Pieces(obs)
.776	.669	1.669	.599	1.782	-	-	0	1	1
.869	.960	1.960	.510	2.288	1.167	.763	1	2	3
1.384	3.163	4.163	.240	3.466	.832	.867	3	4	4

Here m'_o is taken to be the sum of the masses of the projectile pieces observed after perforation and so does not include the mass lost by erosion. Presumably the eroded mass survives as particles too small to measure and breakup of the eroded mass occurs as the projectile exits the target. So m'_o is taken to be the mass to be broken in Equation (176). By using $\overline{N}_B = .669$ for $v_o = .776$ we calculate $S(0;.669) = .512$ so $\tilde{s} = 0$ and the median number of pieces predicted is one in agreement with the observation of an intact projectile. It is meaningless to speak of an average mass of the projectile pieces in this case. By using $\overline{N}_B = .960$ for $v_o = .869$ we find $S(0;.96) = .383$ and $S(1;.96) = .751$ so $\hat{s} = 1$ and the median number of pieces is two. If the two smaller pieces observed, namely .739 gm and .311 gm, had been one piece of mass 1.050 gm, then the observed number of pieces would have been two (as predicted) while the observed average mass would have been $(1.050+1.238)/2 = 1.144$ gm which is close to the predicted value of 1.167 gm. Such deviations are expected of course because of the small sample size and the large variance. Surprisingly, both the number of pieces and the average mass observed at $v_o = 1.384$ km/s are quite close to the values predicted.

This is encouraging. However, much more information is required before we can say that this model has been validated by comparison with experiment. This too will be the subject of future work.

IX. CONCLUSION

The advantages and limitations of a number of previous descriptions of target penetration by a projectile have been reviewed, and new approaches have been proposed which incorporate these advantages and overcome many of these limitations. A deterministic particle model for an eroding penetrator has been proposed and the simplest versions of this model have been illustrated by comparisons with simple experiments. The model seems capable of describing three dimensional trajectories in a target consisting of various density components distributed in an arbitrary manner. Although the illustrations given here have been for single plate or semi-infinite targets, extensions to other targets of interest such as multiple (possibly spaced) plates, convex or concave cubes, etc., are obvious. In addition, a stochastic model has been proposed for projectile breakup and illustrated both for chunky fragment projectiles and long rod penetrators. Thus, the principle features of penetration in the ordnance range can be described in a theoretically sound yet simple manner, readily adapted to practical calculations and suitable for obtaining a broader fundamental understanding of penetration.

Much work still remains to be done. In order to consolidate the gains already made here, many more comparisons with experiment are in order. From a theoretical point of view it would be advantageous to find closed-form expressions for $s(t)$ and $m(t)$ using a force which depends on the first and second powers of the speed as well as on at least the first power of the depth of penetration. In view of the long history of this unsolved problem, this may not be easy to do and approximate solutions may have to be employed in order to describe hypervelocity penetrations by this technique. This reminds us also of the desirability of obtaining a simple, closed-form solution for both projectile and shaped charge jet penetration in a unified theory as well as a unified model of projectile breakup, jet particulation and high explosive fragmentation. Another area where much work remains to be done involves the mass and velocity distributions which describe the target debris. Little experimental information is available to guide or check the model maker much less the vulnerability analyst who might use such a model. However, now that a simple method is available to describe ricochet, this long-neglected feature can be incorporated into vulnerability codes after suitable experimental checks have been made.

ACKNOWLEDGMENTS

100

A COMPUTER CODE

```
10 REM THIS PROGRAM FOR THE HP 9830A CALCULATOR COMPUTES AND PLOTS EXIT
20 REM SPEEDS AND ANGLES VERSUS STRIKING SPEED FOR A PENETRATOR OF GIVEN
30 REM MASS M(GM) STRIKING A PLATE TARGET OF GIVEN THICKNESS T(MM) AT A
40 REM GIVEN OBLIQUITY THETA(DEG). THE Z COMPONENTS OF THE RICOCHET AND
50 REM PERFORATION LIMIT VELOCITIES (KM/S) ARE REQUESTED AND USED TO COMPUTE
60 REM AZ AND CZ FROM DZ INSTEAD OF USING THE VALUES GIVEN. IF THESE LIMITS
70 REM ARE UNKNOWN,SET THEM TO ZERO AND THE GIVEN AZ AND CZ WILL BE USED.
80 REM ANY VALUES ARE ALLOWED FOR AX,BX,CX,DX,AZ,BZ AND CZ BUT ONLY
90 REM DZ<M*(BZ/2)+2 IS ACCEPTED AS WRITTEN TO KEEP BETAZ REAL.
100 DIM V[100],C[100],X[100],Z[100],S[100],P[20],Q[20],R[20],A[61],G[100]
110 R=0
120 DISP "M,THETA,T,V0ZRL,V0ZPL";
130 INPUT M,T7,T8,V8,V9
140 PRINT "MASS=";M;"  OBLIQUITY=";T7;"  THICKNESS=";T8;"V0ZRL=";V8;"V0ZPL=";V9
150 DISP "VMIN,VMAX,VSTEP";
160 INPUT P1,P2,P3
170 PRINT "VMIN=";P1;"VMAX=";P2;"VSTEP=";P3
180 DISP "AZ,BZ,CZ,DZ";
190 INPUT C5,C6,C7,C8
200 A2=0.5*C6/M
210 IF (A2+2-C8/M)<0 THEN 180
220 B2=SQR(A2+2-C8/M)
230 G2=-A2+B2
240 H2=-A2-B2
250 IF V8=0 THEN 290
260 IF V9=0 THEN 290
270 C5=(V8/(V9-V8))*C8
280 C7=(-T8/(V9-V8))*C8
290 PRINT "AZ=";C5;"  BZ=";C6;"  CZ=";C7;"  DZ=";C8
300 DISP "AX,BX,CX,DX";
310 INPUT C1,C2,C3,C4
320 A1=0.5*C2/M
330 W1=0
340 B1=1
350 IF (A1+2-C4/M)<0 THEN 400
360 B1=SQR(A1+2-C4/M)
370 G1=-A1+B1
380 H1=-A1-B1
390 GOTO 410
400 W1=SQR(C4/M-A1+2)
410 PRINT "AX=";C1;"  BX=";C2;"  CX=";C3;"  DX=";C4
420 T6=T7*PI/180
430 PRINT
440 DISP "THANK YOU. I'LL WORK ON IT"
450 WAIT 1000
460 PRINT TAB2"V0"TAB9"TIME"TAB23"VX"TAB38"VZ"
470 K=0
480 FOR V0=P1 TO P2 STEP P3
490 K=K+1
500 S[K]=V0
```

```
510 IF V0=0 THEN 1050
520 S1=V0*SIN(T6)
530 S2=V0*COS(T6)
540 D1=-(C1*T8*TAN(T6)+C3*S1)/C4
550 D2=-(C5*T8+C7*S2)/C8
560 IF S2<V8 THEN 970
570 IF S2<V9 THEN 930
580 REM***PERFORATION***
590 IF R=1 THEN 740
600 I=1
610 T0=0
620 FOR T=T0 TO 500 STEP I
630 IF B2=0 THEN 660
640 J=FNA(T)
650 GOTO 670
660 J=FNE(T)
670 IF J>T8 THEN 690
680 NEXT T
690 IF (J-0.01)<T8 THEN 730
700 T0=T-I
710 I=I/10
720 GOTO 620
730 G[K]=T
740 T=G[K]
750 IF B2=0 THEN 780
760 V2=FNB(T)
770 GOTO 790
780 V2=FNF(T)
790 IF B1=0 THEN 850
800 IF W1>0 THEN 830
810 V1=FND(T)
820 GOTO 860
830 V1=FNL(T)
840 GOTO 860
850 V1=FNH(T)
860 V[K]=SQR(V1↑2+V2↑2)
870 C[K]=ATN(V1/V2)*(180/PI)
880 WRITE (15,890)V0,T,V1,V2
890 FORMAT F5.2,F9.2,E15.3,E15.3
900 GOTO 1370
910 IF D2>0 THEN 970
920 REM***EMBEDMENT***
930 V[K]=0
940 C[K]=0
950 GOTO 1370
960 REM***RICOCHET***
970 I=1
980 IF R=1 THEN 1220
990 IF K>2 THEN 1100
1000 IF B2=0 THEN 1030
1010 T1=LOG((H2/G2)*(S2+G2*D2)/(S2+H2*D2))/(G2-H2)
1020 GOTO 1040
1030 T1=(S2/A2)/(S2-A2*D2)
1040 IF T1>0 THEN 1100
1050 V[K]=0
```

```
1060 C[K]=180-T7
1070 G[K]=0
1080 WRITE (15,890)V0,V0,V0,V0
1090 GOTO 1370
1100 FOR T=T1 TO 500 STEP I
1110 IF B2=0 THEN 1140
1120 J=FNA(T)
1130 GOTO 1150
1140 J=FNE(T)
1150 IF J<0 THEN 1170
1160 NEXT T
1170 IF (J+0.01)>0 THEN 1210
1180 T1=T-I
1190 I=I/10
1200 GOTO 1100
1210 G[K]=T
1220 T=G[K]
1230 IF B2=0 THEN 1260
1240 V2=FNB(T)
1250 GOTO 1270
1260 V2=FNF(T)
1270 IF B1=0 THEN 1330
1280 IF W1>0 THEN 1310
1290 V1=FND(T)
1300 GOTO 1340
1310 V1=FNL(T)
1320 GOTO 1340
1330 V1=FNH(T)
1340 V[K]=SQR(V1↑2+V2↑2)
1350 C[K]=ATN(V1/V2)*(180/PI)+180
1360 WRITE (15,890)V0,T,V1,V2
1370 NEXT V0
1380 PRINT "IMPACT SPEED"TAB20"EXIT SPEED"TAB40"EXIT ANGLE (DEGREES)"
1390 FOR L=1 TO K
1400 WRITE (15,1410)S[L],V[L],C[L]
1410 FORMAT F10.2,E20.3,F20.3
1420 NEXT L
1430 REM (REMOVE REM TO RECYCLE) GO TO 290
1440 DISP "PLOT THESE VALUES? (YES=1,NO=0)";
1450 INPUT P5
1460 IF P5=0 THEN 2710
1470 REM PLOT SPEEDS AND ANGLES
1480 DISP "DATA FILE NUMBER? (0=NONE)";
1490 INPUT N1
1500 IF N1=0 THEN 1600
1510 LOAD  DATA N1,A
1520 I1=2
1530 FOR I=1 TO A[1]
1540 P[I]=A[I1]
1550 Q[I]=A[I1+1]
1560 R[I]=A[I1+2]
1570 I1=I1+3
1580 NEXT I
1590 GOTO 1680
1600 DISP "# DATA POINTS,FILE #";
```

```
1610 INPUT A[1],N1
1620 FOR I=2 TO 3*A[1]+1 STEP 3
1630 DISP "V0,V,THETA";
1640 INPUT A[I],A[I+1],A[I+2]
1650 NEXT I
1660 STORE DATA N1,A
1670 GOTO 1520
1680 P4=(P2-P1)/10
1690 SCALE P1-P4,P2+0.5*P4,-P4,P2+0.5*P4
1700 PLOT P1,P2,1
1710 CPLOT 10,0
1720 IF W1>0 THEN 1750
1730 LABEL (1760)"EXIT SPEED (KM/S)    BETAX=",B1,"   BETAZ=",B2
1740 GOTO 1770
1750 LABEL (1760)"EXIT SPEED (KM/S)   OMEGAX=",W1,"   BETAZ=",B2
1760 FORMAT 2F8.3
1770 PLOT P1,P2,1
1780 CPLOT 10,-2
1790 LABEL (1800)"M=",M,"   OBLIQUITY=",T7,"   T=",T8
1800 FORMAT 4F8.4
1810 LABEL (1800)"AX=",C1,"   BX=",C2,"   CX=",C3,"   DX=",C4
1820 LABEL (1800)"AZ=",C5,"   BZ=",C6,"   CZ=",C7,"   DZ=",C8
1830 LABEL (*)" "
1840 CPLOT 0,-3
1850 LABEL (*)"          V0            V"
1860 LABEL (*)" "
1870 FOR I=1 TO K STEP INT(K/8)
1880 LABEL (1890)S[I],V[I]
1890 FORMAT 2F10.3
1900 NEXT I
1910 XAXIS 0,0.2,P1,P2
1920 LABEL (*)
1930 FOR X=P1 TO P2 STEP 0.2
1940 PLOT X,0,1
1950 CPLOT -2,-2
1960 LABEL (1970)X
1970 FORMAT F4.1
1980 NEXT X
1990 YAXIS P1,0.2,0,P2
2000 LABEL (*)
2010 FOR Y=0 TO P2 STEP 0.2
2020 PLOT 0,Y,1
2030 CPLOT -5,-0.3
2040 LABEL (1970)Y
2050 NEXT Y
2060 PLOT P2,0.1,1
2070 CPLOT -20,0
2080 LABEL (*)"IMPACT SPEED (KM/S)"
2090 FOR I=1 TO A[1]
2100 PLOT P[I],Q[I],1
2110 CPLOT -0.3,-0.3
2120 LABEL (*)"X"
2130 NEXT I
2140 FOR L=1 TO K
2150 PLOT S[L],V[L]
```

104

```
2160 NEXT L
2170 PEN
2180 DISP "CHANGE PAPER, THEN CONTINUE"
2190 STOP
2200 P4=(P2-P1)/10
2210 SCALE P1-P4,P2+P4/2,-20,210
2220 PLOT P1,206,1
2230 CPLOT 10,0
2240 IF W1>0 THEN 2270
2250 LABEL (2280)"EXIT ANGLE (DEGREES)    BETAX=",B1,"  BETAZ=",B2
2260 GOTO 2290
2270 LABEL (2280)"EXIT ANGLE (DEGREES)    OMEGAX=",W1,"  BETAZ=",B2
2280 FORMAT 2F8.3
2290 PLOT P1,200,1
2300 CPLOT 10,-0.5
2310 LABEL (2320)"M=",M"  OBLIQUITY=",T7,"  T=",T8
2320 FORMAT 4F8.4
2330 LABEL (2320)"AX=",C1,"   BX=",C2,"   CX=",C3,"   DX=",C4
2340 LABEL (2320)"AZ=",C5,"   BZ=",C6,"   CZ=",C7,"   DZ=",C8
2350 LABEL (*)" "
2360 CPLOT 25,-2
2370 LABEL (*)"      V0        THETA"
2380 LABEL (*)" "
2390 FOR I=1 TO K STEP INT(K/8)
2400 LABEL (2410)S[I],C[I]
2410 FORMAT 2F10.3
2420 NEXT I
2430 XAXIS 0,0.2,P1,P2
2440 LABEL (*)
2450 FOR X=P1 TO P2 STEP 0.2
2460 PLOT X,0,1
2470 CPLOT -2,-2
2480 LABEL (2490)X
2490 FORMAT F4.1
2500 NEXT X
2510 YAXIS P1,20,0,200
2520 LABEL (*)
2530 FOR Y=0 TO 200 STEP 40
2540 PLOT 0,Y,1
2550 CPLOT -6,-0.3
2560 LABEL (2570)Y
2570 FORMAT F5.0
2580 NEXT Y
2590 PLOT P2,10,1
2600 CPLOT -20,0
2610 LABEL (*)"IMPACT SPEED (KM/S)"
2620 FOR I=1 TO A[1]
2630 PLOT P[I],R[I],1
2640 CPLOT -0.3,-0.3
2650 LABEL (*)"X"
2660 NEXT I
2670 FOR L=1 TO K
2680 PLOT S[L],C[L]
2690 NEXT L
```

105

```
2700 PEN
2710 STOP
2720 END
2730 DEF  FNA(T)=((S2+D2*H2)*EXP(G2*T)-(S2+D2*G2)*EXP(H2*T))/(G2-H2)+D2
2740 DEF  FNB(T)=((S2+D2*H2)*G2*EXP(G2*T)-(S2+D2*G2)*H2*EXP(H2*T))/(G2-H2)
2750 DEF  FNC(T)=((S1+D1*H1)*EXP(G1*T)-(S1+D1*G1)*EXP(H1*T))/(G1-H1)+D1
2760 DEF  FND(T)=((S1+D1*H1)*G1*EXP(G1*T)-(S1+D1*G1)*H1*EXP(H1*T))/(G1-H1)
2770 DEF  FNE(T)=EXP(-A2*T)*((S2-A2*D2)*T-D2)+D2
2780 DEF  FNF(T)=EXP(-A2*T)*((S2-A2*D2)*(1-A2*T)+A2*D2)
2790 DEF  FNG(T)=EXP(-A1*T)*((S1-A1*D1)*T-D1)+D1
2800 DEF  FNH(T)=EXP(-A1*T)*((S1-A1*D1)*(1-A1*T)+A1*D1)
2810 DEF  FNK(T)=EXP(-A1*T)*((S1-A1*D1)*SIN(W1*T)/W1-D1*COS(W1*T))+D1
2820 DEF  FNL(T)=EXP(-A1*T)*(S1*COS(W1*T)-(A1*S1-D1*C4/M)*SIN(W1*T)/W1)
2830 STOP
2840 END
```

106

DISTRIBUTION LIST

No. of Copies	Organization	No. of Copies	Organization
12	Commander Defense Documentation Center ATTN: DDC-DDA Cameron Station Alexandria, VA 22314	1	Commander US Army Communications Rsch and Development Command ATTN: DRDCO-PPA-SA Fort Monmouth, NJ 07703
1	Commander US Army Materiel Development and Readiness Command ATTN: DRCDMD-ST 5001 Eisenhower Avenue Alexandria, VA 22333	1	Commander US Army Electronics Research and Development Command Technical Support Activity ATTN: DELSD-L Fort Monmouth, NJ 07703
2	Commander US Army Armament Research and Development Command ATTN: DRDAR-TSS (2 cys) Dover, NJ 07801	2	Commander US Army Missile Research and Development Command ATTN: DRDMI-R DRDMI-YDL Redstone Arsenal, AL 35809
3	Commander US Army Armament Research and Development Command ATTN: J. Frasier J. Pearson G. Randers-Pehrson Dover, NJ 07801	1	Commander US Army Tank Automotive Research & Development Cmd ATTN: DRDTA-UL Warren, MI 48090
1	Commander US Army Armament Materiel Readiness Command ATTN: DRSAR-LEP-L, Tech Lib Rock Island, IL 61299	1	Director US Army TRADOC Systems Analysis Activity ATTN: ATAA-SL, Tech Lib White Sands Missile Range NM 88002
1	Commander US Army Aviation Research and Development Command ATTN: DRSAV-E P. O. Box 209 St. Louis, MO 63166	1	Director Army Research Office ATTN: E. Saibel P. O. Box 12211 Research Triangle Park, NC 27709
1	Director US Army Air Mobility Research and Development Laboratory Ames Research Center Moffett Field, CA 94035	1	Commander Naval Weapons Center ATTN: M. E. Backman, Code 3831 China Lake, CA 93555

DISTRIBUTION LIST

No. of Copies	Organization	No. of Copies	Organization
2	Sandia Laboratories ATTN: R. K. Byers W. Herrmann Albuquerque, NM 87115	1	University of California Dept of Applied Mechanics ATTN: W. Goldsmith Berkeley, CA 94720
1	National Aeronautics and Space Adminstration Lyndon B. Jonson Space Center ATTN: B. G. Cour-Palais Houston, TX 77058	1	University of California Los Alamos Scientif Lab ATTN: R. Darpp P. O. Box 808 Livermore, CA 94550
1	National Aeronautics and Space Administration Langley Research Center ATTN: D. H. Humes Hampton, VA 23665	1	University of Calfornia Lawrence Livermore Laboratory ATTN: M. L. Wilkins Livermore, CA 94550
1	Boeing Aerospace Company ATTN: Mr. R. G. Blaisdell Seattle, WA 98124	1	University of Delaware ATTN: J. Vinson Newark, DE 19711
1	Falcon Research and Development ATTN: R. Pipens 696 Fairmount Ave Baltimore, MD 21204	1	University of Dayton Research Institute ATTN: S. J. Bless Dayton, OH 45469
1	Falcon Research and Development ATTN: D. Parks 1225 S. Huron Denver, CO 80223	1	Denver Research Institute University of Denver ATTN: R. F. Recht 2390 S. University Blvd. Denver, CO 80208
1	International Applied Physics Inc ATTN: H. F. Swift 7546 Mc Ewen Rd Dayton, OH 45459	1	Drexel University Dept. of Mechanical Engineering ATTN: P.C. Chou 32nd and Chestnut Streets Philadelphia, PA 19104
1	Systems, Science and Software ATTN: R. T. Sedgwick P. O. Box 1620 La Jolla, CA 92038	1	Michigan Technical University ATTN: W. Predebon Houghton, MI 49931
		1	New Mexico Institute of Mining and Technology ATTN: TERA Group Socorro, NM 8780

108

DISTRIBUTION LIST

No. of
Copies   Organization

  1 Princeton University
     ATTN: A. C. Eringen
     Princeton, N.J. 08540

  1 Southwest Research Institute
     ATTN: W. Baker
     8500 Culebra Rd
     San Antonio, TX 78228

  1 Stanford Research Institute
     Poulter Laboratory
     ATTN: D. R. Curran
     Menlo Park, CA 94025

Aberdeen Proving Ground

     Dir, USAMSAA
       ATTN: Dr. J. Sperrazza
              DRXSY-MP, H. Cohen
              B. Cummings
     Cdr, USATECOM
       ATTN: DRSTE-TO-F
     Dir, Wpns Sys Concepts Team,
       Bldg. E3516, EA
         ATTN: DRDAR-ACW

USER EVALUATION OF REPORT

Please take a few minutes to answer the questions below; tear out this sheet and return it to Director, US Army Ballistic Research Laboratory, ARRADCOM, ATTN: DRDAR-TSB, Aberdeen Proving Ground, Maryland 21005. Your comments will provide us with information for improving future reports.

1. BRL Report Number _____

2. Does this report satisfy a need? (Comment on purpose, related project, or other area of interest for which report will be used.)

_____

_____

_____

3. How, specifically, is the report being used? (Information source, design data or procedure, management procedure, source of ideas, etc.) _____

_____

_____

4. Has the information in this report led to any quantitative savings as far as man-hours/contract dollars saved, operating costs avoided, efficiencies achieved, etc.? If so, please elaborate.

_____

_____

5. General Comments (Indicate what you think should be changed to make this report and future reports of this type more responsive to your needs, more usable, improve readability, etc.)_____

_____

_____

6. If you would like to be contacted by the personnel who prepared this report to raise specific questions or discuss the topic, please fill in the following information.

Name: _____

Telephone Number: _____

Organization Address: _____

_____

_____